ASI

SEED

خوشحال خیبر پختونخوا

UK International Development

Partnership | Progress | Prosperity

Assessment of Climate Change Impacts on Floods in the Indus River Basin of Khyber Pakhtunkhwa

# REPORT ON

# HYDROLOGICAL MODELLING AND FLOOD ESTIMATION

## (CLIMATE CHANGE INCLUSIVE FLOOD MODELLING REPORT)

(February 2024)

# EXECUTIVE SUMMARY

S1. Concern has been growing in recent years regarding the potential impact of climate change on Pakistan's already stressed water and agriculture resources. Rising temperatures, shrinking glaciers, early snow- and glacier-melt, variability in flows, rise in intense and frequent droughts and floods, rise in sea-level, increasing sea water intrusion, the growing threat of more intense rainfall, and changes in monsoon and winter rainfall patterns are just a few of how climate change is already affecting Pakistan's hydrologic resources. These risks amplify an already problematic situation given that Pakistan is among the most water-stressed countries in the world. Per capita access to surface and groundwater resources is expected to continue to decline in the decades ahead, driven largely by rapid population growth and urbanization.

S2. As the first step for climate change assessment, historic climate datasets have been collected and assessed. The available climate stations are sparse and have limited time-series data. Therefore, the accuracy of more than 25 gridded climate datasets has been evaluated. Of the available gridded datasets, the selection and bias-correction of one gridded climate dataset have been carried out using robust methodology and techniques.

S3. Similarly, a total of 31 Global Climate Models (GCMs) Coupled Model Inter-comparison Project Phase 6 (CMIP6) data performance has been assessed using the bias-corrected climate dataset, using different statistical methods. Out of these 31 models, seven models perform relatively better in capturing the annual variations as well as absolute deviations in precipitation compare to the observations. The performance of all the models to capture the variability in temperature was found satisfactory. Due to the limited availability of variables at the daily resolution, five out of these seven models have finally been selected for further analysis. For each of the five models, the dataset is obtained for the middle of the road scenario (SSP 2-4.5) and extreme scenario (SSP 5-8.5) for the assessment of the projected climate over the study area.

S4. Outputs of GCMs data (precipitation, minimum and maximum temperature) have been used in SWAT model calibration, validation and future projections of floods. Flood frequency analysis have been carried out using flood estimates for the historic and future periods, at basin-scale. The report provides flood estimates at various return periods. However, 100-year return period floods are discussed in summary.

S5. The Gomal River Basin, shows the highest increase across the study area. The increase in 100-year return flood is 98.6%, 92.9%, and 72.9% for 2011-2040, 2041-2070, and 2071-2100 under SSP 2-4.5 scenario. The rise in 100-year flood under SSP 5-8.5 is projected to be 109.1%, 84.9%, and 76.4% for 2011-2040, 2041-2070, and 2071-2100.

S6. Similarly, the Upper Indus Basin, shows the second highest increase across the study area. The increase in 100-year return flood is 36.8%, 59.1%, and 57.9% for 2011-2040, 2041-2070, and 2071-2100 under SSP 2-4.5 scenario. The rise in 100-year flood under SSP 5-8.5 is projected to be 42.3%, 65.4%, and 67.4% for 2011-2040, 2041-2070, and 2071-2100.

S7. In addition, the Swat, Chitral, Kabul, Kurram, Tank, and Kunhar river basins also show an increase in 100-year floods. The increase in 100-year flood ranges between 10% to 40% in various time periods under both scenarios. The maximum increase in various return period may occur in different future time periods.

S8. Furthermore, the potential increase in various return period floods is likely to increase significant sediment, boulders and debris flows in the Gomal, UIB, Kunhar, Swat, Chitral and Kabul River basins. The deposition of these sediments, boulders and debris may block water ways, reduce river carrying capacities (such as witnessed in Swat River during flood 2022) together with reduction in reservoir capacities (such as witnessed in the Tarbela Dam and Chashma Barrage). The future hotter and wetter climate will also increase risk of increase in Glacier Lake Outburst

Flood (GLOF) events, which may also bring large quantity of boulders and debris (particularly in the UIB, Chitral and Swat River Basin). Reduction in water carrying capacities and potential increase in floods may rise risks of inundation and damages in near to far future.

S9. Considering increase in floods in various return periods together with their occurrences warrants basin-level integrated flood management policy measures during the near, mid and long-term basis. The next report will provide policy measures for better climate inclusive flood adaptation and mitigation actions.

# CONTENTS

# LIST OF TABLES

## LIST OF FIGURES

# DELIVERABLE 2.2: REPORT ON CLIMATE CHANGE INCLUSIVE FLOOD MODELING FOR THE INDUS RIVER BASIN IN KP

# A-1. INTRODUCTION

## 1.1. CONTEXT

1. Pakistan is a flood-prone country and one of the 10 countries most affected by climate change in the world (Germanwatch, 2021)[1]. The devastating floods cause economic hardship for the country, such as those seen in the floods of 2010 and 2022. According to the initial reports from June 15, 2022 to September 12, 2022, a total of 303 people lost their lives (147 Male, 41 female and 115 children), due to heavy floods in Khyber Pakhtunkhwa (KP). Over 73,000 houses were also damaged, in addition to 754 schools and 82 Health centers. Well over 60,000 acres of crops and 477 irrigation systems were also destroyed by the floods. Furthermore, a total of 1,503 km Road network and 96 Bridges in 31 districts were either badly damaged or destroyed, with approximate damage cost of PKR 18.2 billion. It is a matter of public urgency that the government should adopt new tools and technology for development of climate resilient infrastructure that protects the most vulnerable and at-risk segments of the population, especially women and children of the province, and their socio-economic fabric plus livelihood activities from future disasters.

2. Climate change inclusive hydrological models are important tools for improving our understanding and predictability of climate behavior on seasonal, annual, decadal, and centennial time scales. Climate Models investigate the degree to which observed climate changes may be due to natural variability, human activity, or a combination of both. Recently, SEED provided technical assistance to the Government of KP (GoKP) for rehabilitation of flood damaged infrastructure in the province. The project named "Integrated Climate Adaptation and Disaster Resilience Assessment of Critical Infrastructure Assets in Khyber Pakhtunkhwa" focused on roads and bridges that had been damaged in the 2022 floods. As a policy decision, GoKP had mandated that these infrastructure assets had to be reconstructed in a manner that they are resilient to the impacts of climate change. Accordingly, hydrological analysis during the design process did not simply rely on consideration of historical flood flow as per the conventional approach. Instead, location specific climate change projections were made for each of the assets included in the project scope. The projected climate data was then used to estimate expected runoff based on the characteristics of the corresponding watersheds. Flood frequency analysis then involved historical stream/river flow data as well as flows expected under climate change scenarios. Results of the exercise revealed deficiencies in the conventional design approach in terms of high flood levels (HFLs) corresponding to various return periods and scour depths and velocities. Based on the significant value addition in terms of improving climate resilience of critical infrastructure through the adopted design approach, it was deemed necessary that climate change projections and consequent flood flows be estimated for all critical river basins in the whole province. This would make available a vital knowledge base that can be utilized by all relevant government departments in planning and design of public infrastructure assets.

3. The current study will carry out climate inclusive hydrological modelling and project floods at various return periods for various basins in KP. The study will identify critical basins, and provide a road-map of policy recommendations for climate resilient infrastructure development in the province.

## 1.2. SCOPE OF THE ASSIGNMENT

### 1.2.1. OBJECTIVES

4. The objective of this study is to support the Government of Khyber Pakhtunkhwa (GoKP) in carrying out a planning level hydro-climatic modelling exercise to estimate the magnitude and frequency of future floods in the Indus River basin of KP. The projected flood estimates will provide baseline for well-informed policy decisions aimed at resilient development/rehabilitation especially

[1] https://www.germanwatch.org/en/19777

for vulnerable population. In particular, the intervention will augment the climate-resilient planning and designing process of the damaged and vulnerable infrastructure assets.

5. The current study will encompass the following scope/objectives:

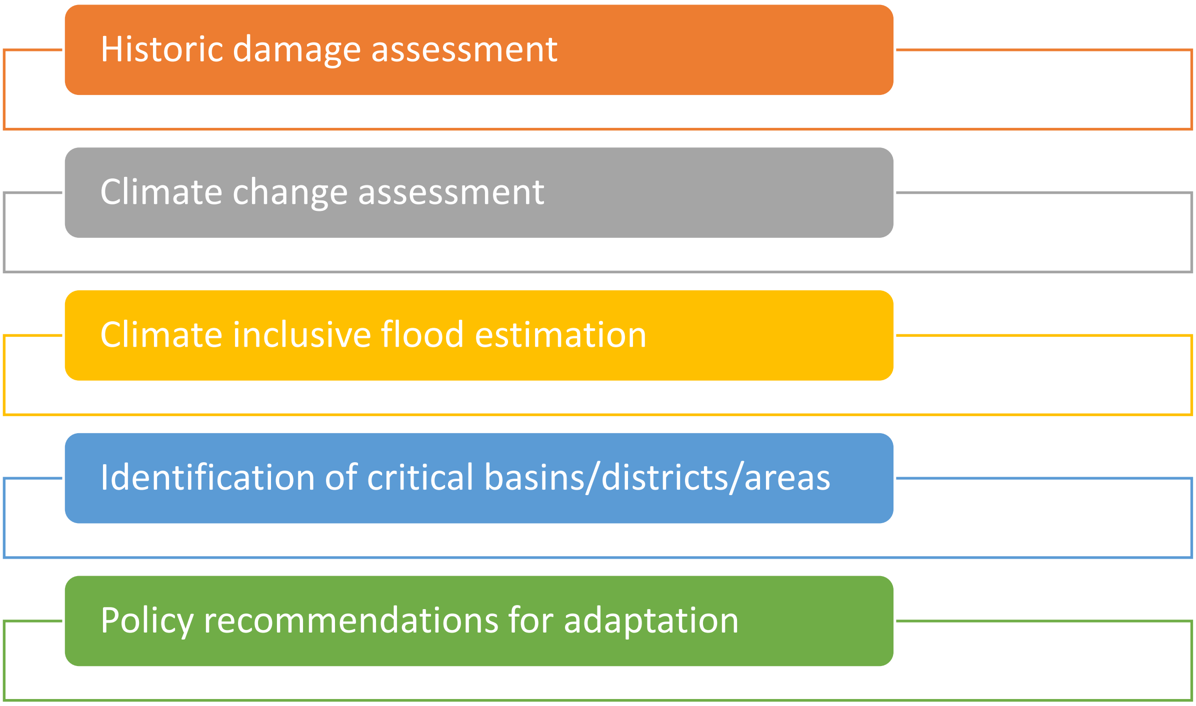


**Figure 1: The scope/objectives of the current study**

### 1.2.2. Deliverables/Reports

6. The consultants' team are supposed to prepare and submit, as a minimum, the following reports:

(i) **D-1: Inception Report.** 1 electronic copy and 1 hard copy to SEED within 2 weeks after the commencement of the services has been provided. The report includes an update of the proposed approach and methodology for key tasks under each output, detailed workflow, staffing schedule, and schedule of deliverables.

(ii) **D-2.1: Report on climate change assessment for the KP.** 1 electronic copy and 1 hard copy to SEED within 6 weeks after the commencement of the services have been submitted. The report provides comprehensive climate change assessment with a focus on floods in various river basins.

(iii) **D-2.2: Report on climate change inclusive flood modelling for the Indus River Basin in KP.** 1 electronic copy and 1 hard copy to SEED within 10 weeks after the commencement of the services will be submitted. The report will provide comprehensive climate inclusive flood modelling and projected estimates at different return periods for various river basins in the KP.

(iv) **D-3: Report on policy recommendations on climate change adaptation and resilient planning.** 1 electronic copy and 1 hard copy to SEED within 14 weeks after the commencement of the services will be submitted. The report will focus on a set of climate resilient planning measures for various river basins, considering structural and non-structural measures based on eco-system-/nature-based adaptation, green infrastructure, early warning systems, and grey infrastructure.

### 1.2.3. Meetings

7. **Meetings.** The consultant team will organize and participate in meetings with the key stakeholders, SEED and the government counterparts, to foster quality outputs. The consultant team will arrange and conduct internal meetings to keep the project on track.

### 1.2.4. Language and Formats

8. **Language and formats.** All reports to SEED will be produced in English. Reports shall be provided in electronic form. One hard copy of each of the final report will be provided upon approval of SEED.

## 1.3. Schedule

9. All the agreed deliverables will be submitted considering the following schedule:

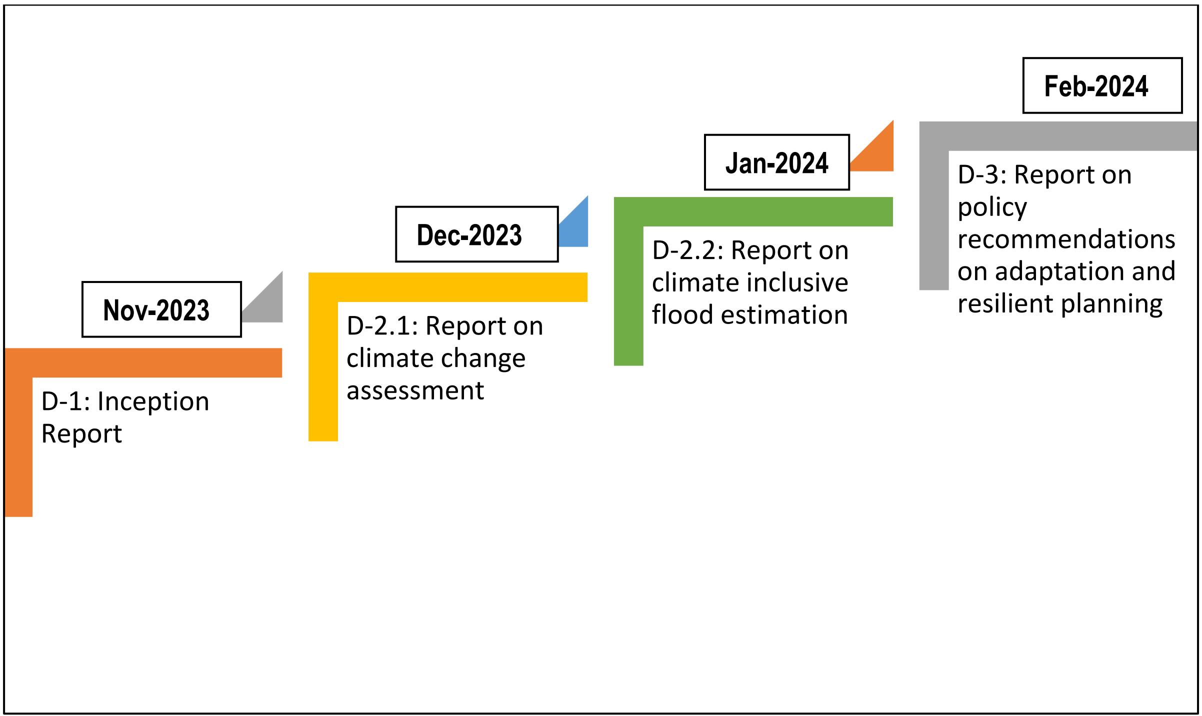


Figure 2: Schedule of the deliverables/reports

10. This report is deliverable D-2.2, which is focused on the climate change inclusive flood modelling of the study area.

# A-2. CLIMATE CHANGE INCLUSIVE HYDROLOGICAL MODELING

## 2.1. SELECTED BASINS FOR HYDROLOGICAL MODELING

11. The current study focusses on climate change inclusive flood modelling for the Indus River Basin of KP. The study area includes eight important river basins of the Indus River flowing within or draining into the KP. Five of these basins—Kabul, Chitral, Swat, the Indus River, and Kunhar—are located in the northern part, while the other three—Gomal, Kurram and Tank—are situated in the southern part of the KP. Climate inclusive flood modelling has been carried out for all the eight basins and detailed in the following sections.

## 2.2. HYDROLOGIC MODELING SYSTEM (SWAT MODEL)

12. The classification of open-source hydrological models typically falls into two categories: temperature/degree-day-based models and energy-based models. The energy-based models are acknowledged for their higher accuracy, however, they come with increased complexity in both structure and data requirements. The temperature-based models are simple, and perform better than energy-based models in data scarce regions, such as the Indus River Basin.

13. Notable hydrological models for consideration encompass SWAT, Snowmelt Runoff Model (SRM), VIC, and HEC-HMS. VIC stands out as a fully distributed model capable of functioning with either energy-based or temperature-based options. SWAT and SRM, on the other hand, are semi-distributed temperature-based models. SRM specifically predicts daily flow resulting from snowmelt and rainfall runoff, while HEC-HMS, although simpler to calibrate and providing output at hourly intervals, lacks sediment outputs.

14. The process of selecting an appropriate model hinge on factors such as data availability, desired output specifications, computation time and facilities, and the level of accuracy required. In light of limited data availability, specific outcome needs, and the primary goal of estimating floods, the SWAT model has been selected for the current study. Figure 1 illustrates the general workflow of the SWAT modeling process.

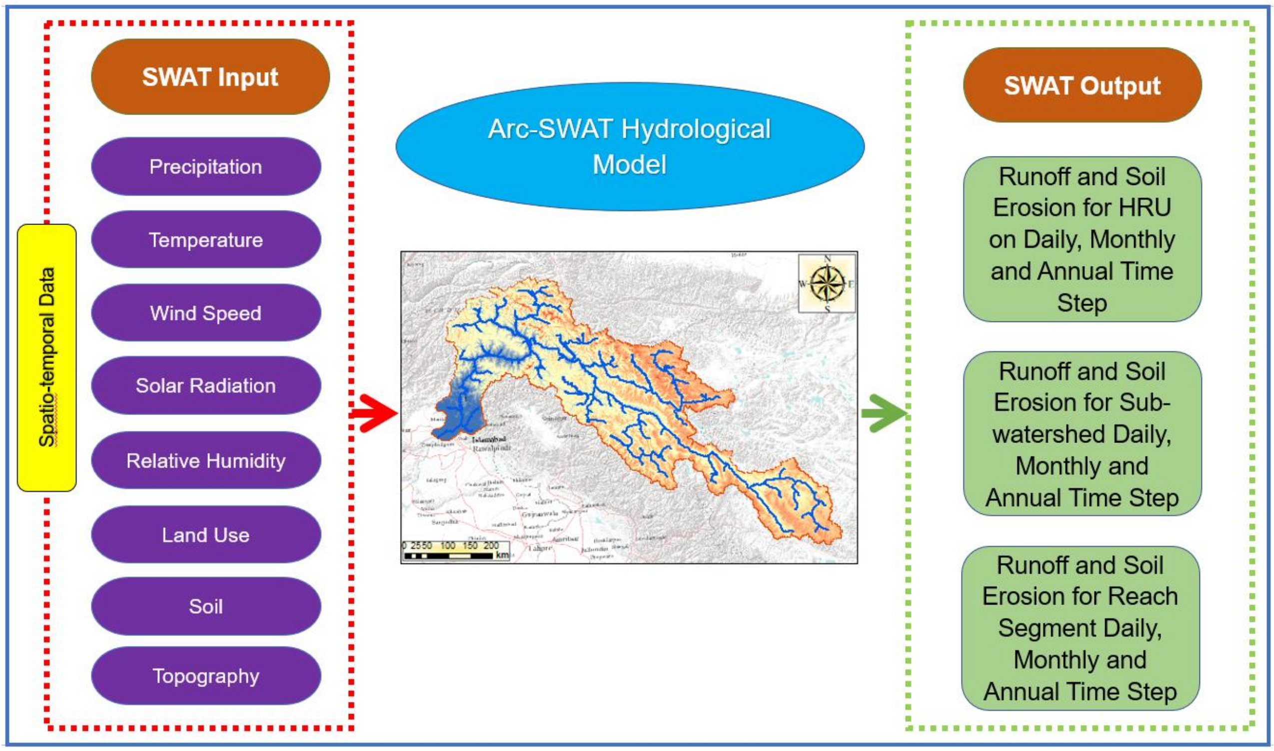


**Figure 3: General workflow of SWAT model**

### 2.2.1. Methodology Of Model Setup For The Base Line Period And Future Projections

15. The methodology for setting up the SWAT model for the baseline period and future projections involves several key steps. These include data collection and preparation, model parameterization, calibration, and validation for the baseline period. For future projections, climate change scenarios are integrated into the model, and simulations are performed using the modified inputs. This methodology enables the evaluation of hydrological changes and the estimation of future flood under different climate change scenarios. Figure 2 shows the methodological framework for SWAT modeling.

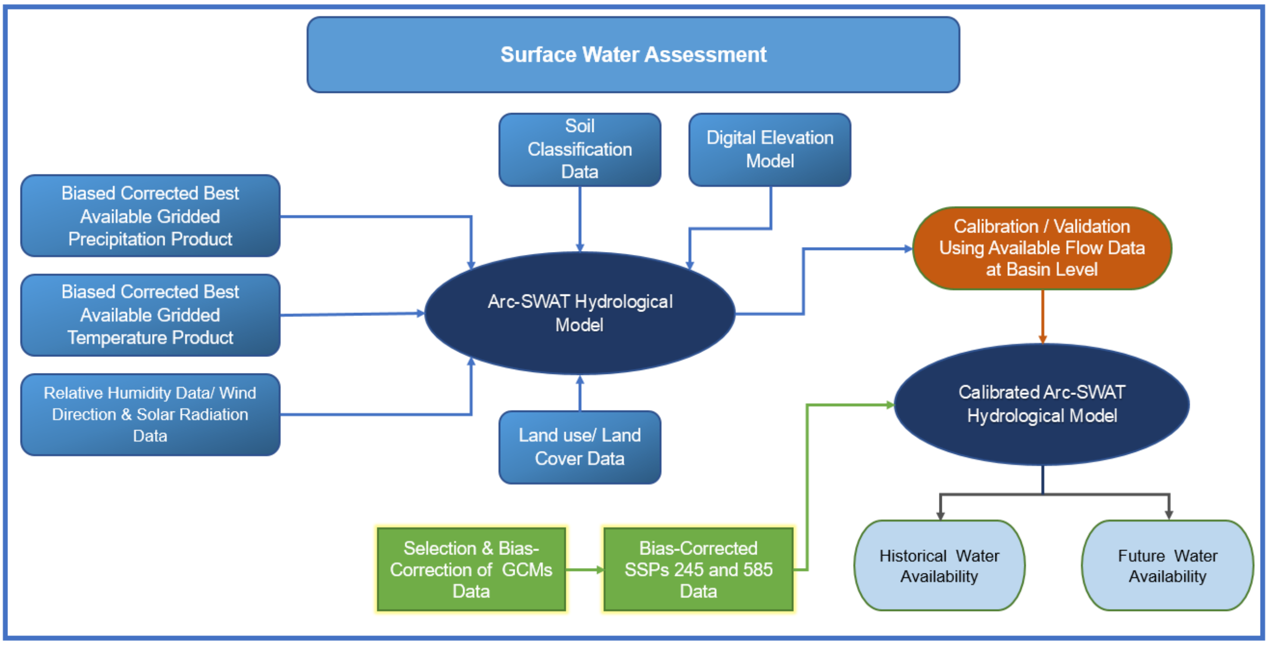


**Figure 4: Methodological framework for the Assessment of Water Availability (Baseline and Future)**

### 2.2.2. Soil And Water Assessment Tool (SWAT)

16. The Soil and Water Assessment Tool (SWAT) is a physically based, semi-distributed model designed for predicting runoff, erosion, sediment, and nutrient transport within agricultural watersheds, considering various management practices (Arnold et al., 1998). The model employs the curve number method (Service, 1972) to compute surface runoff, determining the quantity of runoff based on local soil properties, land use characteristics, and slope conditions. Additionally, SWAT utilizes the ArcGIS interface for defining hydrological features.

17. The watershed is initially divided into sub-watersheds through the Digital Elevation Model (DEM) delineation process. Subsequently, each sub-watershed is further subdivided into smaller units known as Hydrologic Response Units (HRUs). These HRUs are defined based on the unique combination of soil types, land use patterns, and slope characteristics within each unit. The SWAT model simulates discharge independently for each HRU before aggregating the results to simulate the overall basin discharge.

18. In summary, SWAT is a robust modeling tool that integrates the curve number method, ArcGIS interface, DEM delineation, and HRU-based simulation to predict runoff and associated processes within agricultural watersheds, considering the influence of diverse soil, land use, and slope conditions.

19. The hydrological components of the SWAT model are characterized by the water balance equation given below, which forms the basis of its overall hydrological representation (Arnold et al.,1998). This equation captures the interactions between precipitation, evapotranspiration, surface

runoff, and other relevant hydrological processes, providing a comprehensive framework for understanding the movement and distribution of water within the watershed.

20. The water balance equation essentially states that the soil water content at any given time is equal to the initial soil water content plus the cumulative sum of various water inputs (precipitation), outputs (surface runoff, evapotranspiration), and internal movements (percolation, return flow) over time. Each component of the water balance equation and hydrologic processes are explained in detail by Arnold (1998).

$$SWt = \mathrm{SW} + \sum_{j=0}^{t} (\mathrm{Rj} - \mathrm{Qj} - \mathrm{ETj} - \mathrm{Pj} - \mathrm{QRj})$$

SW, Soil water content
T, time
R, precipitation
Q, Surface runoff
ET, Evapotranspiration
P, Percolation
QR, Return Flow
j, Watershed

21. The water balance equation essentially states that the soil water content at any given time is equal to the initial soil water content plus the cumulative sum of various water inputs (precipitation), outputs (surface runoff, evapotranspiration), and internal movements (percolation, return flow) over time. Each component of the water balance equation and hydrologic processes are explained in detail by Arnold (1998).

22. In this study, SWAT hydrologic modeling was carried out for all the river basins of the Indus River flowing within or draining into the KP Province, using the spatiotemporal inputs to assess historical and future floods. However, owing to the unavailability of the reservoir and operational data, the transboundary dams and their reservoirs were not considered in the current study.

### 2.2.3. Data Inputs for SWAT Model

23. Hydrologic modeling involves the integration of spatial and temporal data to simulate and analyze the movement of water through a watershed or river basin. Two essential types of data inputs in this process are spatial data and temporal data. Spatial data comprise of Digital Elevation Model (DEM), Soil Classification, and Land Use Land Cover (LULC), whereas temporal data consist of the hydro-climate data. Details for each are given below.

#### 2.2.3.1. Digital Elevation Model (DEM)

24. DEM provides information about the elevation of the Earth's surface in a specific area. This data is crucial for determining the topography of the landscape, identifying the flow direction of water, and delineating watershed boundaries. DEM assists in creating the terrain model necessary for accurate representation of surface water movement. An SRTM 1 arc-second DEM is available in the public domain (http://srtm.csi.cgiar.org) and have been used in the projected coordinate system UTM-Zone-42/43 N to delineate the watershed and other catchment characteristics for each river basin.

#### 2.2.3.2. Soil Classification

25. Soil data includes information about the types and characteristics of soils within the study area. Different soil types have varying capacities for water retention and infiltration, influencing the flow and storage of water in the hydrologic system. Soil classification helps in understanding how water interacts with the ground, affecting runoff and groundwater recharge.

26. Soil data extraction was carried out for each river basin boundary from Digital Soil Map of the World (DSMW). DSMW was downloaded from Food and Agriculture Organization (FAO) soil portal in vector format and then, using the Arc-Hydro tools, the data were converted from a geographic (WGS-1984) to a projected (UTM-Zone-42/43N) coordinate system. The composition of each soil class, along with soil texture, hydrologic group, and available soil capacity, are available in the soil database.

27. The FAO soil classification system, uses a hierarchical approach to classify soils based on various criteria such as soil properties, horizons, and other characteristics. If different soil classes within the FAO system have the same soil texture, it means that while they share a similar composition of sand, silt, and clay (which determines the soil texture), they differ in other important characteristics such as soil horizons, organic matter content, drainage, or other properties considered in the classification. Thus, in relevant figures there may be same name for various classes of soil.

#### 2.2.3.3. Land Use Land Cover

28. LULC data categorizes the land surface into different classes based on its use and cover, such as urban areas, forests, agricultural land, and water bodies. This information is vital for assessing how human activities and land management practices impact the hydrological cycle. LULC data helps modelers understand the distribution of impervious surfaces, vegetation, and other land features affecting water runoff and absorption. Latest available Sentinal-2 10 m (ESRI) data were downloaded (https://livingatlas.arcgis.com/landcover) and used in this study. There are nine different LULC classes within the database.

29. The Digital Elevation Model, Soil Classification and LULC data, along with percentage slope classification for each river basin, are shown in Figure 3 to Figure 10.

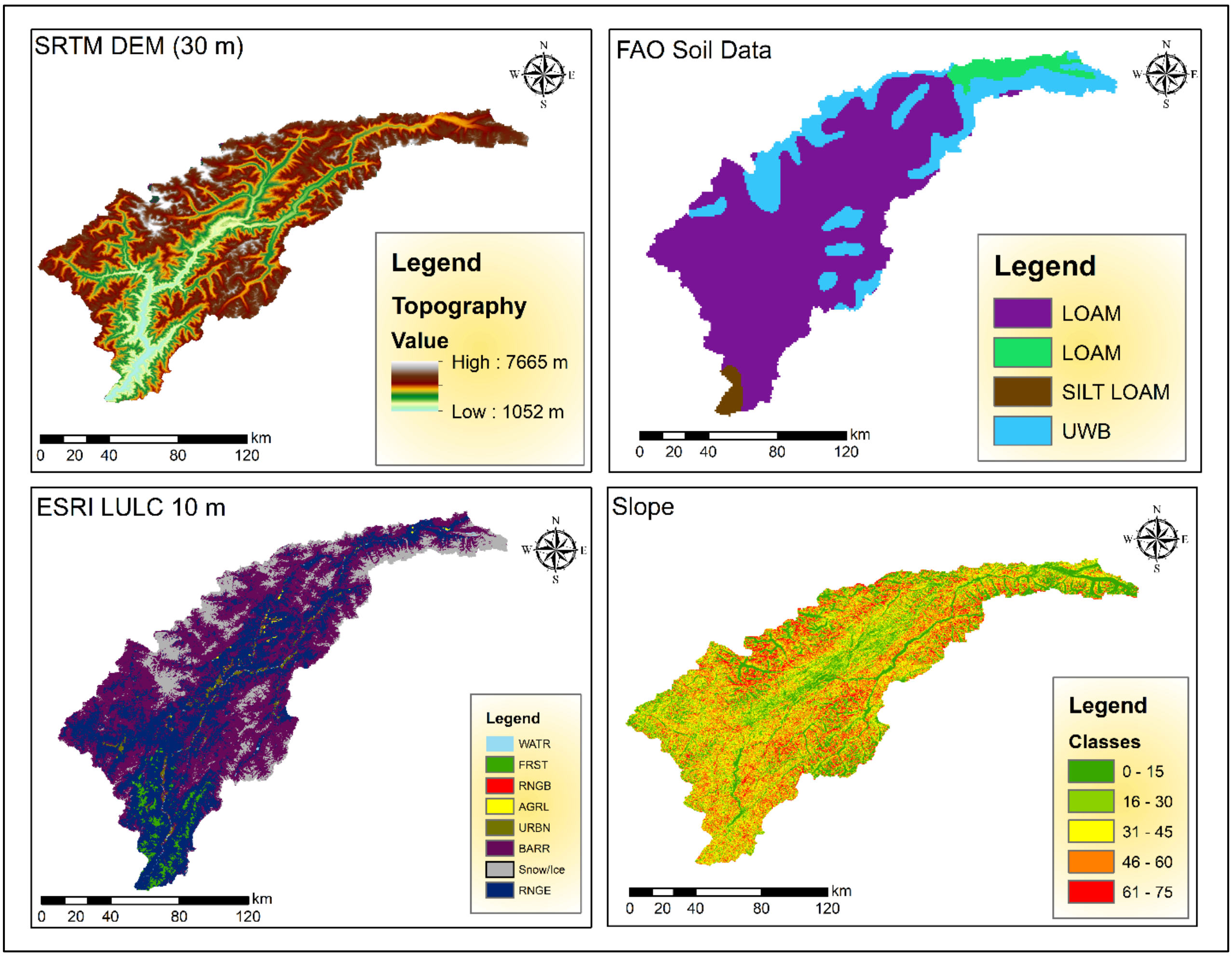


**Figure 5: SRTM Digital Elevation Model (30m x 30m), ESRI LULC and FAO Soil and Slope Classification for Chitral River basin at Chitral**

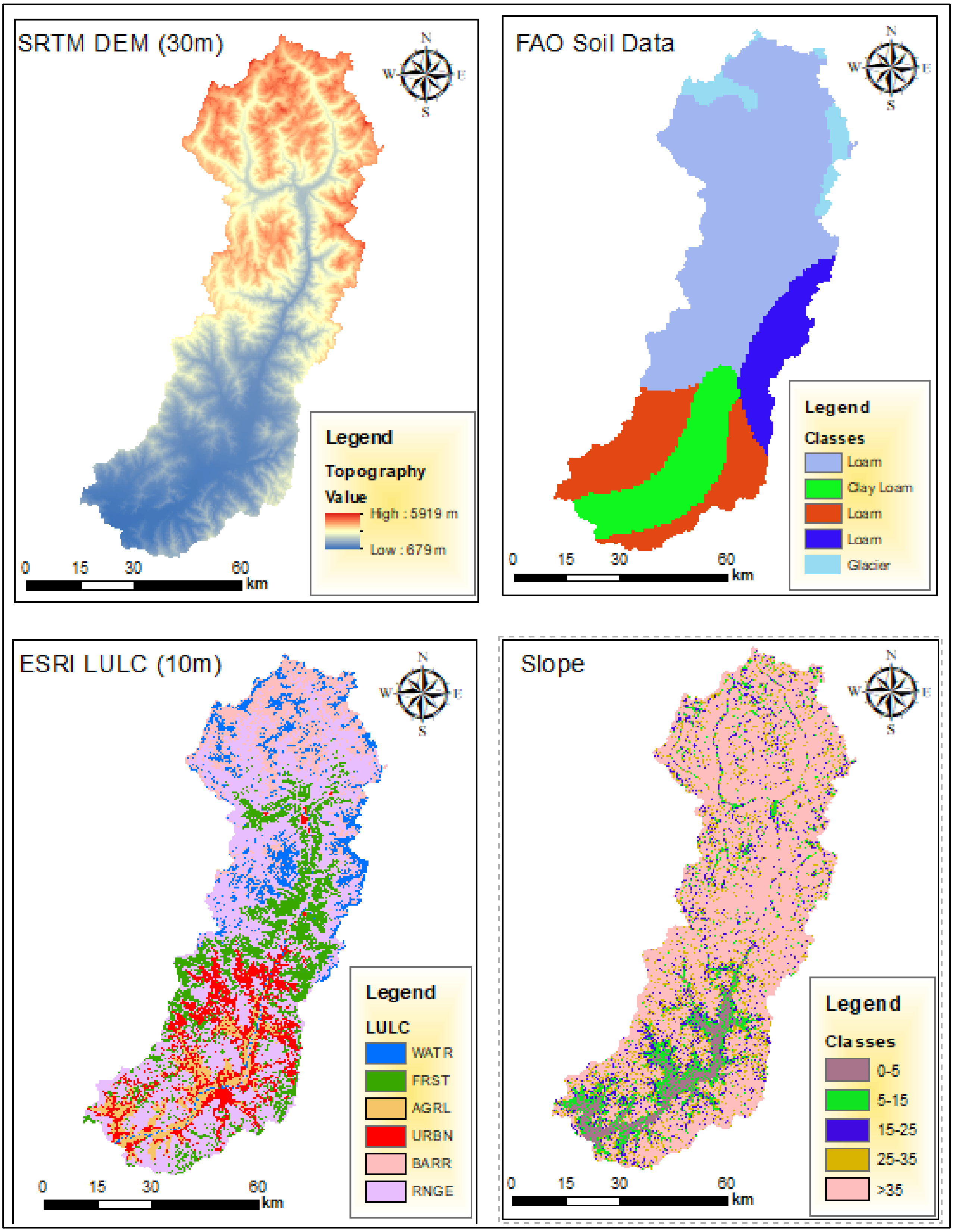


**Figure 6: SRTM Digital Elevation Model (30m x 30m), ESRI LULC and FAO Soil and Slope Classification for Swat River basin at Chakdara**

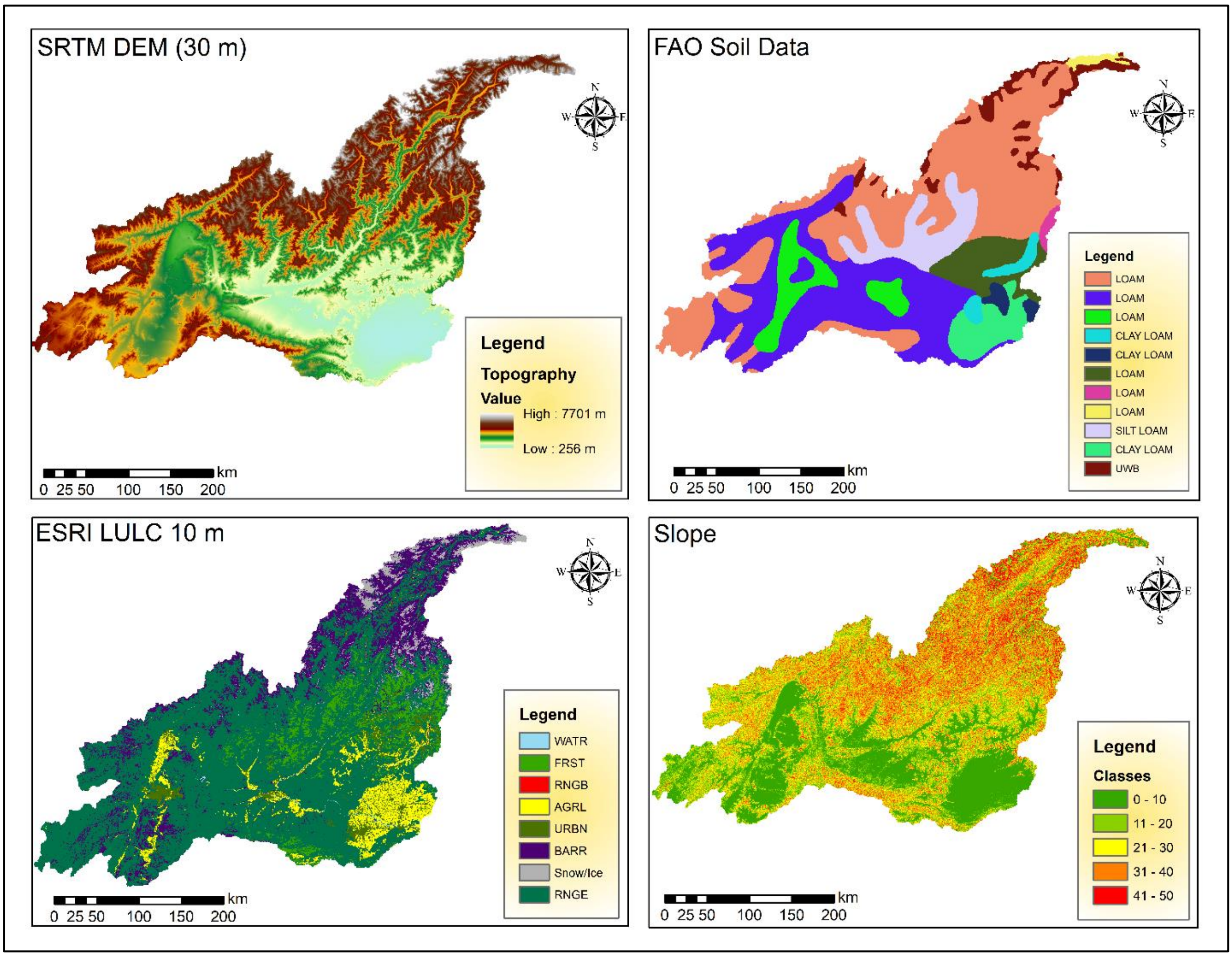


**Figure 7: SRTM Digital Elevation Model (30m x 30m), ESRI LULC and FAO Soil and Slope Classification for Kabul River basin at Nowshera**

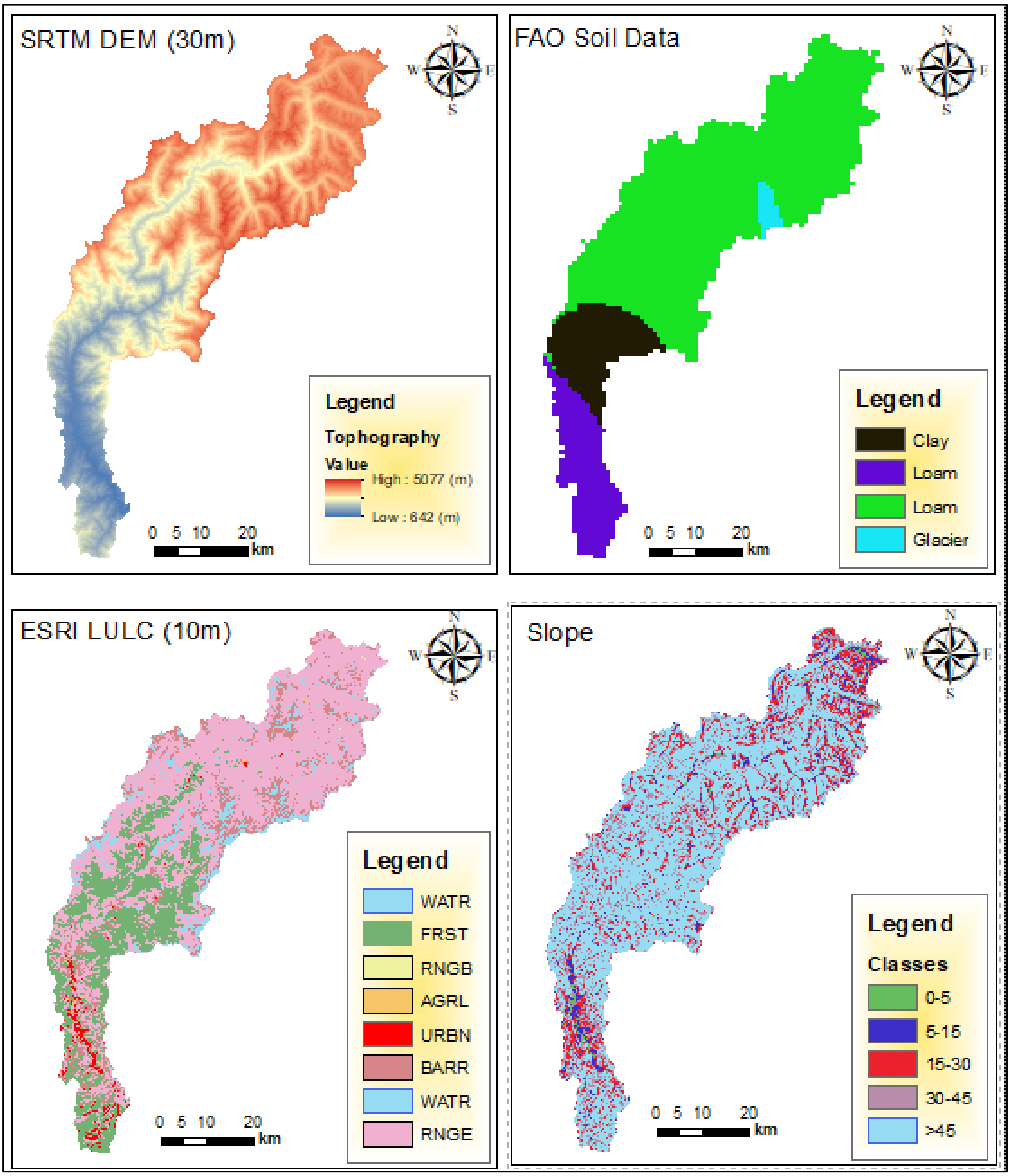


**Figure 8: SRTM Digital Elevation Model (30m x 30m), ESRI LULC and FAO Soil and Slope Classification for Kunhar River Basin**

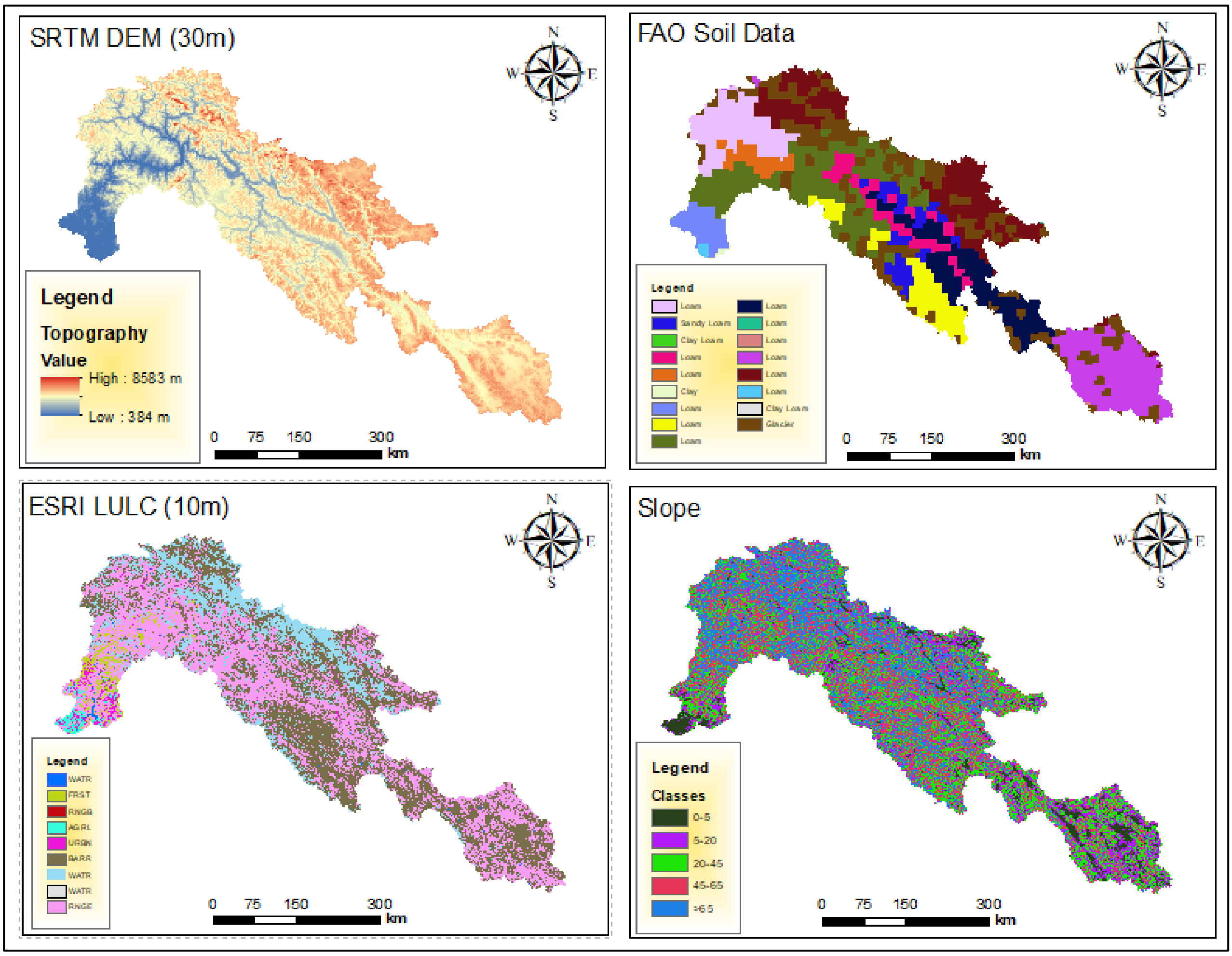


**Figure 9: SRTM Digital Elevation Model (30m x 30m), ESRI LULC and FAO Soil and Slope Classification for the Indus River basin at Tarbela**

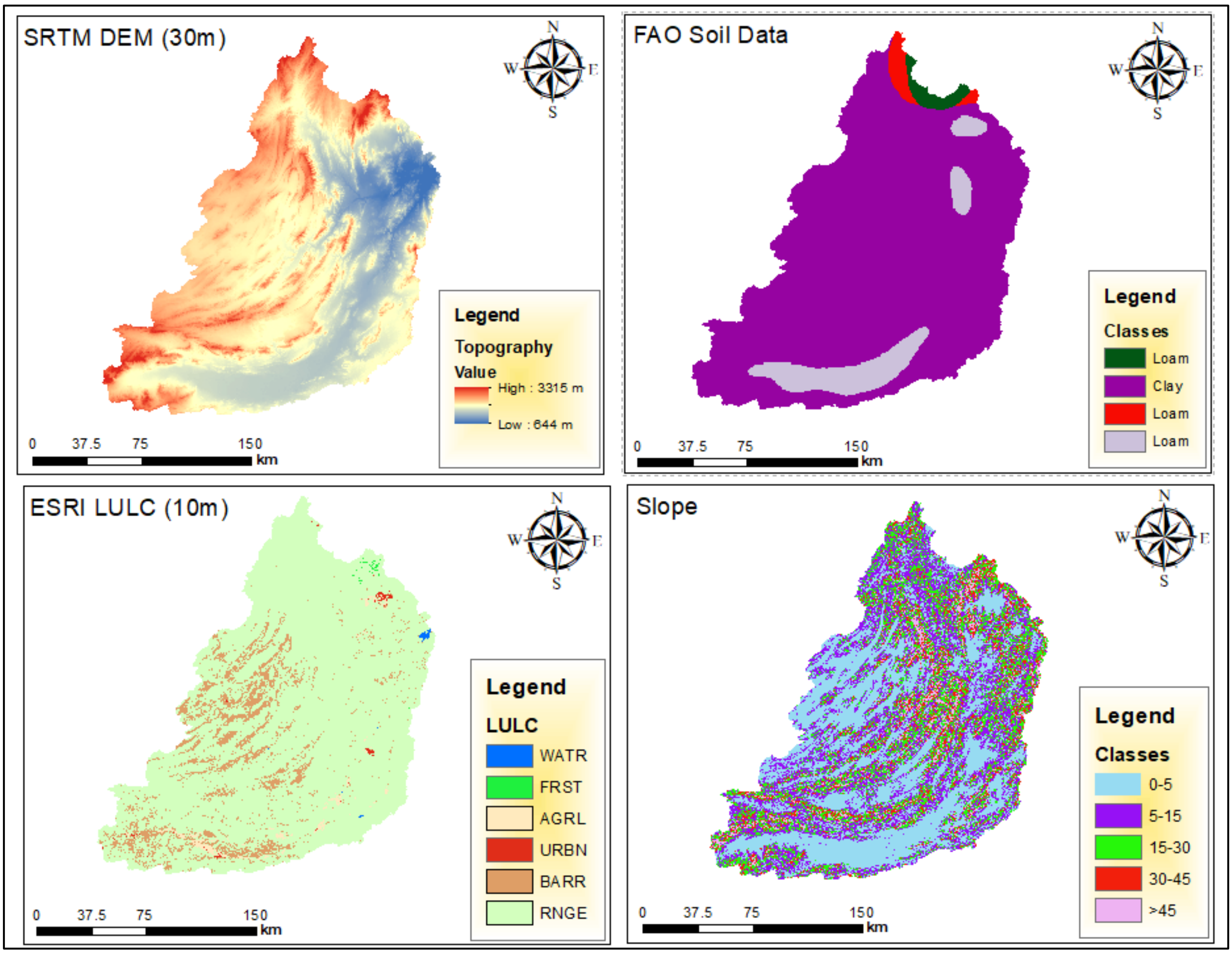


**Figure 10: SRTM Digital Elevation Model (30m x 30m), ESRI LULC and FAO Soil and Slope Classification for Gomal River basin at Khajori Kach**

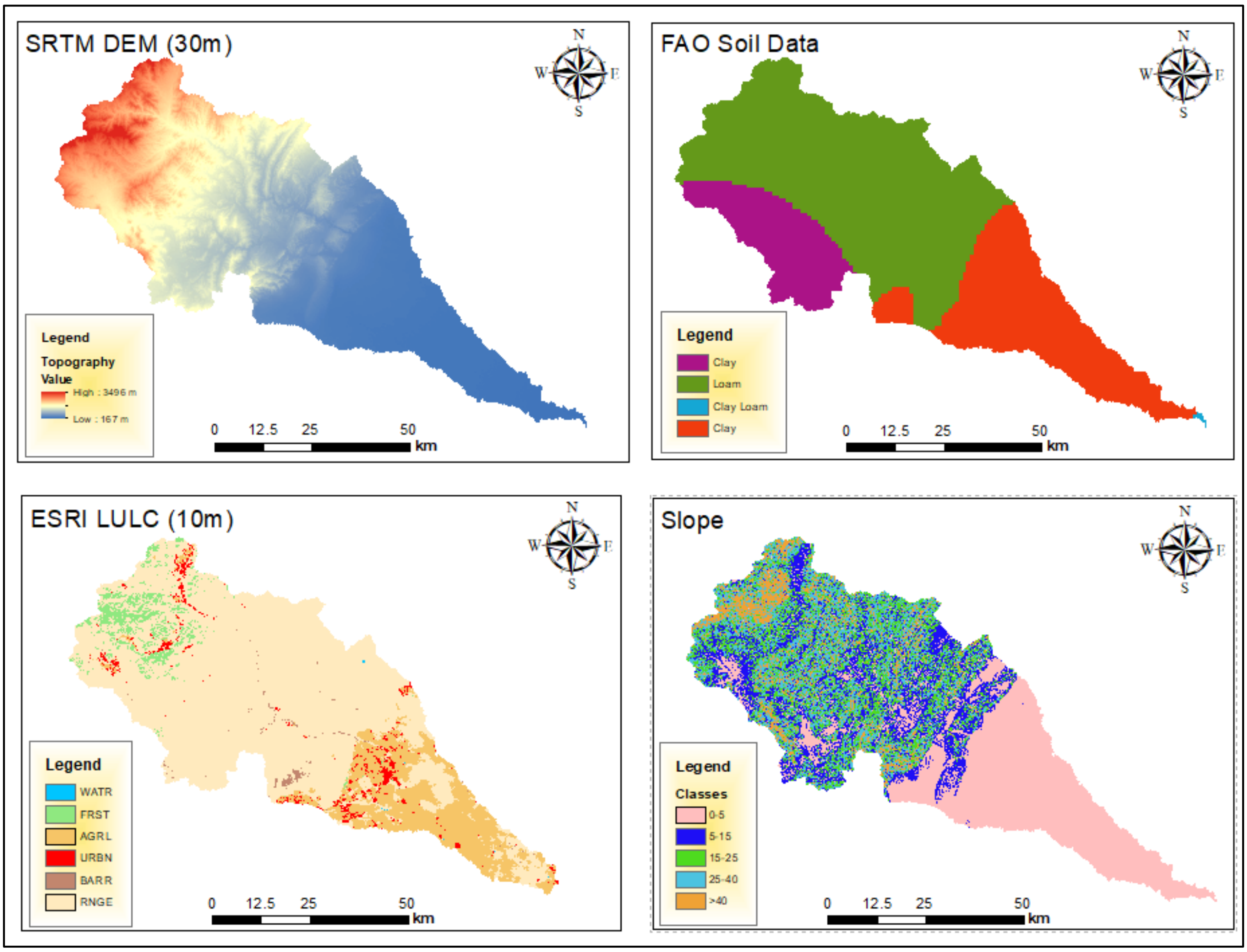


**Figure 11: SRTM Digital Elevation Model (30m x 30m), ESRI LULC and FAO Soil and Slope Classification for Tank River Basin**

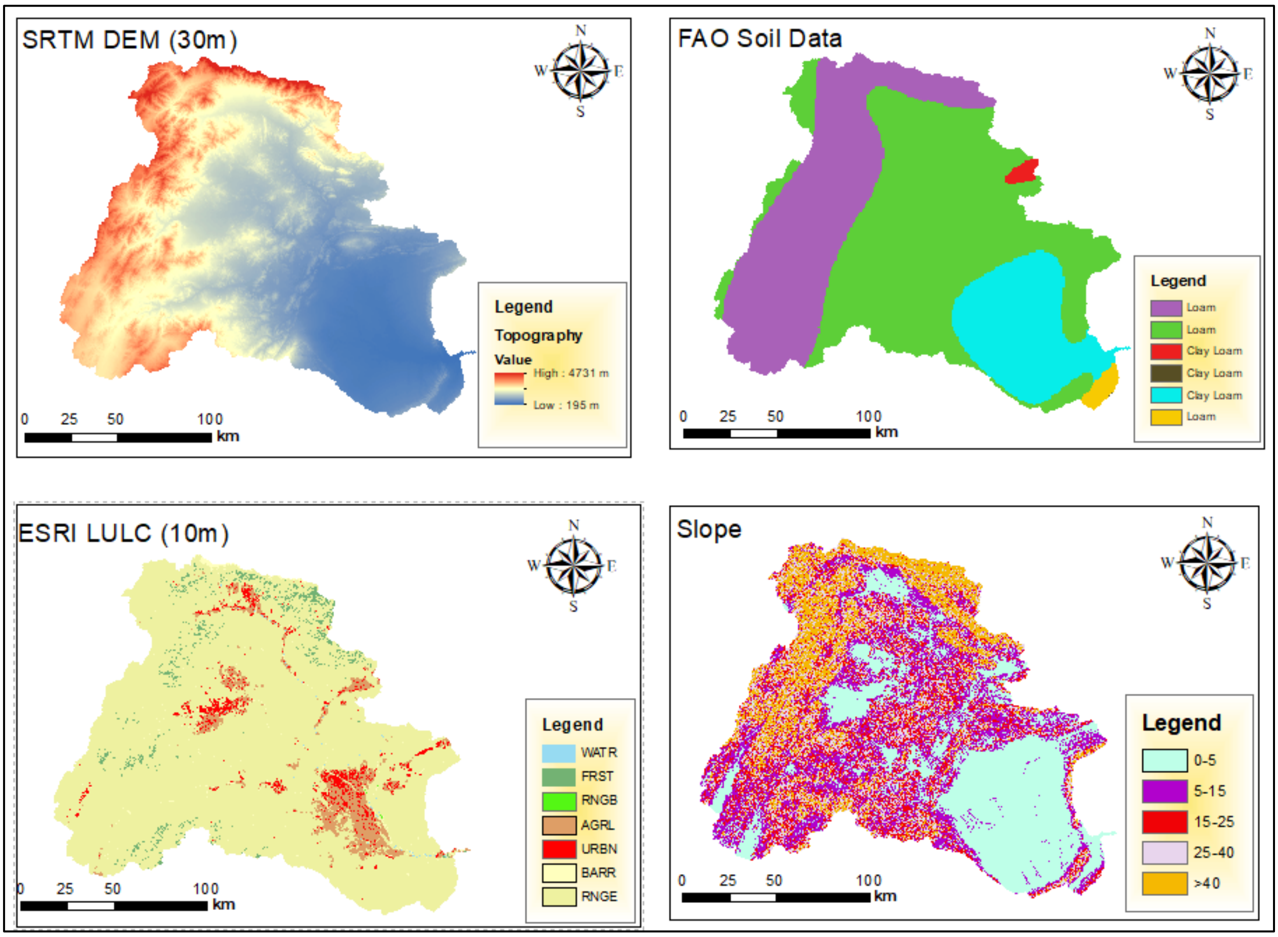


**Figure 12: SRTM Digital Elevation Model (30m x 30m), ESRI LULC and FAO Soil and Slope Classification for Kurram River basin**

#### 2.2.3.4. HISTORIC RAINFALL AND TEMPERATURE DATA

30. The available climate stations are sparse and have limited time-series data. Therefore, out of many historic gridded datasets, the best available (ERA-5 Land) has been used to carry out base hydrologic modeling. Daily precipitation, maximum temperature and minimum temperature data of ERA-5 Land product (1981-2010) have been used as an input to the model for historic model run.

### 2.2.4. FLOWS DATA

31. Flow data are available from WAPDA and Irrigation Department. These river gauges are on the main rivers. The available data records are highly inherited with inconsistencies, uncertainties, and missing values at daily time step. However, keeping in view the model input requirements and available consistent record a reference period was selected to cover all the climatic conditions and have been used for the calibration and validation of the model.

# A-3. CALIBRATION AND VALIDATION OF SWAT MODEL

## 3.1. Calibration And Validation Parameters Selection And Sensitivity Analysis

32. Calibration is an iterative process that establishes the ranges for SWAT process-based input parameters to achieve the best possible match between the modelled and observed output variables. Whereas, validation is further confirmation of the calibration process using independent data of different time period other than calibration period. The SWAT base models were calibrated and validated using the SWAT-CUP (Premium) calibration and uncertainty program after the SWAT base model was successfully developed using the Arc SWAT for ArcGIS 10.3.1 interface. The base models were run for 30 years (1981-2010) with one year as warm-up period. Selection of the time period for calibration and validation was based on the criteria of available stream flow consistent record and to cover all climatic conditions including dry, average and wet years.

33. The models were initially run in SWAT-CUP (Premium) with a neutral parameter WDPQ in order to know the model's initial behavior and check its adequacy for calibration. Most of the watersheds lies in a snow fed mountainous regions, therefore, the models were first improved by incorporating 5 different elevation bands into the models using the SWAT-CUP Premium's inbuilt component (Utility program). The weather parameters chosen for calibration, such as lapse rates and snow parameters, were then assigned physically meaningful ranges based on the original model's results.

34. Following that, global sensitivity analyses for lapse rates, snow parameters, soil parameters, shift parameters and groundwater parameters were performed, and their ranges were fixed independently after many iterative simulations run each 300 simulations. Table 1-7 provides a comprehensive analysis of the sensitivity, calibrated ranges, and best-fitted values for various physically based SWAT parameters. These parameters play a crucial role in modeling hydrological processes. The table highlights the significance of different parameters, such as temperature lapse rate, snow-related variables, runoff curve number, soil properties, and groundwater factors. The findings emphasize the importance of accurately calibrating these parameters within their respective ranges to obtain optimal model performance and improve the simulation of hydrological phenomena.

**Table 1: Parameters sensitivity and their calibrated ranges at Chitral River basin.**

| S.No. | Physically Based SWAT Parameters | | Sensitivity Analysis | | Calibrated Range | | Best Fitted |
|---|---|---|---|---|---|---|---|
| | Name | Description | t-Stat | P-Value | Minimum Value | Maximum Value | Best Simulation |
| 1 | v__TLAPS.sub | Temperature lapse rate (°C) | -24.4 | 0 | -8 | -2 | -6 |
| 2 | v__SMFMX.bsn | Maximum melt rate for snow during year (occurs on summer solstice) mm/°C Day | -18.91 | 0 | 0 | 4.5 | -1.23 |
| 3 | v__SMTMP.bsn | Snow melt base temperature (°C) | 14.97 | 0 | -4.5 | 4.5 | -2.81 |
| 4 | v__SFTMP.bsn | Snowfall temperature (°C) | -2 | 0.05 | -5 | 5 | -1.23 |
| 5 | v__TIMP.bsn | Snow pack temperature lag factor (°C) | -2.74 | 0.01 | 0 | 1 | 0.4 |
| 6 | v__SMFMN.bsn | Minimum melt rate for snow during the year (occurs on winter solstice) mm/°C Day | -1.85 | 0.07 | 0 | 4.5 | 0.3 |
| 7 | r__CN2.mgt | SCS runoff curve number | -232.53 | 0 | -0.1 | 0.1 | -0.09 |
| 8 | v__ESCO.hru | Soil evaporation compensation factor | 0.88 | 0.38 | 0.1 | 0.7 | 0.46 |
| 9 | r__SOL_BD().sol | Moist bulk density | 22.39 | 0 | -0.5 | 0.5 | -0.07 |
| 10 | r__SOL_AWC().sol | Available water capacity of the soil layer | -0.26 | 0.8 | -0.2 | 0.2 | 0.02 |
| 11 | r__SOL_K().sol | Saturated hydraulic conductivity | 0.25 | 0.81 | -0.5 | 0.5 | 0.06 |

### Table 2: Parameters sensitivity and their calibrated ranges at Swat River basin (Chakdara).

| S.No. | Physically Based SWAT Parameters | | Sensitivity Analysis | | Calibrated Range | | Best Fitted |
|---|---|---|---|---|---|---|---|
| | Name | Description | t-Stat | P-Value | Minimum Value | Maximum Value | Best Simulation |
| 1 | v__TLAPS.sub | Temperature lapse rate (°C) | -20.4 | 0 | -8 | -2 | -5.2 |
| 2 | v__SMFMX.bsn | Maximum melt rate for snow during year (occurs on summer solstice) mm/°C Day | 1.3 | 0.2 | 0 | 6 | 4.65 |
| 3 | v__SMTMP.bsn | Snow melt base temperature (°C) | 2.47 | 0.02 | -6 | 6 | 0.1 |
| 4 | v__SFTMP.bsn | Snowfall temperature (°C) | -0.95 | 0.35 | -6 | 6 | 0.5 |
| 5 | v__TIMP.bsn | Snow pack temperature lag factor (°C) | -1.02 | 0.31 | 0 | 1 | 0.01 |
| 6 | v__SMFMN.bsn | Minimum melt rate for snow during the year (occurs on winter solstice) mm/°C Day | -2.29 | 0.03 | 0 | 6 | 0.3 |
| 7 | r__CN2.mgt | SCS runoff curve number | -89.29 | 0 | -0.05 | 0.05 | -0.05 |
| 8 | v__ESCO.hru | Soil evaporation compensation factor | -3.42 | 0 | 0.1 | 0.7 | 0.34 |
| 9 | r__SOL_BD().sol | Moist bulk density | -2.12 | 0.04 | -0.6 | 0.6 | 0.47 |
| 10 | r__SOL_AWC().sol | Available water capacity of the soil layer | 0.09 | 0.93 | -0.5 | 0.5 | -0.45 |
| 11 | r__SOL_K().sol | Saturated hydraulic conductivity | -2.34 | 0.02 | -0.8 | 0.8 | -0.68 |

### Table 3: Parameters sensitivity and their calibrated ranges at Kabul River basin (Nowshera).

| S.No. | Physically Based SWAT Parameters | | Sensitivity Analysis | | Calibrated Range | | Best Fitted |
|---|---|---|---|---|---|---|---|
| | Name | Description | t-Stat | P-Value | Minimum Value | Maximum Value | Best Simulation |
| 1 | v__TLAPS.sub | Temperature lapse rate (°C) | -52.4 | 0 | -8 | -2 | -4 |
| 2 | v__SMFMX.bsn | Maximum melt rate for snow during year (occurs on summer solstice) mm/°C Day | -11.63 | 0 | 0 | 5 | 0.42 |
| 3 | v__SMTMP.bsn | Snow melt base temperature (°C) | 6.2 | 0 | -5 | 5 | 1.95 |
| 4 | v__SFTMP.bsn | Snowfall temperature (°C) | -10.12 | 0 | -5 | 5 | -0.95 |
| 5 | v__TIMP.bsn | Snow pack temperature lag factor (°C) | -1.3 | 0.2 | 0 | 1 | 0.47 |
| 6 | v__SMFMN.bsn | Minimum melt rate for snow during the year (occurs on winter solstice) mm/°C Day | -1.26 | 0.21 | 0 | 5 | 0.38 |
| 7 | r__CN2.mgt | SCS runoff curve number | -45.66 | 0 | -0.05 | 0.1 | -0.04 |
| 8 | v__ESCO.hru | Soil evaporation compensation factor | -9.81 | 0 | 0.1 | 0.7 | 0.18 |
| 9 | r__HRU_SLP.hru | Average slope steepness | 14.53 | 0 | -0.5 | 0.5 | 0.36 |
| 10 | r__OV_N.hru | Manning's "n" value for overland flow. | 3.59 | 0 | -0.5 | 0.5 | 0.48 |
| 11 | r__SLSUBBSN.hru | Average slope length. | -7.39 | 0 | -0.5 | 0.5 | 0.17 |
| 12 | r__SOL_BD().sol | Moist bulk density | -0.24 | 0.81 | -1.16 | 0.02 | -1.13 |
| 13 | r__SOL_AWC().sol | Available water capacity of the soil layer | 58.57 | 0 | -0.01 | 0.96 | 0.93 |
| 14 | r__SOL_K().sol | Saturated hydraulic conductivity | 7.51 | 0 | -0.29 | 0.75 | 0.38 |
| 15 | v__GWQMN.gw | Threshold depth of water in the shallow aquifer required for return flow to occur (mm). | 27.92 | 0 | 0 | 2000 | 1950 |
| 16 | v__REVAPMN.gw | Threshold depth of water in the shallow aquifer for "revap" to occur (mm). | -0.26 | 0.79 | 0 | 800 | 612 |
| 17 | v__GW_REVAP.gw | Groundwater "revap" coefficient. | 10.51 | 0 | 0.02 | 0.1 | 0.1 |

**Table 4: Parameters sensitivity and their calibrated ranges at Jhelum River basin (Mangla).**

| S.No. | Physically Based SWAT Parameters | | Sensitivity Analysis | | Calibrated Range | | Best Fitted |
|---|---|---|---|---|---|---|---|
| | Name | Description | t-Stat | P-Value | Minimum Value | Maximum Value | Best Simulation |
| 1 | v__TLAPS.sub | Temperature lapse rate (°C) | -44.4 | 0 | -8 | -2 | -4 |
| 2 | v__SMFMX.bsn | Maximum melt rate for snow during year (occurs on summer solstice) mm/°C Day | 8.04 | 0 | 0 | 6 | 3.51 |
| 3 | v__SMTMP.bsn | Snow melt base temperature (°C) | -4.25 | 0 | -6 | 6 | -4.02 |
| 4 | v__SFTMP.bsn | Snowfall temperature (°C) | -8.92 | 0 | -6 | 6 | -0.9 |
| 5 | v__TIMP.bsn | Snow pack temperature lag factor (°C) | 0.22 | 0.82 | 0 | 1 | 0.02 |
| 6 | v__SMFMN.bsn | Minimum melt rate for snow during the year (occurs on winter solstice) mm/°C Day | -0.69 | 0.49 | 0 | 6 | 2.67 |
| 7 | r__HRU_SLP.hru | Average slope steepness | -30.17 | 0 | -0.97 | 0 | -0.96 |
| 8 | r__OV_N.hru | Manning's "n" value for overland flow. | 6.47 | 0 | -0.2 | 0.39 | 0.15 |
| 9 | r__SLSUBBSN.hru | Average slope length. | 15.8 | 0 | -0.03 | 0.92 | 0.87 |
| 10 | r__SOL_BD().sol | Moist bulk density | 1.01 | 0.32 | -0.6 | 0.6 | -0.5 |
| 11 | r__SOL_AWC().sol | Available water capacity of the soil layer | 18.95 | 0 | -0.5 | 0.5 | 0.47 |
| 12 | r__SOL_K().sol | Saturated hydraulic conductivity | 8.73 | 0 | -0.8 | 0.8 | 0.23 |
| 13 | v__GWQMN.gw | Threshold depth of water in the shallow aquifer required for return flow to occur (mm). | -10.53 | 0 | 1312.42 | 3797.57 | 2666.83 |
| 14 | v__REVAPMN.gw | Threshold depth of water in the shallow aquifer for "revap" to occur (mm). | 0.22 | 0.83 | 188.27 | 365.72 | 249.49 |
| 15 | v__GW_REVAP.gw | Groundwater "revap" coefficient. | 4.66 | 0 | 0.07 | 0.13 | 0.13 |

**Table 5: Parameters sensitivity and their calibrated ranges at the Indus River basin (Tarbela).**

| S.No. | Physically Based SWAT Parameters | | Sensitivity Analysis | | Calibrated Range | | Best Fitted |
|---|---|---|---|---|---|---|---|
| | Name | Description | t-Stat | P-Value | Minimum Value | Maximum Value | Best Simulation |
| 1 | v__TLAPS.sub | Temperature lapse rate (°C) | -46.4 | 0 | -8 | -2 | -4.5 |
| 2 | v__SMFMX.bsn | Maximum melt rate for snow during year (occurs on summer solstice) mm/°C Day | 8.04 | 0 | 0 | 5 | 1.72 |
| 3 | v__SMTMP.bsn | Snow melt base temperature (°C) | 5.91 | 0 | -5 | 5 | 2.69 |
| 4 | v__SFTMP.bsn | Snowfall temperature (°C) | -3.7 | 0 | -6 | 5 | -5.11 |
| 5 | v__TIMP.bsn | Snow pack temperature lag factor (°C) | -2.49 | 0.01 | 0 | 1 | 0.93 |
| 6 | v__SMFMN.bsn | Minimum melt rate for snow during the year (occurs on winter solstice) mm/°C Day | -6.12 | 0 | 0 | 5 | 0.84 |
| 7 | r__SOL_BD().sol | Moist bulk density | 1.68 | 0.11 | -0.6 | 0.6 | -0.5 |
| 8 | r__SOL_AWC().sol | Available water capacity of the soil layer | 0.47 | 0.64 | -0.5 | 0.5 | 0.47 |
| 9 | r__SOL_K().sol | Saturated hydraulic conductivity | 1.19 | 0.25 | -0.8 | 0.8 | 0.23 |
| 10 | r__CN2.mgt | SCS runoff curve number | -23.08 | 0 | -0.05 | 0.1 | -0.04 |
| 11 | v__ESCO.hru | Soil evaporation compensation factor | 1.82 | 0.08 | 0.1 | 0.7 | 0.18 |

**Table 6: Parameters sensitivity and their calibrated ranges at Gomal River basin (Khajori Kach).**

| S.No. | Physically Based SWAT Parameters | | Sensitivity Analysis | | Calibrated Range | | Best Fitted |
|---|---|---|---|---|---|---|---|
| | Name | Description | t-Stat | P-Value | Minimum Value | Maximum Value | Best Simulation |
| 1 | v__SMFMX.bsn | Maximum melt rate for snow during year (occurs on summer solstice) mm/°C Day | -1.91 | 0.06 | 0 | 10 | 0.83 |
| 2 | v__SMTMP.bsn | Snow melt base temperature (°C) | 6.59 | 0 | -10 | 10 | 4.65 |
| 3 | v__SFTMP.bsn | Snowfall temperature (°C) | 1.79 | 0.08 | -10 | 10 | 7.75 |
| 4 | v__TIMP.bsn | Snow pack temperature lag factor (°C) | 0.92 | 0.36 | 0 | 1 | 0.83 |
| 5 | v__SMFMN.bsn | Minimum melt rate for snow during the year (occurs on winter solstice) mm/°C Day | -4.31 | 0 | 0 | 10 | 4.43 |
| 6 | r__SOL_BD().sol | Moist bulk density | 12.87 | 0 | -0.24 | 0.49 | 0.1 |
| 7 | r__SOL_AWC().sol | Available water capacity of the soil layer | 12.46 | 0 | -0.52 | 0.16 | -0.01 |
| 8 | r__SOL_K().sol | Saturated hydraulic conductivity | 4.03 | 0 | -0.07 | 1.4 | 0.76 |
| 9 | r__SLSUBBSN.hru | Average slope length | 13.72 | 0 | -0.5 | 0.5 | 0.39 |
| 10 | r__HRU_SLP.hru | Average slope steepness | 4.16 | 0 | -0.5 | 0.5 | 0.48 |
| 11 | r__OV_N.hru | Manning's "n" value for overland flow | 3.33 | 0 | -0.5 | 0.5 | 0.49 |
| 12 | v__GWQMN.gw | Threshold depth of water in the shallow aquifer required for return flow to occur (mm) | 14.96 | 0 | 0 | 5000 | 1208.33 |
| 13 | v__REVAPMN.gw | Threshold depth of water in the shallow aquifer for "revap" to occur (mm) | 0.92 | 0.36 | 0 | 1000 | 451.67 |
| 14 | v__GW_REVAP.gw | Groundwater "revap" coefficient | 0.88 | 0.38 | 0.02 | 0.1 | 0.02 |

**Table 7: Parameters sensitivity and their calibrated ranges at Kurraml River basin (Thal).**

| S.No. | Physically Based SWAT Parameters | | Sensitivity Analysis | | Calibrated Range | | Best Fitted |
|---|---|---|---|---|---|---|---|
| | Name | Description | t-Stat | P-Value | Minimum Value | Maximum Value | Best Simulation |
| 1 | v__SMFMX.bsn | Maximum melt rate for snow during year (occurs on summer solstice) mm/°C Day | -3.2 | 0.04 | 0 | 10 | 0.73 |
| 2 | v__SMTMP.bsn | Snow melt base temperature (°C) | 8 | 0 | -10 | 10 | 4.1 |
| 3 | v__SFTMP.bsn | Snowfall temperature (°C) | 1.79 | 0.05 | -10 | 10 | 5.65 |
| 4 | v__TIMP.bsn | Snow pack temperature lag factor (°C) | 0.78 | 0.35 | 0 | 1 | 0.72 |
| 5 | v__SMFMN.bsn | Minimum melt rate for snow during the year (occurs on winter solstice) mm/°C Day | -8.31 | 0 | 0 | 10 | 4.5 |
| 6 | r__SOL_BD().sol | Moist bulk density | 22 | 0 | -0.25 | 0.5 | 0.1 |
| 7 | r__SOL_AWC().sol | Available water capacity of the soil layer | 34 | 0 | -0.5 | 0.2 | -0.01 |
| 8 | r__SOL_K().sol | Saturated hydraulic conductivity | 6 | 0 | -0.1 | 1.5 | 0.71 |
| 9 | r__SLSUBBSN.hru | Average slope length | 21.34 | 0 | -0.5 | 0.5 | 0.39 |
| 10 | r__HRU_SLP.hru | Average slope steepness | 6.54 | 0 | -0.5 | 0.5 | 0.48 |
| 11 | r__OV_N.hru | Manning's "n" value for overland flow | 9.54 | 0 | -0.5 | 0.5 | 0.49 |
| 12 | v__GWQMN.gw | Threshold depth of water in the shallow aquifer required for return flow to occur (mm) | 25 | 0 | 0 | 4000 | 1260 |
| 13 | v__REVAPMN.gw | Threshold depth of water in the shallow aquifer for "revap" to occur (mm) | 0.82 | 0.36 | 0 | 900 | 463.67 |
| 14 | v__GW_REVAP.gw | Groundwater "revap" coefficient | 0.89 | 0.38 | 0.02 | 0.1 | 0.02 |

## 3.2. Criteria for Assessment of Calibration and Validation

35. Six performance evaluation indicators were used to check the performance of SWAT to project stream flow, namely: (a) the p-factor (b) the r-factor (c) the coefficient of determination ($R^2$), (d) Nash-Sutcliffe efficiency (NSE), and (e) Kling Gupta Efficiency (KGE) and (f) Percent Bias (PBIAS). The P-factor, which ranges from 0 to 1, represents model accuracy. In other words, it is the percentage of measured data that is within the 95PPU band. The model error is defined as (1 - P-factor).

36. The r-factor represents model uncertainty, dividing the average thickness of the 95PPU by the standard deviation of the measured data the value we get is the r-factor. It can range from 0 to a fairly large number. A value of around 1 for the R-factor is desirable because it equals the standard deviation of the observation. These two factors completely describe the calibrated model's performance. The closer the P-factor and r-factor to 1, the better the calibrated model depicts the measurements (Abaspour, 2021). Based on latest available literature, one should bracket approximately 70% of the measured data for river discharge in the 95PPU band, ideally (P-factor ≥ 0.7, r-factor ≤ 1.5) (Abaspour, 2022). $R^2$ expresses the degree of collinearity between simulated and measured data, or the proportion of variance. $R^2$ values range from 0 to 1, with higher values indicating less error variance, and values greater than 0.5 are typically considered acceptable. Whereas NSE shows how well the observed plot matches the simulated plot. NSE values range from 0 to 1, with higher values indicating less error and values greater than 0.5 considered acceptable.

37. The Kling Gupta Efficiency (KGE) assesses correlation, variability error and bias error. It has a range, 0-1, Ideal model performance should have a KGE-score of 1. The criteria for KGE rating are given below as: (1) satisfactory performance when (0.4 ≥ KGE < 0.6); (2) good performance when (KGE ≥ 0.6); very good performance when (KGE ≥ 0.7); and excellent performance when (KGE ≥ 0.8).

38. The percentage bias (PBIAS) measures the simulated data's average tendency to be larger or smaller than their observed counterparts. PBIAS has an optimal value of 0.0, however, ± 25% is satisfactory and acceptable. Positive values indicate underestimation bias in the model, while negative values indicate overestimation bias in the model.

39. The results of all the statistical performance indicators both for calibration and validation were compared to the reported acceptable performance ratings from the literature and the model's performance was assessed and ranked accordingly.

**Table 8: Reported performance ratings for different statistical performance indicators.**

| Performance Rating | $R^2$ | NSE | PBIAS (%)<br>Streamflow |
|---|---|---|---|
| Very good | 0.75 < $R^2$ ≤ 1.00 | 0.75 < NSE ≤ 1.00 | PBIAS < ±10 |
| Good | 0.65 < $R^2$ ≤ 0.75 | 0.65 < NSE ≤ 0.75 | ±10 PBIAS < ±15 |
| Satisfactory | 0.50 < $R^2$ ≤ 0.65 | 0.50 < NSE ≤ 0.65 | ±15 ≤ PBIAS < ±25 |
| Unsatisfactory | $R^2$ < 0.50 | NSE < 0.50 | PBIAS ≥ ±25 |

## 3.3. Chitral River Basin Calibration And Validation Results

40. The Chitral River is the main tributary of the Kabul River, which eventually flows into the Indus near Attock. The river gets the majority of its water from melting snow and glaciers in the

Hindukush Mountain range, where winter precipitation is the main source of replenishment. Approximately 14.5% of the basin area occupies snow/glacier cover, which is the key source of water supply to the Chitral River and its tributaries. Chitral Valley's climate is characterized as cold and dry. The summer monsoon has little influence over the Chitral Basin, while the majority of rainfall comes during winter and spring, primarily as snow, and is generated from the Mediterranean's westerly winter disturbance. The average annual precipitation observed at Chitral from 1992 to 2017 is 465 mm.

41. The SWAT base model for the Chitral River basin was developed and run using ERA-5 Land data for a historic period of 30 years (1981-2010). The model was calibrated and validated using the SWAT-CUP Premium SWAT Parameter Estimator (SPE) program, using stream flow data from the Chitral River gauging station. Stream flow data for the Chitral River is available for a historic period of 25 years (1991-2015) at a daily time step. However, due to data inconsistencies, missing values, and uncertainties, specific time periods were selected for calibration and validation.

42. For the calibration period, a time span of 10 years (1991-2000) was chosen, while a period of 10 years (2001-2010) was selected for validation. These time periods fulfill criteria such as consistent data availability, representation of different climate conditions, and nearly similar statistical characteristics. The SWAT base model for the Chitral River basin underwent several improvements and calibration steps. Initially, a neutral parameter setting was used to understand the model's initial behavior. Due to the region's significant altitudinal variation and snow-fed nature, five elevation bands were introduced using SWAT-CUP Premium.

43. To account for the influence of precipitation, temperature, and snow parameters, lapse rates for weather variables were fixed, followed by independent calibration of snow parameters. Global sensitivity analyses were performed for each set of parameters, and their ranges were determined through iterative simulations. This iterative process was repeated until satisfactory model performance statistics were achieved for both calibration and validation. Figure 11 depicts a graphical comparison of the modeled and measured flows at Chitral, along with their corresponding statistics.

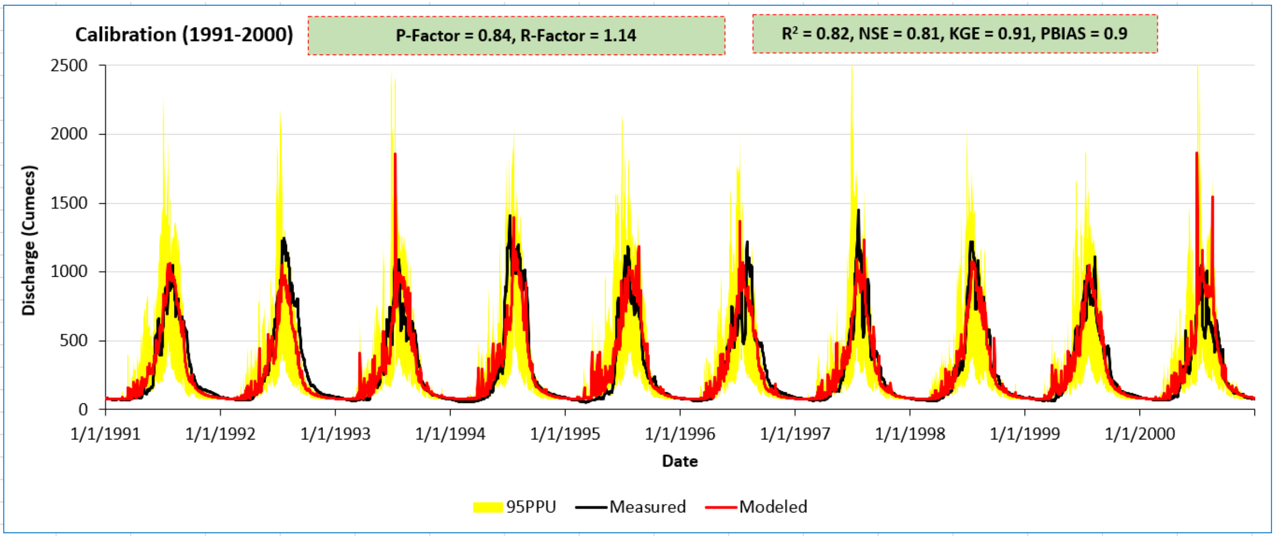

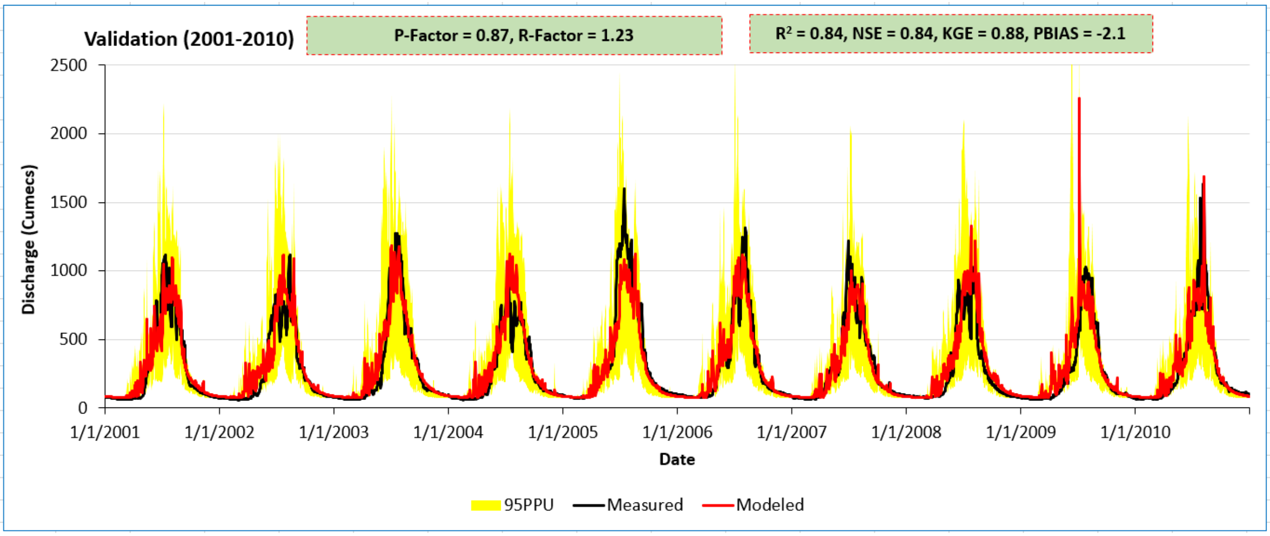


**Figure 13: Graphical representation of calibration and validation result of Chitral River at Chitral along with all the statistical performance indicators**

**Table 9: Calibration summary statistics and remarks for Chitral River Basin at Chitral**

| S.No. | Name | Guage Station Location | Available Record | Calibration Period | Calibration Summary Statistics | | | | | | Remarks (Based on 5 indicators) | Remarks (Based on KGE) |
|---|---|---|---|---|---|---|---|---|---|---|---|---|
| | | | | | p-factor | r-factor | $R^2$ | NS | KGE | PBIAS | | |
| 1a | Chitral River Basin | Chitral | 1991-2015 | 1991-2000 | 0.84 | 1.14 | 0.82 | 0.81 | 0.91 | 0.9 | Very Good | Excellent |

**Table 10: Validation summary statistics and remarks for Chitral River Basin at Chitral**

| S.No. | Name | Guage Station Location | Available Record | Calibration Period | Validation Summary Statistics | | | | | | Remarks (Based on 5 indicators) | Remarks (Based on KGE) |
|---|---|---|---|---|---|---|---|---|---|---|---|---|
| | | | | | p-factor | r-factor | $R^2$ | NS | KGE | PBIAS | | |
| 1b | Chitral River Basin | Chitral | 1991-2015 | 2001-2010 | 0.87 | 1.23 | 0.84 | 0.84 | 0.88 | -2.1 | Very Good | Excellent |

44. For the Chitral River Basin, the model performance during the calibration period (1991-2000) indicates a high level of agreement between observed and simulated values. The p-factor of 0.84 suggests that 84% of the observed values are captured within the model uncertainty band, and the model exhibits a slight overestimation with an r-factor of 1.14. The $R^2$ value of 0.82 indicates that 82% of the observed variability is explained by the model, and the NS value of 0.81 reflects a strong performance in capturing flow variability. Despite a minor negative bias, as indicated by the PBIAS of 0.91%, the KGE value stands at 0.90, emphasizing the excellent overall model performance in projecting the key aspects of flow behavior in the Chitral River Basin during the calibration period.

45. Moving to the validation period (2001-2010), the model for the Chitral River Basin continues to demonstrate a very good level of agreement between observed and simulated values. The p-factor of 0.87 signifies an extended capture of 87% of observed values within the uncertainty band, and the model exhibits a slightly higher overestimation with an r-factor of 1.23. The $R^2$ value of 0.84 indicates that 84% of the observed variability is explained, and the NS value of 0.84 reflects a strong ability to capture flow variability. Despite a PBIAS of -2.1%, the KGE value remains high at 0.88, highlighting an excellent overall model performance in capturing key aspects of flow behavior in the Chitral River Basin during the validation period. In conclusion,

the model consistently demonstrates a very good to excellent performance, making it a reliable tool for water resource management and decision-making in the Chitral River Basin.

## 3.4. Swat River Basin Calibration And Validation Results

46. The Swat River is a right bank branch of the Indus River that originates in the Swat-Kohistan high mountains in northwestern Pakistan. On a north-to-south slope, glaciers, snow, and rain feed the Swat River. The basin's climate can be classified as sub-humid, humid, or semi-arid. The region is part of the monsoon and western disturbance-influenced strip, having a short warm summer and a long chilly winter. June is the warmest month of the year, with average maximum and lowest temperatures of 33 and 16 °C, respectively. January is the coldest month, with regular snowfalls and average high and low temperatures of 11 and -2°C, respectively. The average annual rainfall varies between 700 mm and 1630 mm, with summer precipitation at 246.4 mm and winter precipitation reaching 815.3 mm. Swat River plays an important role in the economy of the valley, as it provides water for drinking and agriculture, and it recharges to the underlying groundwater reserve. Often floods hit the area due to outburst of glaciers at the top and riverine flash floods — Therefore. Precise and accurate hydro-climate study of the Swat River basin is aimed to understand its hydrology, provide support in designing and implementing the interventions which could safeguard the area from the climate risks particularly, floods.

47. To carry out detailed hydrologic assessment of the Swat River basin, the SWAT hydrologic base model was developed and run using ERA-5 Land data for a historic period of 30 years (1981-2010). The model was calibrated and validated using the SWAT-CUP Premium SWAT Parameter Estimator (SPE) program, using stream flow data of the Chakdara gauging station. Stream flow data for the Swat River is available for a historic period of 31 years (1988-2018) at a daily time step. However, due to data inconsistencies, missing values, and uncertainties, specific time periods were selected for calibration and validation.

48. For the calibration period, a time span of 10 years (1991-2000) was chosen, while a period of 9 years (2001-2009) was selected for validation. These time periods fulfill criteria such as consistent data availability, representation of different climate conditions, and nearly similar statistical characteristics. The SWAT base model for the Swat River basin at Chakdara underwent several improvements and calibration steps. Initially, a neutral parameter setting was used to understand the model's initial behavior. Due to the region's significant altitudinal variation and snow-fed nature, five elevation bands were introduced using SWAT-CUP Premium.

49. To account for the influence of precipitation, temperature, and snow parameters, lapse rates for weather variables were fixed, followed by independent calibration of snow parameters. Global sensitivity analyses were performed for each set of parameters, and their ranges were determined through iterative simulations. The iterations continued until a satisfactory model performance statistic were achieved both for calibration and validation. Figure 12 depicts a graphical comparison of the modeled and measured flows at Swat River at Chakdara, along with their corresponding statistics.

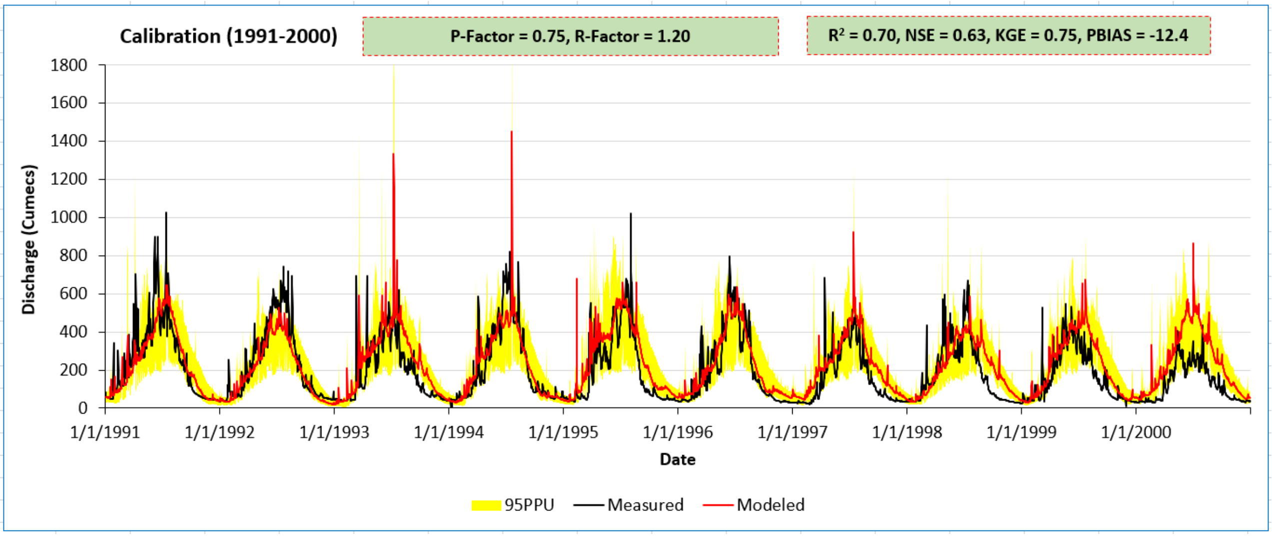


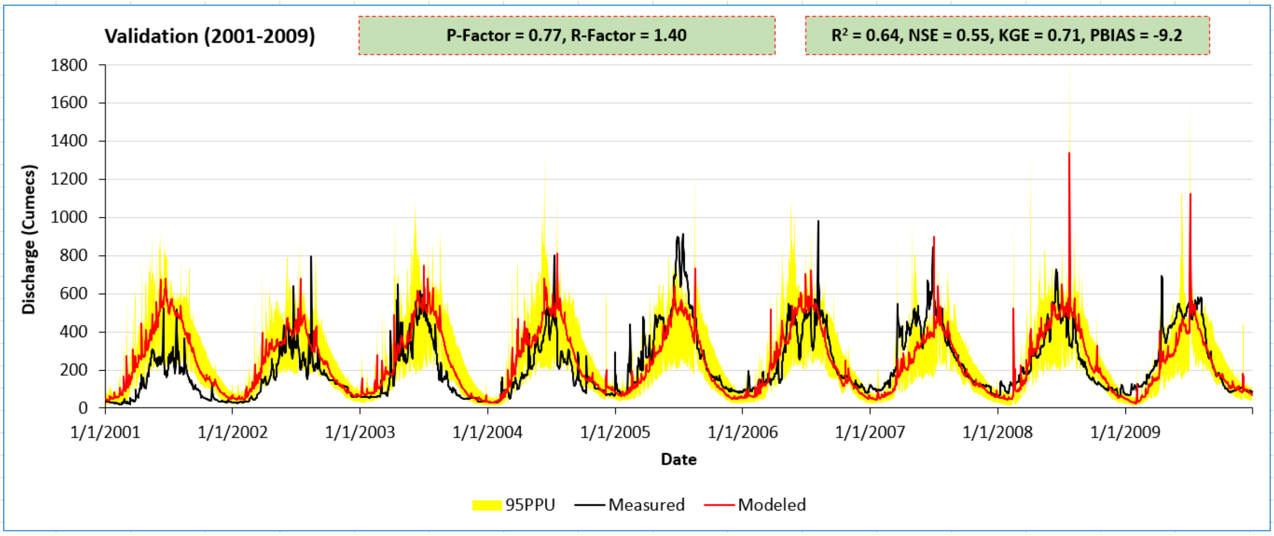


**Figure 14: Graphical representation of calibration and validation result of Swat River at Chakdara along with all the statistical performance indicators**

**Table 11: Calibration summary statistics and remarks for Swat River Basin at Chakdara**

| S.No. | Name | Guage Station Location | Available Record | Calibration Period | Calibration Summary Statistics | | | | | | Remarks (Based on 5 indicators) | Remarks (Based on KGE) |
|---|---|---|---|---|---|---|---|---|---|---|---|---|
| | | | | | p-factor | r-factor | $R^2$ | NS | KGE | PBIAS | | |
| 2a | Swat River Basin | Chakdara | 1988-2018 | 1991-2000 | 0.75 | 1.2 | 0.7 | 0.63 | 0.75 | -12.4 | Good to Satisfactory | Very Good |

**Table 12: Validation summary statistics and remarks for Swat River Basin at Chakdara**

| S.No. | Name | Guage Station Location | Available Record | Calibration Period | Validation Summary Statistics | | | | | | Remarks (Based on 5 indicators) | Remarks (Based on KGE) |
|---|---|---|---|---|---|---|---|---|---|---|---|---|
| | | | | | p-factor | r-factor | $R^2$ | NS | KGE | PBIAS | | |
| 2b | Swat River Basin | Chakdara | 1988-2018 | 2001-2009 | 0.77 | 1.4 | 0.64 | 0.55 | 0.71 | -9.2 | Good to Satisfactory | Very Good |

50. The model performance for the Swat River Basin during the calibration period (1991-2000) exhibits a satisfactory level of agreement between observed and simulated values. The p-factor of 0.75 suggests a capture of 75% observed values by the model uncertainty band, while the model tends to slightly overestimate values, as indicated by the r-factor of 1.20. The $R^2$ value of 0.70 implies that 70% of the observed variability is explained by the model, and the NS value of 0.63

reflects a moderate performance in capturing flow variability. However, a noticeable negative bias is observed with a PBIAS of -12.4%. Despite this bias, the KGE value of 0.75 indicates a very good overall model performance, emphasizing the model's capability to capture key aspects of flow behavior in the Swat River Basin.

51. Moving to the validation period (2001-2009), the model continues to demonstrate a satisfactory level of agreement, with a p-factor of 0.76 confirming a good capture of the observed data within the uncertainty band (95PPU). The r-factor of 1.42 indicates a slight tendency to overestimate observed values. The $R^2$ value of 0.66 implies that 66% of the observed variability is explained, and the NS value of 0.53 reflects a moderate ability to capture flow variability. Despite a negative bias of -9.5%, the KGE value remains high at 0.75, showcasing a very good overall model performance in capturing the key aspects of the flow behavior in the Swat River basin during the validation period. In conclusion, the model consistently demonstrates a satisfactory to very good performance, making it a valuable tool for water resource management and decision-making in the Swat River Basin.

## 3.5. Kabul River Basin Calibration And Validation Results

52. The Kabul River originates from the Hindu Kush Mountains and is a major tributary of the Indus River. The basin's climate is semi-arid and highly temperate. During the winter months, the maximum precipitation averages 110 mm. The highest maximum temperature has been observed in July, with an average value of around 28 °C, while the lowest minimum temperature is approximately -6 °C during the winter. Due to the complex terrain, there is a significant seasonal variation in the amount of precipitation received. Historical data reveals that the northern regions of the basin had the highest mean annual precipitation of more than 1600 mm. During the winter season, the basin receives nearly all of its precipitation. The precipitation is primarily "snow precipitation," which is stored over the mountains to recharge rivers during the melt season.

53. The SWAT base model for Kabul River basin was developed and run for base historic period of 30 years (1981-2010) using ERA-5 Land data. The base model was then calibrated and validated using SWAT-CUP Premium SWAT Parameter Estimator (SPE) program at Nowshera stream flow gauging station. The stream flow at Nowshera is available for a historic period of 38 years (1982-2020) at daily time step. However, the data is highly inherited with inconsistencies, missing values and uncertainties at different time slices of the years. Selection of time period for calibration and validation was based on the following criteria: (a) Data must be available consistently throughout the period at daily time step. (b) The Calibration and Validation period must cover all climate conditions i.e. Dry, Wet and Average years. (c) The mean and standard deviation should be more or less the same for Calibration and validation period. Considering the above-mentioned criteria, data constraints and model output requirements a reference period of 8 years (1991-1998) was chosen for calibration and 7 years (2003-2009) for validation.

54. The SWAT base model backup was initially run in SWAT-CUP Premium with a neutral parameter to have an idea of the model initial behavior. As the watershed exhibits significant altitudinal variation and lies in a snow-fed mountainous region, therefore, the model was first improved by introducing five different elevation bands using the inbuilt capability of the SWAT-CUP Premium. As precipitation, temperature and snow parameters are driving variables and can’t be calibrated in combination with other parameters, therefore, the lapse rates were then fixed for weather variables followed by snow parameters calibration independently.

55. Following that, global sensitivity analyses for each set of parameters have been carried out, and their ranges were fixed independently after many iterative simulations run each 300 simulations. This iterative process was continued till we got satisfactory model performance statistics both for calibration and validation. Figure 13 shows a graphical comparison of the modelled and measured flows at Nowshera along with their calculated statistics.

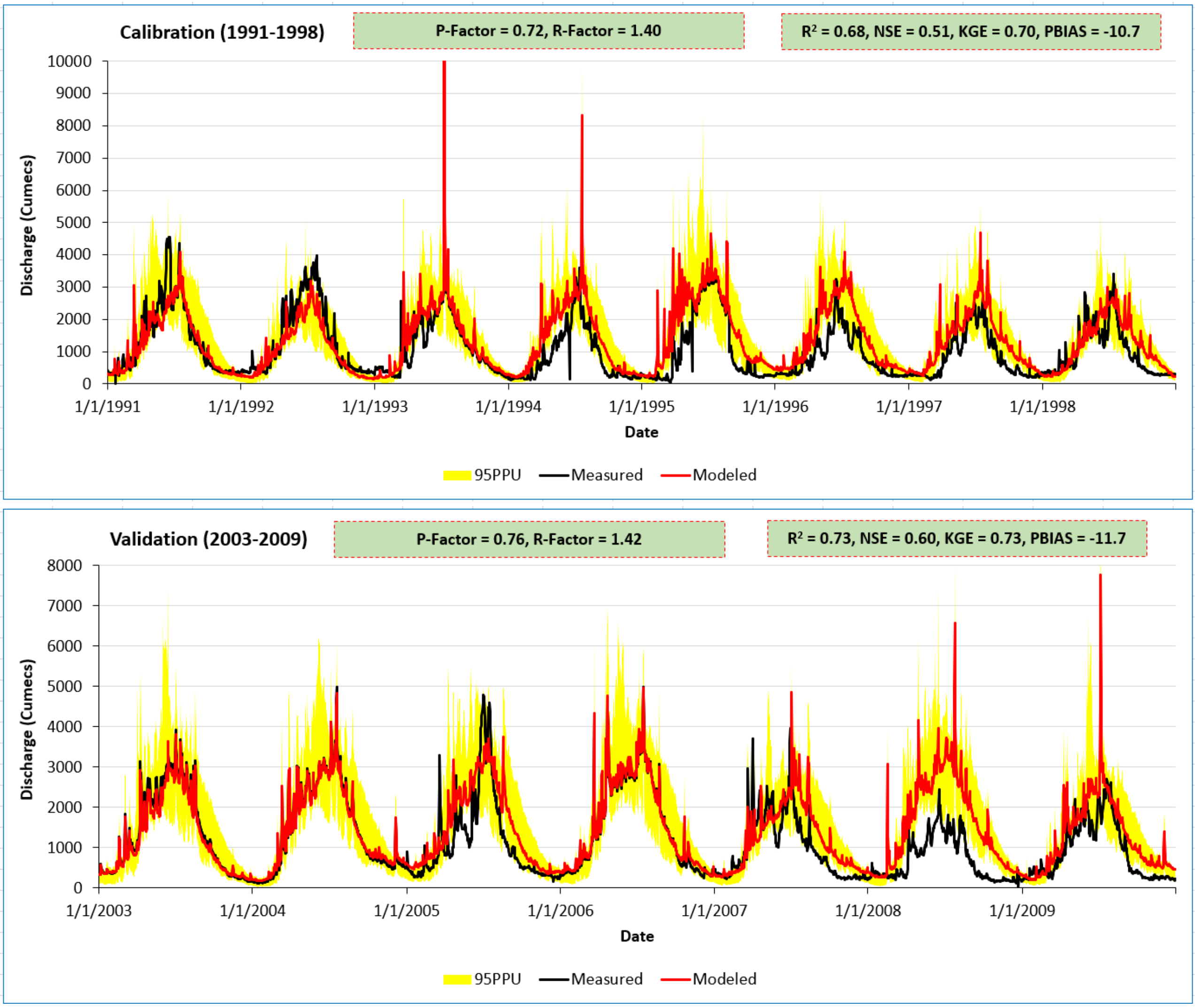


**Figure 15: Graphical representation of calibration and validation result of Kabul River at Nowshera along with all the statistical performance indicators**

**Table 13: Calibration summary statistics and remarks for Kabul River Basin at Nowshera**

| S.No. | Name | Guage Station Location | Available Record | Calibration Period | Calibration Summary Statistics | | | | | | Remarks (Based on 5 indicators) | Remarks (Based on KGE) |
|---|---|---|---|---|---|---|---|---|---|---|---|---|
| | | | | | p-factor | r-factor | $R^2$ | NS | KGE | PBIAS | | |
| 3a | Kabul River Basin | Nowshera | 1982-2020 | 1991-1998 | 0.72 | 1.4 | 0.68 | 0.51 | 0.7 | -10.7 | Good to Satisfactory | Very Good |

**Table 14: Validation summary statistics and remarks for Kabul River Basin at Nowshera**

| S.No. | Name | Guage Station Location | Available Record | Calibration Period | Validation Summary Statistics | | | | | | Remarks (Based on 5 indicators) | Remarks (Based on KGE) |
|---|---|---|---|---|---|---|---|---|---|---|---|---|
| | | | | | p-factor | r-factor | $R^2$ | NS | KGE | PBIAS | | |
| 3b | Kabul River Basin | Nowshera | 1982-2020 | 2003-2009 | 0.76 | 1.42 | 0.73 | 0.6 | 0.73 | -11.7 | Good to Satisfactory | Very Good |

56. Based on the six indicators (p-factor, r-factor, $R^2$, NS, and PBIASE and KGE), the calibration performance is assessed. For calibration, the p-factor of 0.72 indicates a good level of agreement between observed and simulated values during the calibration period. The r-factor of 1.40 suggests that the model tends to overestimate the observed values. The $R^2$ value of 0.68 indicates that 68% of the observed variability is captured by the model. The NS value of 0.51 suggests a moderate level of model performance in capturing the flow variability. The PBIAS of -10.7% indicates a negative bias, suggesting that the model underestimates the observed values on average. However, the KGE value remains high at 0.70, showcasing a very good overall model performance in capturing the key aspects of the flow behavior in the Kabul River basin during the calibration period.

57. For Validation, the p-factor of 0.76 suggests a slightly improved agreement between observed and simulated values during the validation period compared to the calibration period. The r-factor remains at 1.42, indicating the model's tendency to overestimate the observed values. The $R^2$ value of 0.73 indicates that the model captures 73% of the observed variability. The NS value of 0.60 suggests a satisfactory level of model performance in capturing the flow variability during the validation period. Despite of the negative PBIAS of -11.7%, the KGE value at 0.73, showcasing a very good overall model performance in capturing the key aspects of the flow behavior in the Kabul River basin during the validation period. In summary, the model shows a reasonable level of performance in simulating flow in the Kabul River basin, with some overestimation and negative bias. The agreement between observed and simulated values is considered good to satisfactory, as indicated by the remarks for both the calibration and validation periods collectively based on five performance indicators. Whereas, based on single KGE statistics, the model performance is ranked at “Very Good” category both for calibration and validation period.

## 3.6. KUNHAR RIVER BASIN CALIBRATION AND VALIDATION RESULTS

58. Kunhar is the main river in the Naran Valley. It originates from the Lulusar Lake, near the Babusar Pass at the elevation of 3455m, in the Kaghan Valley. Melting snow and natural tributaries are the main source of water for the Kunhar river. It joins Jhelum river at Pattan and is the main western tributary of Jhelum river basin. The Jhelum River Basin is a transboundary basin that borders Pakistan and India, and it is located in Pakistan's high-altitude north-east. The Jhelum River and its major tributaries, the Kunhar and Neelum rivers, drain the southern Himalayan foothills and the northern slopes of Jammu and Kashmir's Pir Punjal Mountain range. Because of high and steep mountains in the north and warm to temperate plains in the south, the climate of the Jhelum River basin varies from north to south. Based on data from 14 different climatic stations in the watershed, the Naran climate station in the north and Jhelum climate station in the south are the coldest and warmest, with mean monthly temperatures of 6.14 °C and 23.53 °C, respectively. The average monthly temperature in the basin, however, remains at 13.72 °C. The basin's annual average precipitation varies considerably by location, with 1893 mm in the north compared to 846 mm in the south, indicating that precipitation in the north is 223.75% higher than in the south.

59. While attempting to study the hydrology of the Kunhar river basin, we lacked sufficient data of stream flow for SWAT model calibration and validation at Kunhar river. Therefore, we took a broader perspective. Since the Kunhar river is a major tributary of the Jhelum River as shown in Figure 14, a detailed SWAT modeling was carried out at at Mangla to understand stream flow patterns in the larger Jhelum River basin. This helped us estimate historical and future flood estimation at sub-basin level. Although we couldn't model directly for Kunhar river basin, this approach still provided insights into how Kunhar river stream flow behaves in that area and how it's connected to the bigger picture. This adaptive strategy provides valuable information for making informed decisions on water resource management in the Kunhar river basin.

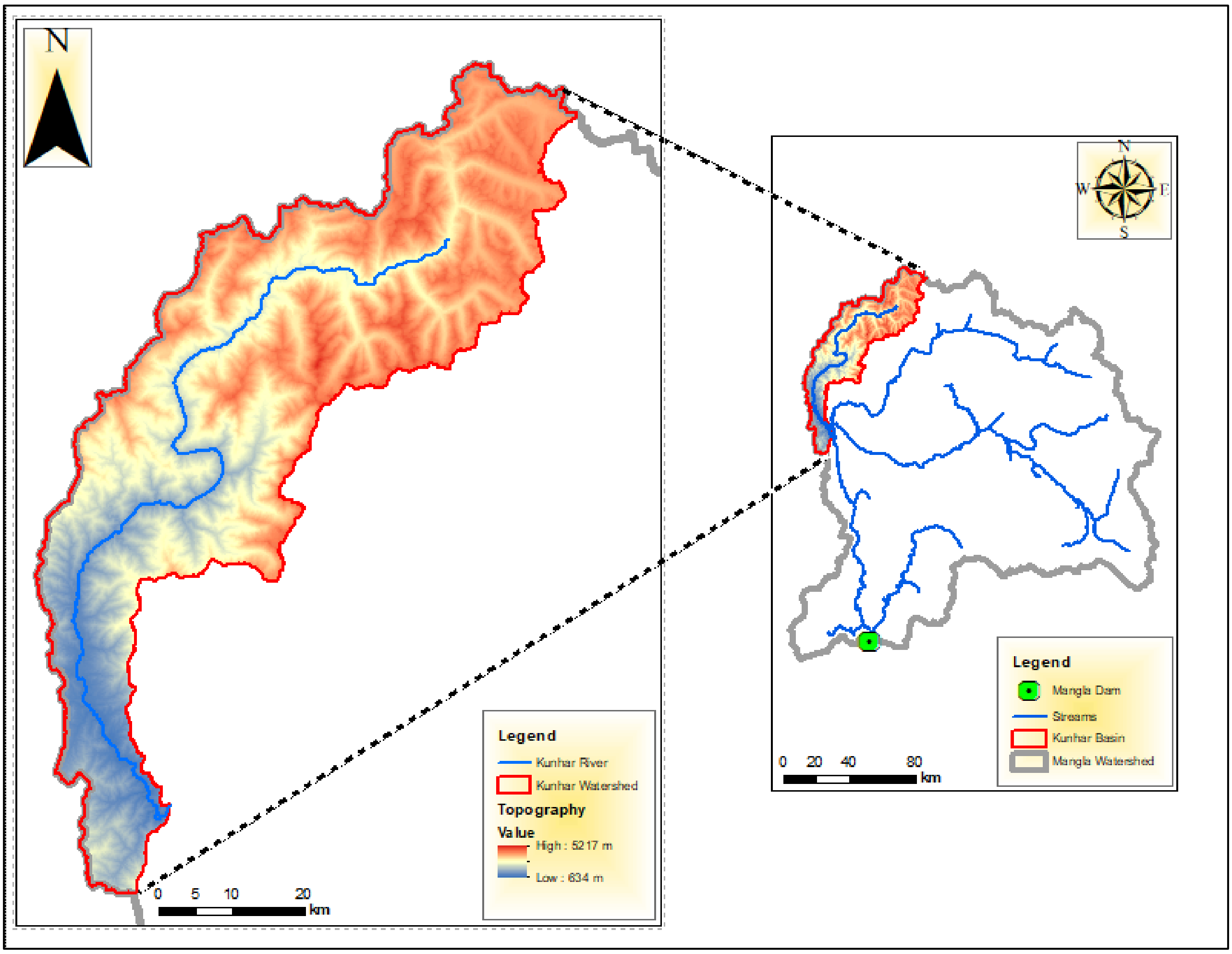


**Figure 16: Location map of Kunhar river basin and Jhelum River basin at Mangla**

60. For the Jhelum River basin at Mangla, the SWAT base model was developed and run using ERA-5 Land data for a historic period of 30 years (1981-2010). The model calibration and validation were performed using stream flow data from the available record spanning from 1982 to 2020 at Mangla. Due to data inconsistencies and uncertainties, specific time periods were selected for calibration and validation. The calibration period chosen was from 1991 to 2000, while the validation period covered 2003 to 2010. These time periods were selected based on consistent data availability, coverage of different climate conditions, and similar statistical characteristics.

61. Similar to other basins, the SWAT base model for the Jhelum River basin undergone several improvements and calibration steps. The model's initial behavior was assessed using a neutral parameter setting. Considering the region's physiographical characteristics, such as significant altitudinal variation and snow influence, specific adjustments were made in terms of elevation bands definition. Lapse rates for weather variables were fixed, followed by independent calibration of snow parameters.

62. Global sensitivity analyses were performed to determine appropriate parameter ranges through iterative simulations. The calibration and validation process continued until satisfactory model performance statistics were achieved. Graphical comparisons of the modeled and measured flows at Mangla, along with their corresponding statistics, were generated to assess the model's performance Figure 15.

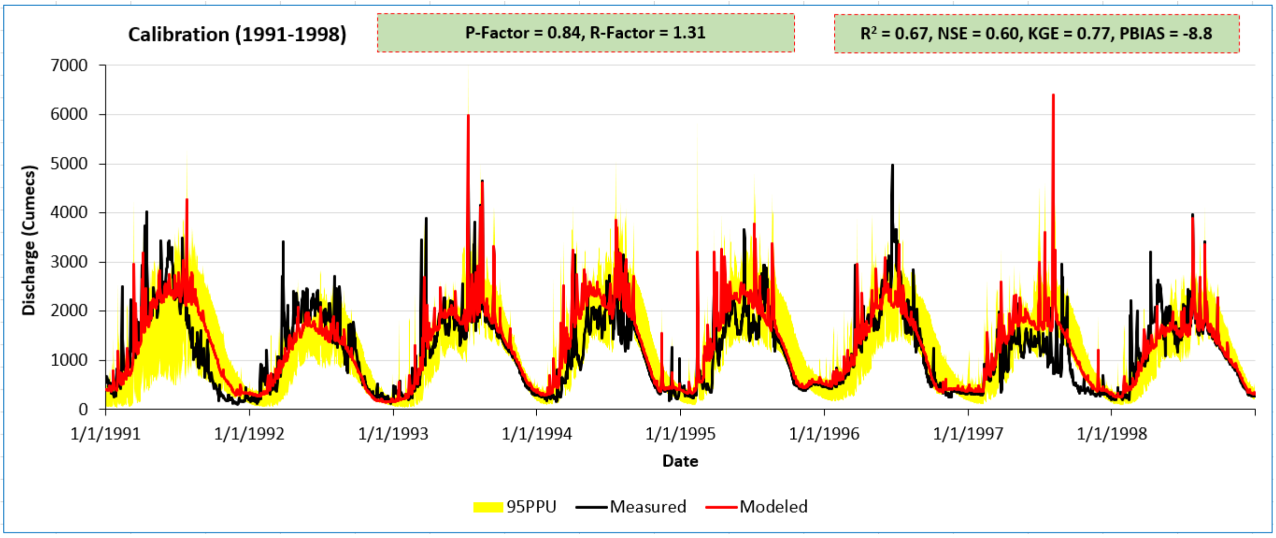


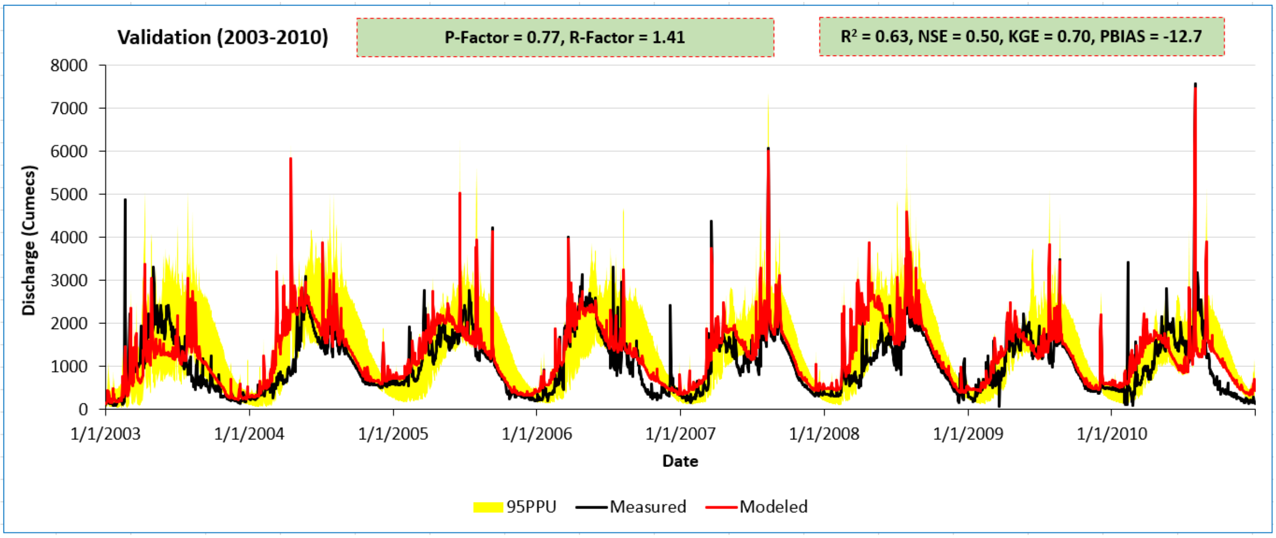


**Figure 17: Graphical representation of calibration and validation result of Jhelum River at Mangla along with all the statistical performance indicators**

**Table 15: Calibration summary statistics and remarks for Jhelum River Basin at Mangla**

| S.No. | Name | Guage Station Location | Available Record | Calibration Period | Calibration Summary Statistics | | | | | | Remarks (Based on 5 indicators) | Remarks (Based on KGE) |
|---|---|---|---|---|---|---|---|---|---|---|---|---|
| | | | | | p-factor | r-factor | $R^2$ | NS | KGE | PBIAS | | |
| 4a | Jhelum River Basin | Mangla | 1982-2020 | 1991-2000 | 0.84 | 1.31 | 0.67 | 0.6 | 0.77 | -8.8 | Good to Satisfactory | Very Good |

**Table 16: Validation summary statistics and remarks for Jhelum River Basin at Mangla**

| S.No. | Name | Guage Station Location | Available Record | Calibration Period | Validation Summary Statistics | | | | | | Remarks (Based on 5 indicators) | Remarks (Based on KGE) |
|---|---|---|---|---|---|---|---|---|---|---|---|---|
| | | | | | p-factor | r-factor | $R^2$ | NS | KGE | PBIAS | | |
| 4b | Jhelum River Basin | Mangla | 1982-2020 | 2003-2010 | 0.77 | 1.41 | 0.63 | 0.5 | 0.7 | -12.7 | Good to Satisfactory | Very Good |

63. The calibration results for the Jhelum River at Mangla, based on the available record and the calibration period from 1991 to 2000, showcase a generally good performance of the simulation model. The p-factor of 0.84 indicates a commendable level of agreement between observed and simulated values, underlining the model's ability to capture the flow dynamics during the calibration period. However, the r-factor of 1.31 suggests a tendency of the model to slightly overestimate the observed values, leading to a moderate negative bias indicated by the PBIAS of -8.8%. Despite this

bias, the $R^2$ value of 0.67 highlights that 67% of the observed variability is captured by the model, reflecting a satisfactory level of performance in replicating the hydrological patterns of the Jhelum River at Mangla.

64. Further insights from the Nash-Sutcliffe efficiency (NS) value of 0.60 reinforce a moderate level of model performance in capturing flow variability. The comprehensive Kling-Gupta efficiency (KGE) value of 0.77 provides additional support, signifying a very good overall model performance during the calibration period.

65. Moving to the validation period (2003-2010), there is a slight decrease in the p-factor from o.84 to 0.77. Additionally, the model still tends to overestimate values (r-factor of 1.41). The $R^2$ value of 0.63 indicates that 63% of the observed variability is captured, while the NS value of 0.50 suggests a satisfactory level of performance in capturing flow variability during the validation period. Despite a negative PBIAS of -12.7%, the KGE value remains high at 0.70, showcasing a very good overall model performance. In summary, the model exhibits a reasonable level of performance in simulating flow in the Jhelum River at Mangla, with some overestimation and negative bias. The agreement between observed and simulated values is considered good to satisfactory, as indicated by the remarks for both the calibration and validation periods based on five performance indicators. Based on the single KGE statistic, the model performance is consistently ranked in the "Very Good" category for both calibration and validation periods.

## 3.7. THE INDUS RIVER BASIN CALIBRATION AND VALIDATION RESULTS

66. The Indus River, also known as Sindhu, originates from the Kailash Range in Tibet, flowing through Ladakh, Karakoram, and the Greater Himalayas. After a sharp turn at the Hindu Kush Mountains, it journeys southward through the Lesser Himalayas, Siwalik Ranges, and plains of Punjab and Sindh, forming a delta at the Arabian Sea. Renowned for nurturing the ancient Indus Valley civilization, the river's upstream, known as the Upper Indus sub-basin, covers a huge area from its source to the Tarbela reservoir. This region covers remarkable glaciers, towering peaks like K2 and Nanga Parbat, and major tributaries such as the Shyok, Nubra, Hushe, Zanskar, Shingo, Shigar, Hunza, Gilgit, and Astore, making it a crucial and diverse part of the Indus River's course.

67. The Upper Indus Basin exhibits a diverse and challenging climate marked by significant physiographic variations. Covering arid to semi-arid climatic zones, the basin experiences spatial and seasonal fluctuations in precipitation and temperature. Annual rainfall ranges from 200-400 mm to 2000-2500 mm, reflecting the basin's varied topography. Northern parts face harsh winters with freezing temperatures and substantial snowfall, while the middle and southern regions have milder winters and extremely hot summers exceeding 35°C. Altitude plays a crucial role, resulting in a transition from hot and moist tropical conditions in lower valleys to cooler temperatures at 1500-2000 m, ultimately reaching an extreme polar type at the highest altitudes. The basin encounters two major climatic systems: mid-latitude westerlies from December to March and the South Asian monsoon from June to September. The Himalayas act as an orographic barrier, creating rain shadows in the north and contributing to the scarcity of rainfall in the Upper Indus sub-basin, with an average of approximately 300 mm. Precipitation in the Karakoram primarily occurs at elevations higher than 4000-5000 m, and orographic enhancement results in increased precipitation with altitude. The region's climate intricacies significantly influence snowfall patterns, contributing to the unique hydrological dynamics of the Upper Indus Basin.

68. Precise and accurate hydro-climate modeling has been carried out for the Indus River basin at Tarbela. The study aimed to provide valuable insights for informed decision-making and proactive interventions to deal with climate-related challenges in the Upper Indus Basin.

69. For the Indus River basin at Tarbela, the SWAT base model was developed and run using ERA-5 Land data for a historic period of 28 years (1981-2010). The model calibration and validation were performed using stream flow data from the available record spanning from 1983 to 2020 at Tarbela. Due to data inconsistencies and uncertainties, specific time periods were selected for calibration and validation. The calibration period chosen was from 1983 to 2000, while the validation period covered 2001 to 2010. These time periods were selected based on consistent data availability, coverage of different climate conditions, and similar statistical characteristics.

70. The SWAT base model for the Indus River basin underwent iterative improvements and calibration steps, commencing with an evaluation of its initial behavior using a neutral parameter setting. Tailoring the model to the region's distinctive physiographical features, such as notable altitudinal variations and the influence of snow, involved specific adjustments in elevation bands definition and fixing lapse rates for weather variables. Independent calibration of snow parameters was also conducted. Global sensitivity analyses iteratively determined appropriate parameter ranges. The calibration and validation processes persisted until achieving satisfactory model performance statistics. Graphical comparisons of modeled and measured flows at Tarbela, accompanied by corresponding statistics (Figure 16), were helpful in assessing the effectiveness of the model in replicating hydrological dynamics.

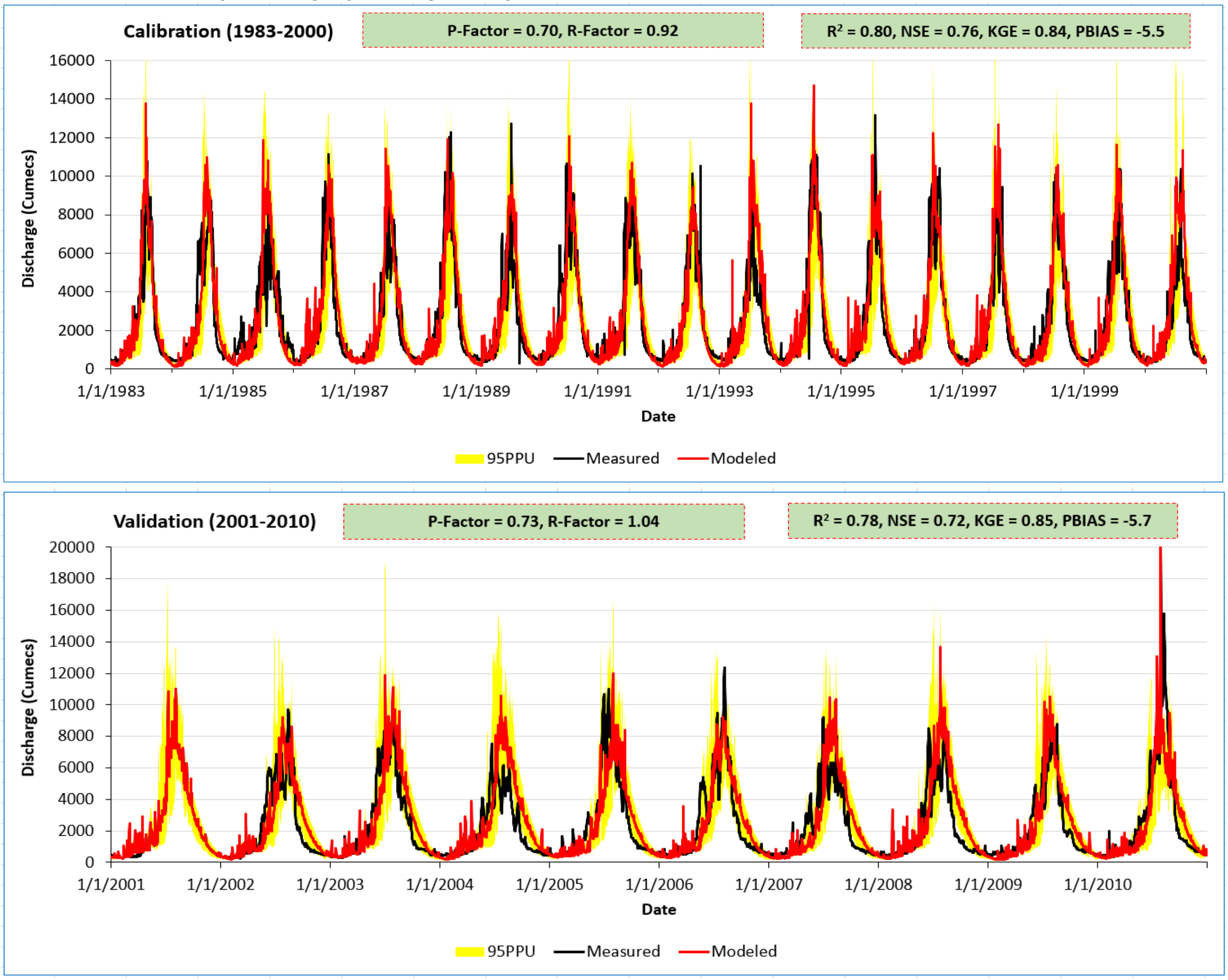


**Figure 18: Graphical representation of calibration and validation result of the Indus River at Tarbela along with all the statistical performance indicators**

**Table 17: Calibration summary statistics and remarks for The Indus River Basin at Tarbela**

| S.No. | Name | Guage Station Location | Available Record | Calibration Period | Calibration Summary Statistics | | | | | | Remarks (Based on 5 indicators) | Remarks (Based on KGE) |
|---|---|---|---|---|---|---|---|---|---|---|---|---|
| | | | | | p-factor | r-factor | $R^2$ | NS | KGE | PBIAS | | |
| 5a | The Indus River Basin | Tarbela | 1983-2020 | 1983-2000 | 0.7 | 0.92 | 0.8 | 0.76 | 0.84 | -5.5 | Good | Very Good |

**Table 18: Validation summary statistics and remarks for The Indus River Basin at Tarbela**

| S.No. | Name | Guage Station Location | Available Record | Calibration Period | Validation Summary Statistics | | | | | | Remarks (Based on 5 indicators) | Remarks (Based on KGE) |
|---|---|---|---|---|---|---|---|---|---|---|---|---|
| | | | | | p-factor | r-factor | $R^2$ | NS | KGE | PBIAS | | |
| 5b | The Indus River Basin | Tarbela | 1983-2020 | 2001-2010 | 0.73 | 1.04 | 0.78 | 0.72 | 0.85 | -5.7 | Good | Very Good |

71. The model's performance for the Indus River Basin at Tarbela, during the calibration period from 1983 to 2000, reveals encouraging results. The calibration summary statistics indicate a p-factor of 0.70, denoting a good level of agreement between observed and simulated values. The r-factor of 0.92 suggests the model uncertainty band is well in range and close to the ideal value of 1, the $R^2$ value of 0.80 indicates that 80% of the observed variability is captured by the model. The NS value of 0.76 suggests a high level of model performance in capturing flow variability, and the PBIAS of -5.5% indicates a slight negative bias. Furthermore, based on the KGE value of 0.84, the model demonstrates excellent overall performance during the calibration period.

72. Moving to the validation period from 2001 to 2010, the model's performance remains robust. The p-factor of 0.73 signifies a good level of agreement, while the r-factor of 1.04 indicates a slight tendency to overestimate observed values. The $R^2$ value of 0.78 showcases that 78% of the observed variability is captured. The NS value of 0.72 suggests effective model performance in capturing flow variability during the validation period. The PBIAS of -5.7% indicates a slight negative bias, and the KGE value of 0.85 reflects excellent overall model performance.

73. In summary, the Indus River Basin model at Tarbela consistently demonstrates very good to excellent performance in simulating flow, both during the calibration and validation periods. The agreement between observed and simulated values is consistently high across multiple indicators, including p-factor, r-factor, $R^2$, NS, and KGE, making it a reliable tool for water resource management and decision-making in the region.

## 3.8. Gomal River Basin Calibration And Validation Results

74. Gomal River is a 400 km long river and it runs across Afghanistan and Pakistan. It originates from the northern province of Afghanistan Paktika and ends when it meets the Indus River near to DI Khan. Within Pakistan, it forms the boundary between South Waziristan and Balochistan. On upstream of its confluence with the Indus River, it also receives water from Zhob River near to Khajuri Kach. The climate of the basin is semi-arid with hot summers and cold winters . The region is prone to droughts and floods due to its irregular rainfall patterns.

75. Similar to other basins, the SWAT base model for the Gomal River basin underwent several improvements and calibration steps. The initial assessment of the model's behavior was conducted using a neutral parameter setting. Acknowledging the physiographical characteristics unique to the Gomal River basin, such as significant altitudinal variation, specific adjustments were made, particularly in terms of defining elevation bands. Fixed lapse rates for weather variables were

established, and independent calibration of snow parameters ensued. Global sensitivity analyses were instrumental in determining appropriate parameter ranges through iterative simulations. The calibration and validation process persevered until achieving satisfactory model performance statistics.

76. To assess the model's efficiency, graphical comparisons of the modeled and measured flows at Khajori Kach, are provided. The corresponding statistics derived from these comparisons were crucial in evaluating the model's performance, as depicted in Figure 17. The challenges encountered during calibration due to biases and inconsistencies in observed stream flow data highlight the importance of addressing data limitations and refining modeling techniques for accurate representation of hydrological processes in the Gomal River basin.

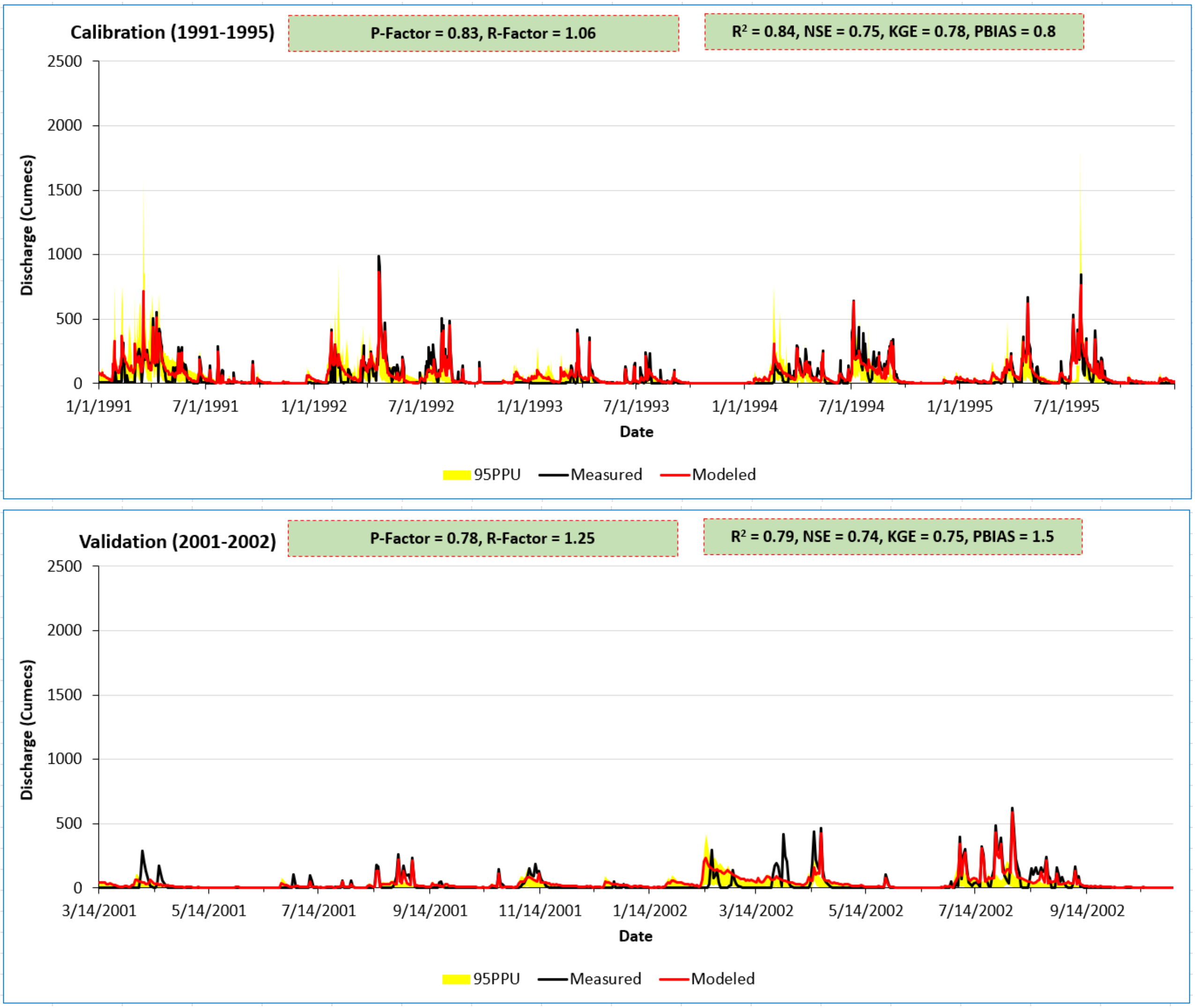


**Figure 19: Graphical representation of calibration and validation result of the Gomal River at Khajori Kach along with all the statistical performance indicators**

**Table 19: Calibration summary statistics and remarks for Gomal River Basin at Khajori Kach**

| S.No. | Name | Guage Station Location | Available Record | Calibration Period | Calibration Summary Statistics | | | | | | Remarks (Based on 5 indicators) | Remarks (Based on KGE) |
|---|---|---|---|---|---|---|---|---|---|---|---|---|
| | | | | | p-factor | r-factor | $R^2$ | NS | KGE | PBIAS | | |
| 6a | Gomal River Basin | Khajori Kach | 1991-1995 | 1991-1995 | 0.83 | 1.06 | 0.84 | 0.75 | 0.78 | 0.8 | Very Good | Excellent |

Table 20: Validation summary statistics and remarks for Gomal River Basin at Khajori Kach

| S.No. | Name | Guage Station Location | Available Record | Calibration Period | Validation Summary Statistics | | | | | | Remarks (Based on 5 indicators) | Remarks (Based on KGE) |
|---|---|---|---|---|---|---|---|---|---|---|---|---|
| | | | | | p-factor | r-factor | $R^2$ | NS | KGE | PBIAS | | |
| 6b | Gomal River Basin | Khajori Kach | 2001-2003 | 2001-2003 | 0.78 | 1.25 | 0.79 | 0.74 | 0.75 | 1.5 | Very Good | Excellent |

77. The calibration period for the Gomal River basin, focusing on the Khajori-Kach gauge station from 1991 to 1995, reveals a robust model performance. The statistical indicators showcase a well-fitted model, with a p-factor of 0.83, r-factor of 1.06, $R^2$ value of 0.84, NS of 0.75, KGE of 0.78, and PBIAS of 0.8. These indicators collectively yield a "Very Good" assessment for the calibration phase. Particularly noteworthy is the excellent KGE value, indicating a high level of agreement between the simulated and observed data. This implies that the model accurately captures the hydrological dynamics of the Gomal River during the calibration period, demonstrating reliability and effectiveness.

78. During the validation period (2001-2003) at the Khajori-Kach gauge station, the model's performance for the Gomal River basin remains consistently strong. The statistical indicators reveal a sound fit between the simulated and observed data, with a p-factor of 0.78, r-factor of 1.25, $R^2$ value of 0.79, NS of 0.74, KGE of 0.75, and PBIAS of 1.5. These values collectively warrant a "Very Good" assessment for the validation phase. The model's ability to maintain an excellent KGE rating during validation reinforces its accuracy in reproducing the hydrological behavior of the Gomal River. Overall, these results affirm the reliability of the SWAT model in simulating the complex hydrological processes of the Gomal River basin, both in calibration and validation scenarios.

## 3.9. Tank River Basin Calibration And Validation Results

79. Tank river basin is one of the nearest river basins to Gomal River basin with a catchment area of 4541 Sq.-Km. Due to the unavailability of sufficient stream flow data at Tank River, The SWAT base model was first developed at Gomal River (Khajori-Kach) for which the stream flow data is consistently available for 8 years (1991-1995) and (2001-2003) at daily time step as discussed in the preceding section. The stream flow data for the Khajori-Kach was collected from the Water and Power Development Authority (WAPDA). This data has been used to calibrate and validate the base model at Gomal River (Khajori-Kach). The calibrated parameters were then regionalized for the Tank River basin based on the hydrologic similarity approach. Using the calibrated back-up, historic and future stream flows were projected for the Tank River basin considering the climate change scenarios.

## 3.10. Kurram River Basin Calibration And Validation Results

80. The Kurram River starts in Spin Ghar, Afghanistan, and the Kurram district of Pakistan. It flows through North Waziristan, passes Bannu, and then flattens out. Finally, it joins the Indus River just 20 km upstream of Chashma barrage, near Isa Khel. This meeting point is significant for the local water system. The Kurram River journey, from mountains to plains, is vital for the environment and communities along its path. The climate of the Kurram River Basin is characterized by diverse conditions shaped by its geographical features. Being a region that spans across Afghanistan and Pakistan, the basin experiences varying climatic patterns. In general, the climate can be described as semi-arid, with distinctive seasons.

81. During summers, the basin encounters hot temperatures, creating warm and dry conditions. The mountainous terrain contributes to temperature variations, providing relief in higher elevations. Winters, on the other hand, tend to be relatively cooler, especially in the elevated areas of Spin Ghar. The river basin may also witness cold temperatures in the Kurram district of Pakistan. Rainfall in the Kurram River Basin is a crucial factor, influencing the overall climate. The basin may experience irregular rainfall patterns, making it susceptible to both droughts and floods. These climatic extremes can impact the river's water flow and the surrounding ecosystems.

82. Like other basins, the SWAT base model for the Kurram River basin underwent enhancements and calibration steps. The model's initial evaluation used a neutral parameter setting, with adjustments made for the unique physiographical characteristics, including significant altitudinal variation. Specific changes were implemented in elevation bands and fixed lapse rates for weather variables, along with independent calibration of snow parameters.

83. Global sensitivity analyses helped establish appropriate parameter ranges through iterative simulations. Calibration and validation persisted until achieving satisfactory model performance statistics. Graphical comparisons of modeled and measured flows at Thal gauge station along with corresponding statistics, were crucial for evaluating the model's efficiency (see Figure 18). Challenges in calibration underscore the importance of addressing data limitations for accurate representation of hydrological processes in the Kurram River basin. The calibration process faced challenges due to biases and inconsistencies in observed stream flow data.

84. Upon reviewing the plots for the Kurram River at Thal, it is evident that there's a noticeable difference between the modeled and observed flows. This divergence, however, can be attributed to potential issues with the accuracy of the observed flow data. The USAID (2013) Supplemental Report on Hydrology (https://pdf.usaid.gov/pdf_docs/PA00KB13.pdf) highlights concerns raised by SWH at Thal regarding flow measurement errors. Acknowledging these potential inaccuracies in the observed data is crucial when trying to understand and interpret the variations between the modeled and observed flow values for the Kurram River at Thal.

85.

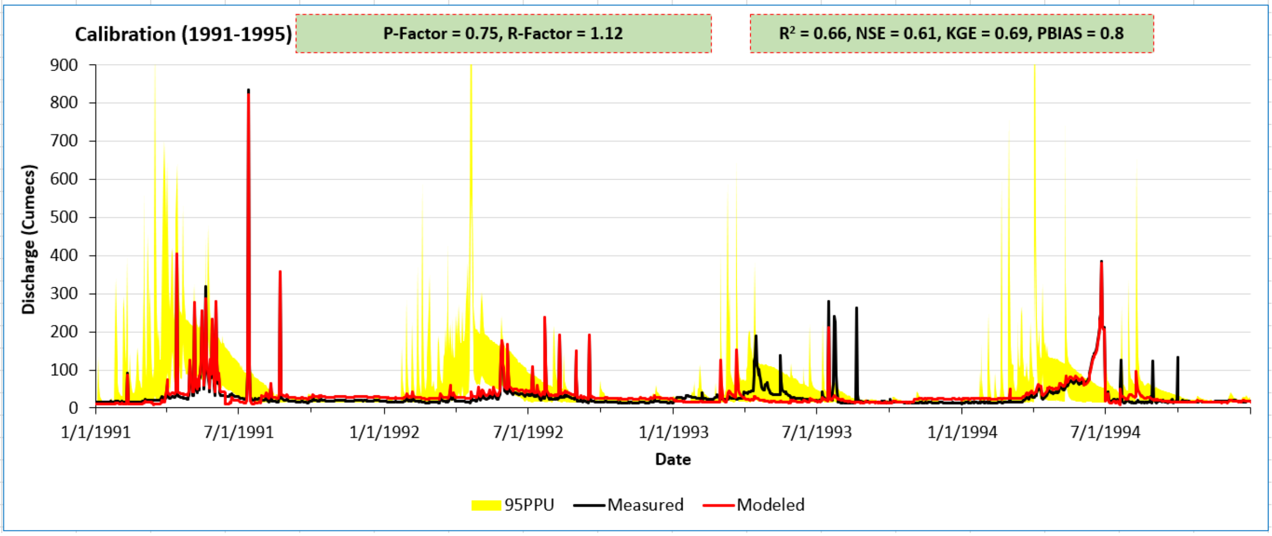

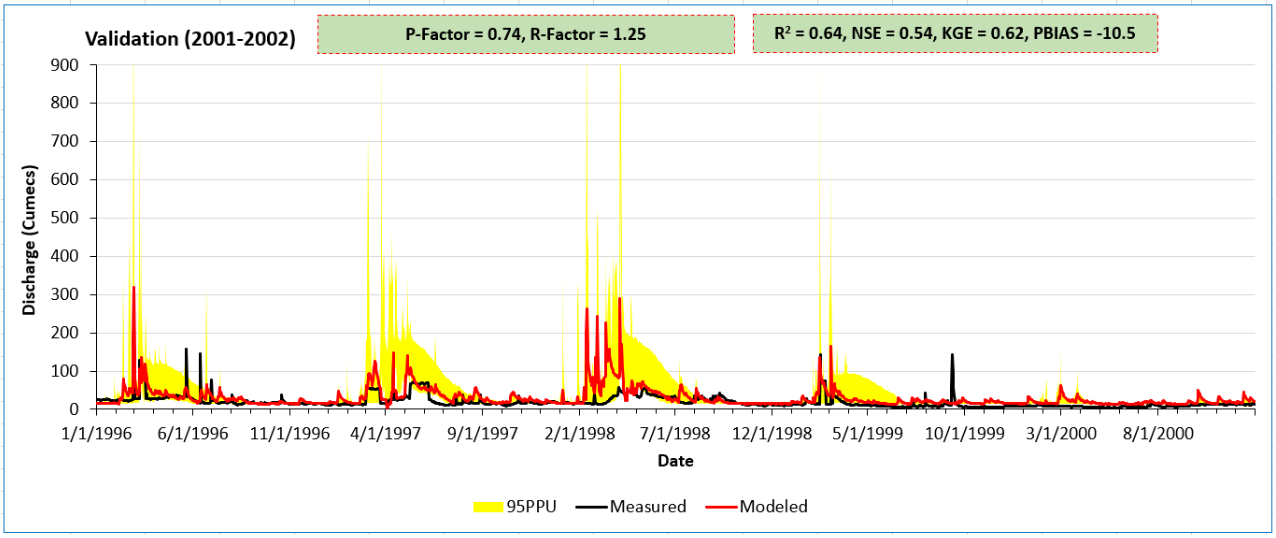


**Figure 20: Graphical representation of calibration and validation result of the Kurram river at Thal along with all the statistical performance indicators**

**Table 21: Calibration summary statistics and remarks for Kurram River Basin at Thal**

| S.No. | Name | Guage Station Location | Available Record | Calibration Period | Calibration Summary Statistics | | | | | | Remarks (Based on 5 indicators) | Remarks (Based on KGE) |
|---|---|---|---|---|---|---|---|---|---|---|---|---|
| | | | | | p-factor | r-factor | $R^2$ | NS | KGE | PBIAS | | |
| 7a | Kurram River Basin | Thal | 1991-1995 | 1991-1995 | 0.75 | 1.12 | 0.66 | 0.61 | 0.69 | 0.8 | Good to Satisfactory | Good |

**Table 22: Validation summary statistics and remarks for Kurram River Basin at Thal**

| S.No. | Name | Guage Station Location | Available Record | Calibration Period | Validation Summary Statistics | | | | | | Remarks (Based on 5 indicators) | Remarks (Based on KGE) |
|---|---|---|---|---|---|---|---|---|---|---|---|---|
| | | | | | p-factor | r-factor | $R^2$ | NS | KGE | PBIAS | | |
| 7b | Kurram River Basin | Thal | 2001-2002 | 2001-2002 | 0.74 | 1.25 | 0.64 | 0.54 | 0.62 | -10.5 | Good to Satisfactory | Good |

86. The calibration period for the Kurram River basin at the Thal gauge station from 1991 to 1995, demonstrates a reasonably good model performance. The statistical indicators illustrate a well-fitted model, featuring a p-factor of 0.75, r-factor of 1.12, $R^2$ value of 0.66, NS of 0.61, KGE of 0.69, and PBIAS of 0.8. These values result in a "Good to Satisfactory" assessment for the calibration phase. Notably, the KGE rating suggests a good agreement between the simulated and observed data, showcasing the model's capability in capturing the hydrological dynamics of the Kurram River during the calibration period.

87. Moving on to the validation period (2001-2002) at the Thal gauge station, the model's performance for the Kurram River basin remains relatively low. However, the statistical indicators reveal a reasonable fit between simulated and observed data, with a p-factor of 0.74, r-factor of 1.25, $R^2$ value of 0.64, NS of 0.54, KGE of 0.62, and PBIAS of -10.5. These values result in a "Good to Satisfactory" assessment for the validation phase. Despite a negative PBIAS, the KGE rating remains in the "Good" range, indicating the model's effectiveness in replicating the hydrological behavior of the Kurram River during the validation period. In summary, these results affirm the competency of the SWAT model in simulating the hydrological processes of the Kurram River basin, both in calibration and validation scenarios at the Thal gauge station.

# A-4. BASELINE AND FUTURE FLOOD ESTIMATES

## 4.1. SWAT RIVER BASIN

88. The following Figures 19 and 20 and Table 23 and 24 provide floods at various return periods during base period (1981–2010) and three future periods (2011–2040, 2041–2070, and 2071–2100) under the SSP 245 and SSP 585 scenarios.
The flood magnitudes under SSP 245 for the future periods are generally increasing (except for 5 and 10 years return period) as compared to the historical period. This suggests a higher potential severity of floods in the Swat River basin in the future under the SSP 245 scenario. Similar but more intense floods are projected under SSP 585 scenario.

89. The percentage increase in the 100-year flood magnitude in the future periods (2011–2040, 2041–2070, and 2071–2100) under SSP 245, with respect to the historical period, is quite substantial. The flood magnitude is projected to increase by approximately 4.1% to 9% for the 100-year return period under the SSP 245 Scenario. Considering the SSP 585 scenario, the 100-year return period flood magnitude is projected to increase by approximately 3.3% to 18.2%. This indicates a significant escalation in flood risk compared to historical conditions.

90. Furthermore the 2022 flood recorded on the Swat River at Chakadara was about 7796 cumecs which is almost equivalent to 500-year return period of historical flood. This also indicates a potential escalation in the intensity of future floods.

91. Moreover, the data pertaining to almost all return period floods indicates a heightened risk of more severe and frequent flood occurrences in the Swat River basin under both SSP 245 and SSP 585 scenarios. These results underscore the critical importance of comprehending and readying for potential future flood hazards in the region, underscoring the imperative for implementing effective adaptation and mitigation strategies

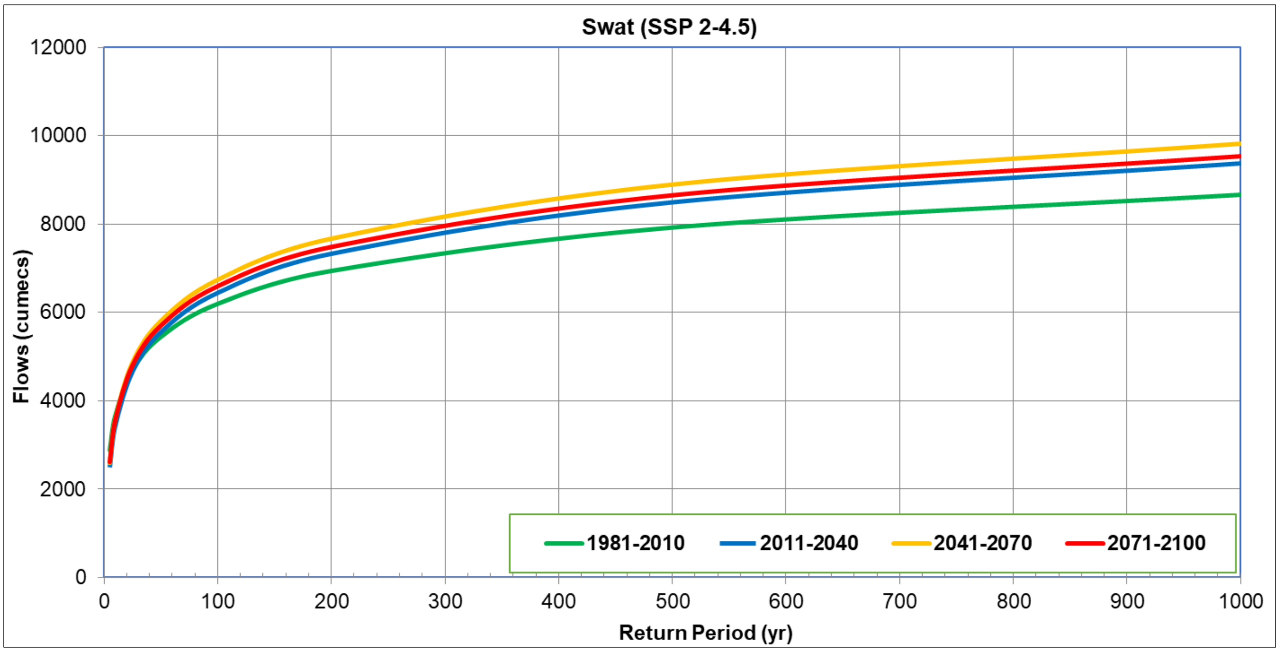


**Figure 21.Flood frequency plots for Swat River Basin under SSP 2-4.5 scenario**

Table 23.Various return period floods for Swat River under SSP 2-4.5 scenario

| Return Period | Historical Period | Swat SSP 245 | | | | | |
|---|---|---|---|---|---|---|---|
| | 1981-2010 | 2011-2040 | | 2041-2070 | | 2071-2100 | |
| Years | $m^3/s$ | $m^3/s$ | % | $m^3/s$ | % | $m^3/s$ | % |
| 5 | 2875 | 2505 | -12.9% | 2604 | -9.4% | 2615 | -9.0% |
| 10 | 3679 | 3463 | -5.9% | 3610 | -1.9% | 3587 | -2.5% |
| 25 | 4694 | 4670 | -0.5% | 4878 | 3.9% | 4806 | 2.4% |
| 50 | 5447 | 5564 | 2.2% | 5818 | 6.8% | 5707 | 4.8% |
| 100 | 6195 | 6451 | 4.1% | 6750 | 9.0% | 6600 | 6.5% |
| 200 | 6939 | 7334 | 5.7% | 7678 | 10.7% | 7488 | 7.9% |
| 500 | 7922 | 8498 | 7.3% | 8903 | 12.4% | 8660 | 9.3% |
| 1000 | 8665 | 9377 | 8.2% | 9828 | 13.4% | 9544 | 10.1% |

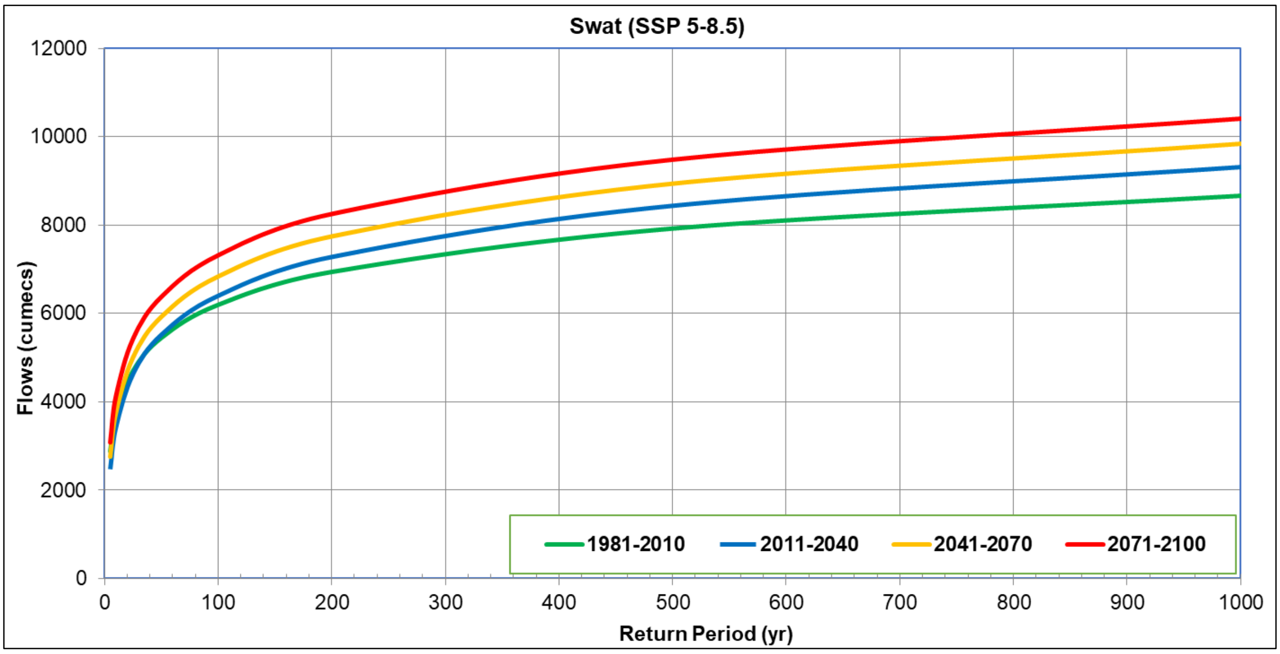


Figure 22.Flood frequency plots for Swat River Basin under SSP 5-8.5 scenario

Table 24.Various return period floods for Swat River under SSP 5-8.5 scenario

| Return Period | Historical Period | Swat SSP 585 | | | | | |
|---|---|---|---|---|---|---|---|
| | 1981-2010 | 2011-2040 | | 2041-2070 | | 2071-2100 | |
| Years | $m^3/s$ | $m^3/s$ | % | $m^3/s$ | % | $m^3/s$ | % |
| 5 | 2875 | 2482 | -13.7% | 2764 | -3.9% | 3082 | 7.2% |
| 10 | 3679 | 3434 | -6.6% | 3762 | 2.3% | 4128 | 12.2% |
| 25 | 4694 | 4633 | -1.3% | 5011 | 6.8% | 5425 | 15.6% |
| 50 | 5447 | 5521 | 1.4% | 5933 | 8.9% | 6378 | 17.1% |
| 100 | 6195 | 6401 | 3.3% | 6845 | 10.5% | 7320 | 18.2% |
| 200 | 6939 | 7278 | 4.9% | 7752 | 11.7% | 8255 | 19.0% |
| 500 | 7922 | 8434 | 6.5% | 8948 | 12.9% | 9485 | 19.7% |
| 1000 | 8665 | 9308 | 7.4% | 9850 | 13.7% | 10413 | 20.2% |

## 4.2. CHITRAL RIVER BASIN

92. The flood frequency analysis results for the Chitral Basin are provided under two different scenarios—SSP 245 and SSP 585 in Figures 21 ,22 and in Tables 25 ,26. Comparing the historical period (1981–2010) to the future scenarios, both SSP 245 and SSP 585 show an increase in flood

estimates during future periods, for various return periods. This suggests a higher risk of more frequent and severe flooding events in the coming years. Under both scenarios, the flood estimates consistently rise from 2011–2040 ,2041-2070 to 2071–2100. However, when comparing SSP 245 and SSP 585, the flood estimates tend to be higher under SSP 585, indicating a potentially greater impact of climate change in terms of flood risk.

93. The flood magnitude is projected to increase by approximately 16.5% to 28.8% for the 100-year return period under the SSP 245 Scenario. Considering the SSP 585 scenario, the 100-year return period flood magnitude is projected to increase by approximately 13.6% to 52.5%. This indicates a significant escalation in flood risk compared to historical conditions.

94. Additionally, the 2022 flood recorded on the Kabul River at Nowshehara reached approximately 9531 cumecs, a figure nearly equivalent to the 100-year return period for historical floods which highlights the potential for a rise in the intensity of future floods.

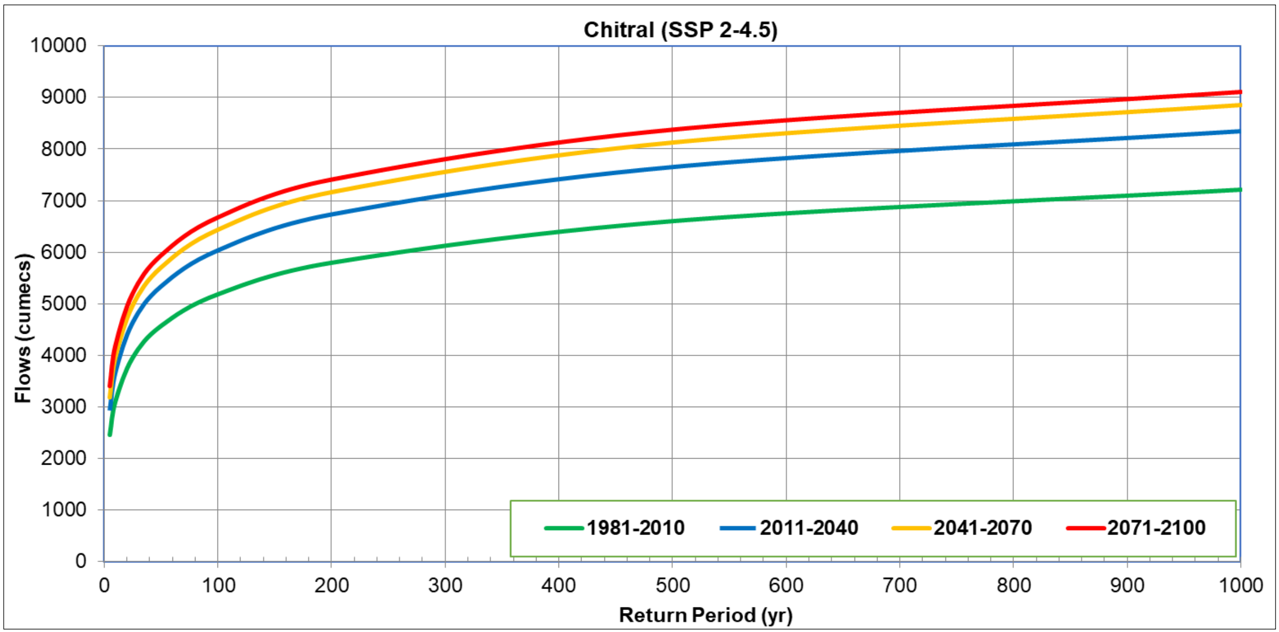


**Figure 23.Flood frequency plots for Chitral River Basin under SSP 2-4.5 scenario**

**Table 25.Various return period flood for Chitral River under SSP 2-4.5 scenario**

| Return Period | Historical Period | Chitral SSP 245 | | | | | |
|---|---|---|---|---|---|---|---|
| | 1981-2010 | 2011-2040 | | 2041-2070 | | 2071-2100 | |
| Years | $m^3/s$ | $m^3/s$ | % | $m^3/s$ | % | $m^3/s$ | % |
| 5 | 2454 | 2931 | 19.4% | 3180 | 29.6% | 3407 | 38.8% |
| 10 | 3114 | 3682 | 18.3% | 3968 | 27.4% | 4197 | 34.8% |
| 25 | 3947 | 4631 | 17.3% | 4964 | 25.8% | 5196 | 31.6% |
| 50 | 4565 | 5336 | 16.9% | 5703 | 24.9% | 5936 | 30.0% |
| 100 | 5179 | 6035 | 16.5% | 6436 | 24.3% | 6671 | 28.8% |
| 200 | 5790 | 6732 | 16.3% | 7166 | 23.8% | 7403 | 27.9% |
| 500 | 6597 | 7650 | 16.0% | 8130 | 23.2% | 8370 | 26.9% |
| 1000 | 7207 | 8345 | 15.8% | 8859 | 22.9% | 9100 | 26.3% |

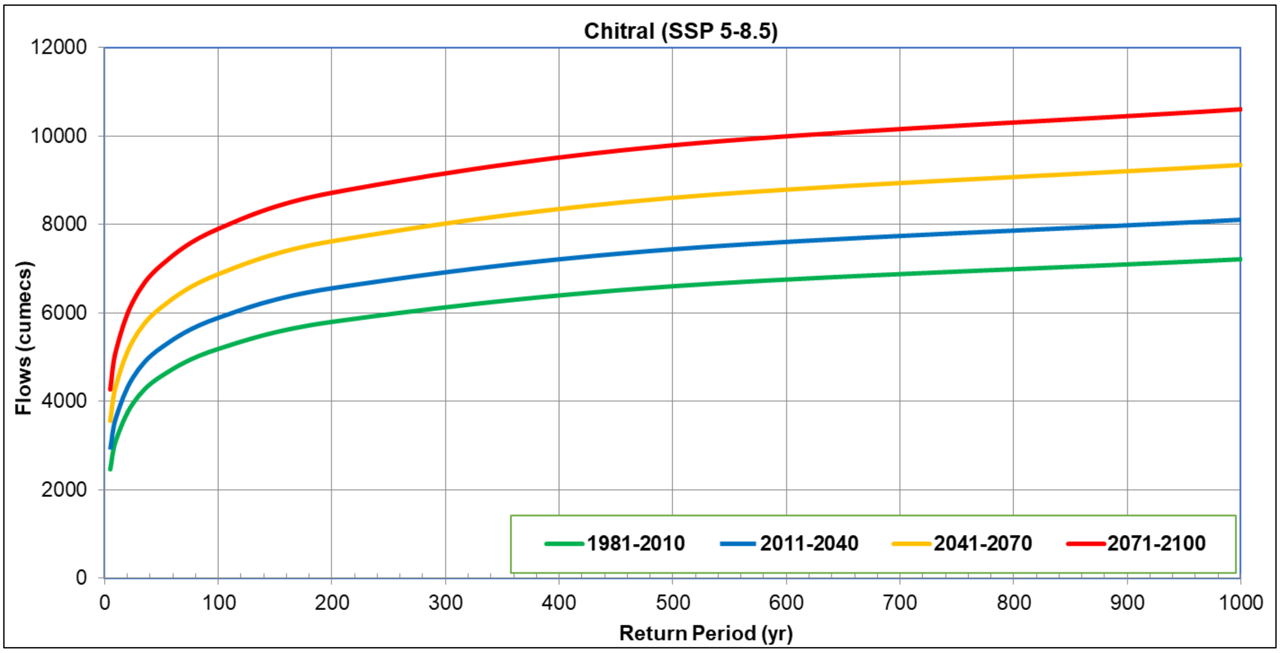


Figure 24.Flood frequency plots for Chitral River Basin under SSP 5-8.5 scenario

Table 26.Various return period flood for Chitral River under SSP 5-8.5 scenario

| Return Period | Historical Period | Chitral SSP 585 | | | | | |
|---|---|---|---|---|---|---|---|
| | 1981-2010 | 2011-2040 | | 2041-2070 | | 2071-2100 | |
| Years | $m^3/s$ | $m^3/s$ | % | $m^3/s$ | % | $m^3/s$ | % |
| 5 | 2454 | 2903 | 18.3% | 3552 | 44.7% | 4267 | 73.9% |
| 10 | 3114 | 3624 | 16.4% | 4355 | 39.9% | 5146 | 65.3% |
| 25 | 3947 | 4535 | 14.9% | 5370 | 36.0% | 6255 | 58.5% |
| 50 | 4565 | 5211 | 14.1% | 6123 | 34.1% | 7079 | 55.1% |
| 100 | 5179 | 5882 | 13.6% | 6870 | 32.6% | 7896 | 52.5% |
| 200 | 5790 | 6550 | 13.1% | 7614 | 31.5% | 8710 | 50.4% |
| 500 | 6597 | 7432 | 12.7% | 8596 | 30.3% | 9785 | 48.3% |
| 1000 | 7207 | 8099 | 12.4% | 9339 | 29.6% | 10596 | 47.0% |

## 4.3. Kabul River Basin

95. The flood frequency analysis results for the Kabul Basin are provided under two different scenarios—SSP 245 and SSP 585. Comparing the historical period (1981–2010) to the future scenarios, both SSP 245 and SSP 585 show an increase in flood estimates during future periods, for various return periods except for 5-year and 10-year return period for SSP 245 which show decrease -5.8% to -7.8% (mid to far future) and for SSP 585 it shows decrease -5.0% to -2.8% (mid to near future) for 5 year return period only. This suggests a higher risk of more frequent and severe flooding events in the coming years. Under both scenarios, the flood estimates rise from near to far future However, when comparing SSP 245 and SSP 585, the flood estimates tend to be higher under SSP 585, indicating a potentially greater impact of climate change in terms of flood risk.

96. The results shown in Figures 23 , 24 and provided in Tables 27 and 28 show that a 100-year return period flood in the Kabul River basin corresponds to a magnitude of 9,575 cumecs based on the base period estimate. Considering the SSP 245 scenario, the projected 100-year flood magnitudes for future periods vary between 10,310 cumecs and 10,420 cumecs. For SSP 585 scenario, the 100-year return period flood ranges between 10,417cumecs and 12,231 cumecs.

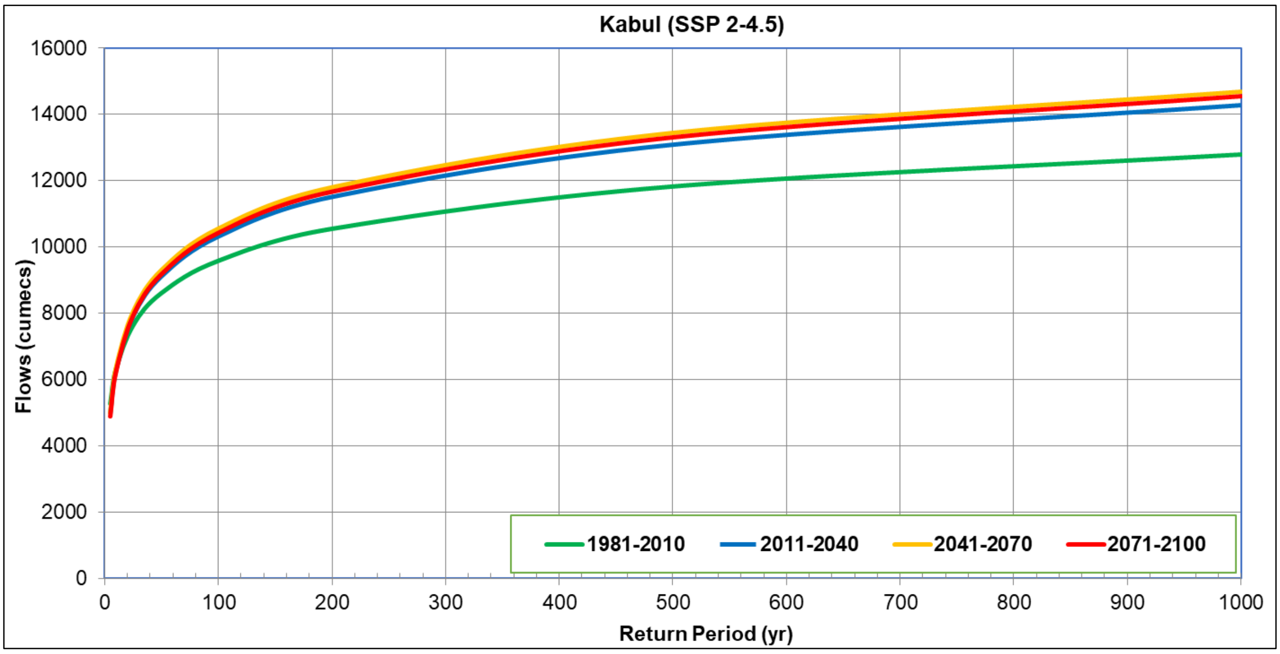

Figure 25.Flood frequency plots for Kabul River Basin under SSP 2-4.5 scenario

Table 27.Various return period flood for Kabul River under SSP 2-4.5 scenario

| Return Period | Historical Period | Kabul SSP 245 | | | | | |
|---|---|---|---|---|---|---|---|
| | 1981-2010 | 2011-2040 | | 2041-2070 | | 2071-2100 | |
| Years | m³/s | m³/s | % | m³/s | % | m³/s | % |
| 5 | 5263 | 4959 | -5.8% | 4990 | -5.2% | 4891 | -7.1% |
| 10 | 6307 | 6258 | -0.8% | 6337 | 0.5% | 6228 | -1.3% |
| 25 | 7626 | 7895 | 3.5% | 8038 | 5.4% | 7918 | 3.8% |
| 50 | 8604 | 9108 | 5.9% | 9301 | 8.1% | 9174 | 6.6% |
| 100 | 9575 | 10310 | 7.7% | 10553 | 10.2% | 10420 | 8.8% |
| 200 | 10543 | 11507 | 9.1% | 11802 | 11.9% | 11662 | 10.6% |
| 500 | 11819 | 13086 | 10.7% | 13449 | 13.8% | 13301 | 12.5% |
| 1000 | 12784 | 14279 | 11.7% | 14693 | 14.9% | 14540 | 13.7% |

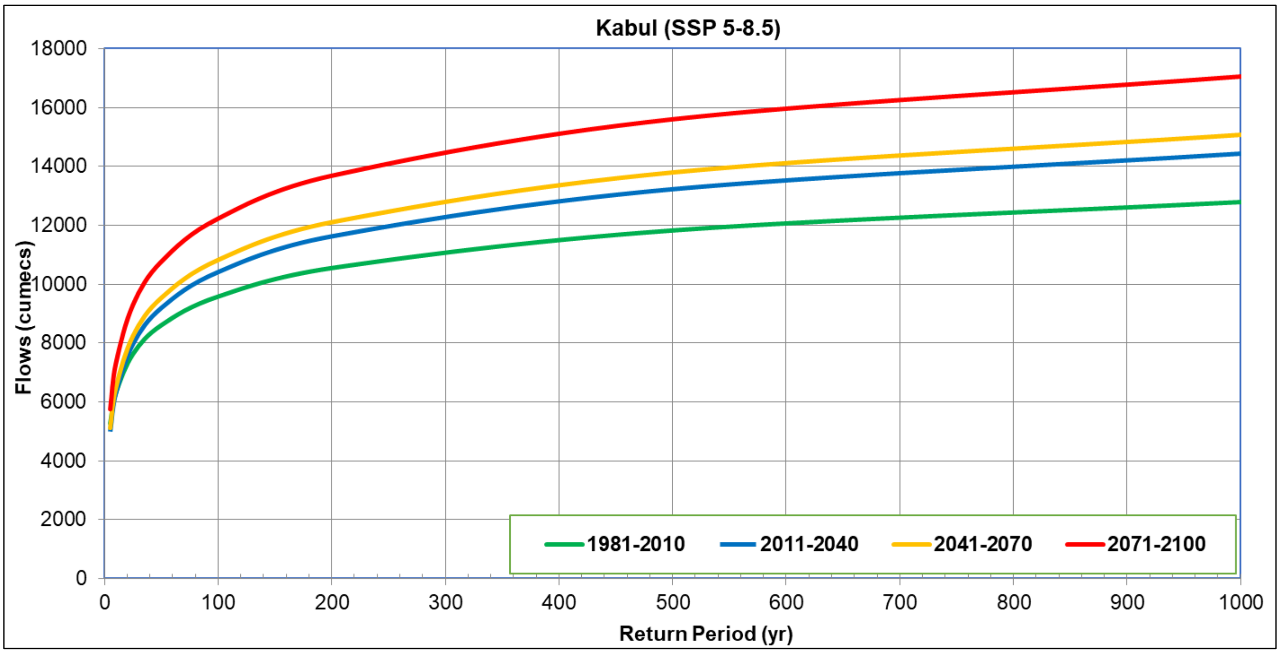


Figure 26.Flood frequency plots for Kabul River Basin under SSP 5-8.5 scenario

Table 28. Various return period flood for Kabul River under SSP 5-8.5 scenario

| Return Period | Historical Period | Kabul SSP 585 | | | | | |
|---|---|---|---|---|---|---|---|
| | 1981-2010 | 2011-2040 | | 2041-2070 | | 2071-2100 | |
| Years | m³/s | m³/s | % | m³/s | % | m³/s | % |
| 5 | 5263 | 5002 | -5.0% | 5114 | -2.8% | 5748 | 9.2% |
| 10 | 6307 | 6316 | 0.1% | 6496 | 3.0% | 7316 | 16.0% |
| 25 | 7626 | 7973 | 4.5% | 8242 | 8.1% | 9299 | 21.9% |
| 50 | 8604 | 9200 | 6.9% | 9538 | 10.9% | 10770 | 25.2% |
| 100 | 9575 | 10417 | 8.8% | 10824 | 13.0% | 12231 | 27.7% |
| 200 | 10543 | 11630 | 10.3% | 12106 | 14.8% | 13688 | 29.8% |
| 500 | 11819 | 13228 | 11.9% | 13796 | 16.7% | 15609 | 32.1% |
| 1000 | 12784 | 14436 | 12.9% | 15074 | 17.9% | 17061 | 33.5% |

## 4.4. KUNHAR RIVER BASIN

97. The flood frequency analysis results for the Kunhar River Basin are provided under two different scenarios—SSP 245 and SSP 585 in Figures 25, 26 and in Tables 29 ,30. Comparing the historical period (1980–2010) to the future scenarios, both SSP 245 and SSP 585 show an increase

in flood estimates during future periods, for various return periods. This suggests a higher risk of more frequent and severe flooding events in the coming years. Under SSP 245 scenarios, for the future 100-year return period the flood estimates rise about 10% to 9.7% from 2011–2040 to 2071–2100 while under SSP 585 scenarios the flood estimates rise about 11% to 20.8% from 2011–2040 to 2071–2100.However, when comparing SSP 245 and SSP 585, the flood estimates tend to be higher under SSP 585, indicating a potentially greater impact of climate change in terms of flood risk.

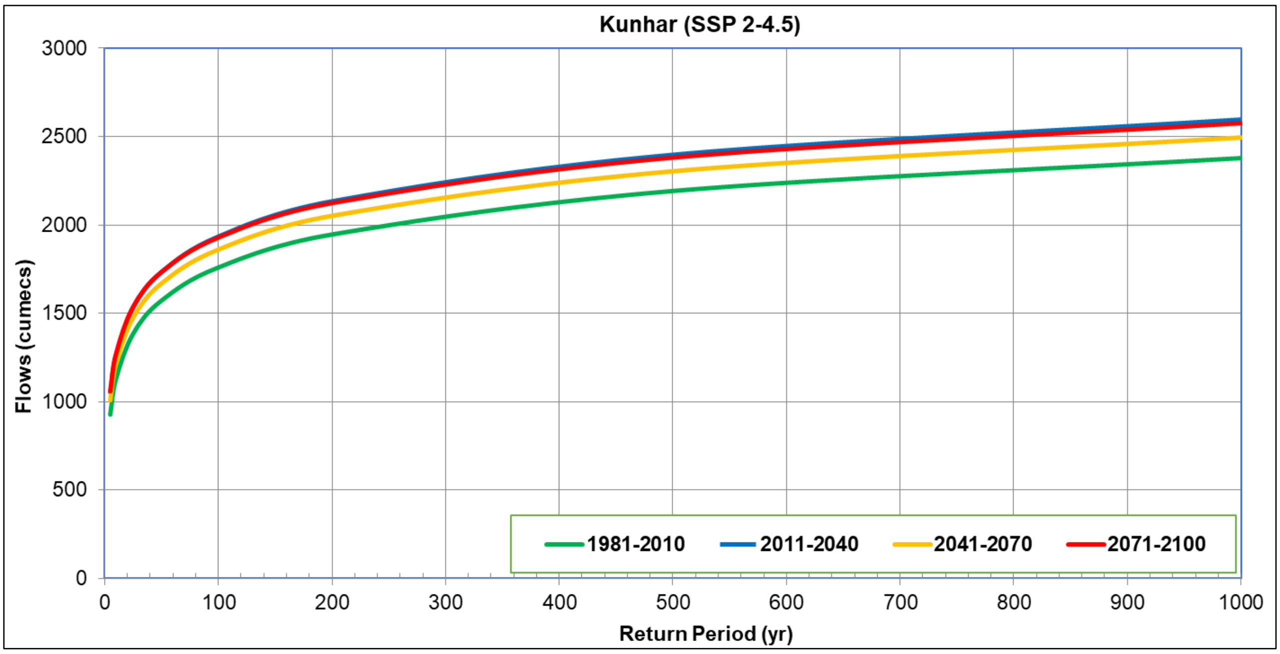


**Figure 27.Flood frequency analysis for Kunhar River Basin under SSP 2-4.5 scenario**

**Table 29. Various return period flood for Kunhar River under SSP 2-4.5 scenario**

| Return Period | Historical Period | Kunhar SSP 245 | | | | | |
|---|---|---|---|---|---|---|---|
| | 1981-2010 | 2011-2040 | | 2041-2070 | | 2071-2100 | |
| Years | $m^3/s$ | $m^3/s$ | % | $m^3/s$ | % | $m^3/s$ | % |
| 5 | 927 | 1046 | 12.8% | 1009 | 8.9% | 1059 | 14.3% |
| 10 | 1128 | 1261 | 11.8% | 1215 | 7.7% | 1270 | 12.6% |
| 25 | 1383 | 1533 | 10.8% | 1475 | 6.6% | 1536 | 11.1% |
| 50 | 1573 | 1735 | 10.3% | 1668 | 6.1% | 1734 | 10.3% |
| 100 | 1760 | 1936 | 10.0% | 1860 | 5.7% | 1930 | 9.7% |
| 200 | 1947 | 2135 | 9.6% | 2051 | 5.3% | 2126 | 9.2% |
| 500 | 2194 | 2399 | 9.3% | 2303 | 5.0% | 2384 | 8.6% |
| 1000 | 2381 | 2598 | 9.1% | 2494 | 4.8% | 2578 | 8.3% |

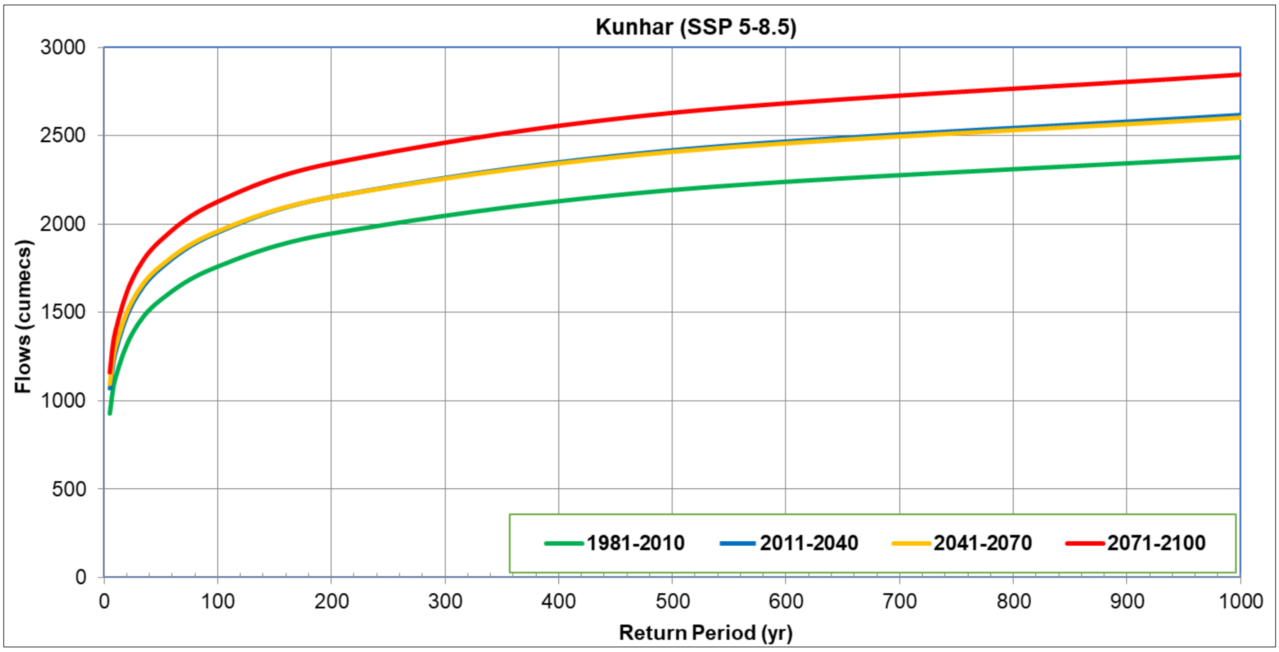


Figure 28.Flood frequency plots for Kunhar River Basin under SSP 5-8.5 scenario

Table 30.Various return period flood for Kunhar River under SSP 5-8.5 scenario

| Return Period | Historical Period | Kunhar SSP 585 | | | | | |
|---|---|---|---|---|---|---|---|
| | 1981-2010 | 2011-2040 | | 2041-2070 | | 2071-2100 | |
| Years | m³/s | m³/s | % | m³/s | % | m³/s | % |
| 5 | 927 | 1062 | 14.6% | 1096 | 18.3% | 1160 | 25.1% |
| 10 | 1128 | 1278 | 13.3% | 1306 | 15.7% | 1394 | 23.5% |
| 25 | 1383 | 1551 | 12.1% | 1570 | 13.5% | 1690 | 22.1% |
| 50 | 1573 | 1753 | 11.5% | 1767 | 12.3% | 1909 | 21.4% |
| 100 | 1760 | 1954 | 11.0% | 1961 | 11.4% | 2127 | 20.8% |
| 200 | 1947 | 2154 | 10.6% | 2156 | 10.7% | 2344 | 20.4% |
| 500 | 2194 | 2418 | 10.2% | 2412 | 9.9% | 2630 | 19.9% |
| 1000 | 2381 | 2617 | 9.9% | 2605 | 9.4% | 2847 | 19.6% |

## 4.5. UPPER INDUS BASIN

98. The flood frequency analysis results for the Upper Indus Basin are provided under two different scenarios—SSP 245 and SSP 585. Comparing the historical period (1981–2010) to the future scenarios, both SSP 245 and SSP 585 show an increase in flood estimates during future periods, for various return. This suggests a higher risk of more frequent and severe flooding events in the coming years. Under both scenarios, the flood estimates rise from near to far future However, when comparing SSP 245 and SSP 585, the flood estimates tend to be higher under SSP 585 in far future indicating a potentially greater impact of climate change in terms of flood risk.

99. The results shown in Figures 27 and 28 and provided in Tables 31 and 32 show that a 100-year return period flood in the Upper Indus basin corresponds to a magnitude of 17,815 cumecs based on the base period estimate. Considering the SSP 245 scenario, the projected 100-year flood magnitudes for future periods vary between 24,379cumecs and 28,139 cumecs. For SSP 585 scenario, the 100-year return period flood ranges between 25,354cumecs and 29,827cumecs.

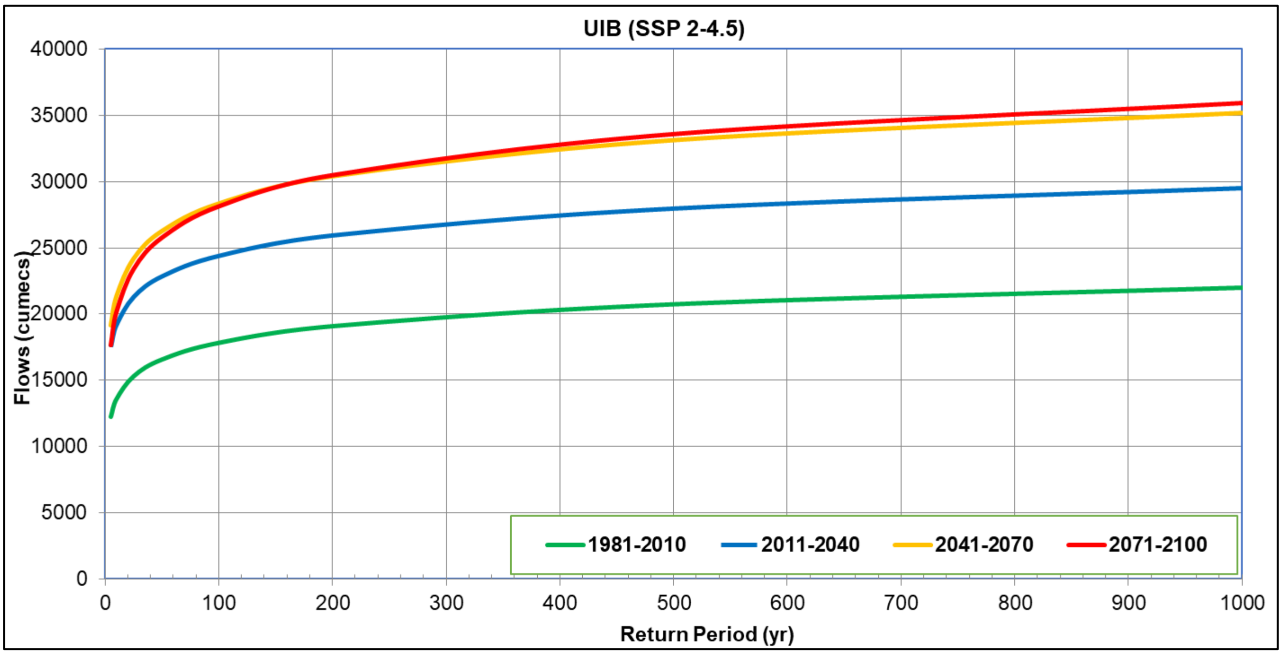


Figure 29.Flood frequency plots for Upper Indus Basin under SSP 2-4.5 scenario

Table 31.Various return period flood for Upper Indus Basin under SSP 2-4.5 scenario

| Return Period | Historical Period | UIB SSP 245 | | | | | |
|---|---|---|---|---|---|---|---|
| | 1981-2010 | 2011-2040 | | 2041-2070 | | 2071-2100 | |
| Years | $m^3/s$ | $m^3/s$ | % | $m^3/s$ | % | $m^3/s$ | % |
| 5 | 12231 | 17498 | 43.1% | 19136 | 56.4% | 17682 | 44.6% |
| 10 | 13583 | 19163 | 41.1% | 21363 | 57.3% | 20213 | 48.8% |
| 25 | 15291 | 21268 | 39.1% | 24176 | 58.1% | 23411 | 53.1% |
| 50 | 16558 | 22829 | 37.9% | 26264 | 58.6% | 25784 | 55.7% |
| 100 | 17815 | 24379 | 36.8% | 28336 | 59.1% | 28139 | 57.9% |
| 200 | 19068 | 25923 | 35.9% | 30400 | 59.4% | 30485 | 59.9% |
| 500 | 20721 | 27960 | 34.9% | 33124 | 59.9% | 33580 | 62.1% |
| 1000 | 21971 | 29499 | 34.3% | 35182 | 60.1% | 35920 | 63.5% |

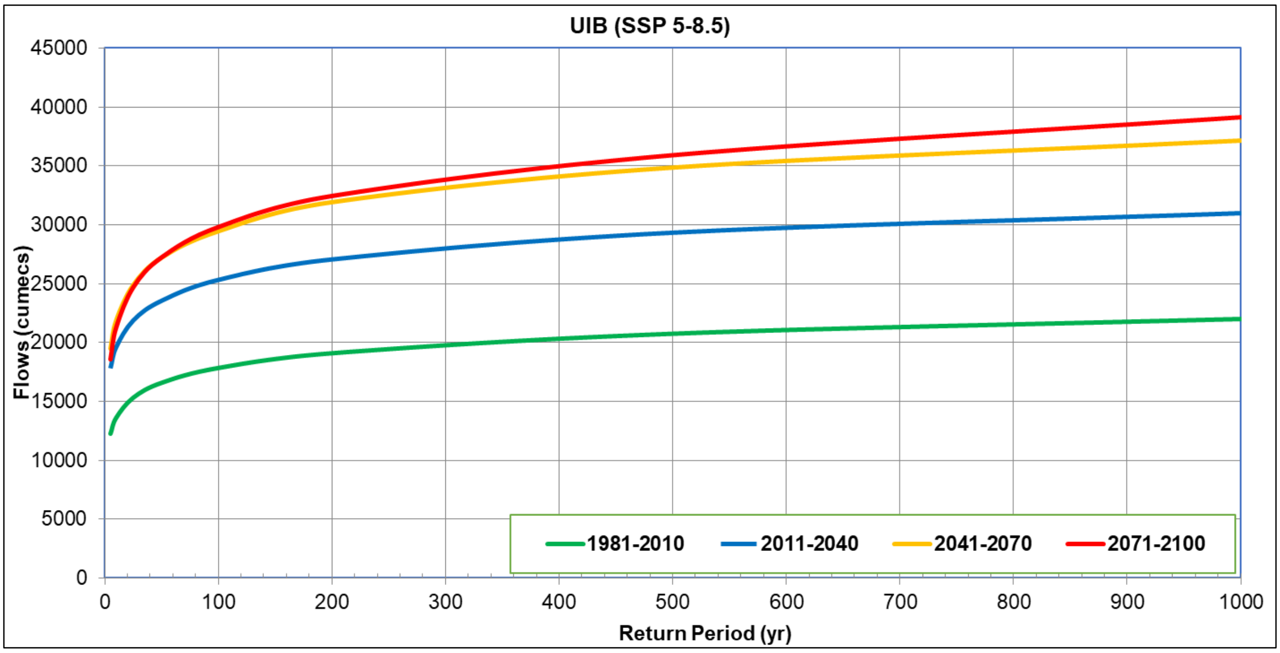

Figure 30.Flood frequency plots for Upper Indus Basin under SSP 5-8.5 scenario

Table 32.Various return period flood for Upper Indus Basin under SSP 5-8.5 scenario

| Return Period | Historical Period | UIB SSP 585 | | | | | |
|---|---|---|---|---|---|---|---|
| | 1981-2010 | 2011-2040 | | 2041-2070 | | 2071-2100 | |
| Years | $m^3/s$ | $m^3/s$ | % | $m^3/s$ | % | $m^3/s$ | % |
| 5 | 12231 | 17848 | 45.9% | 19519 | 59.6% | 18584 | 51.9% |
| 10 | 13583 | 19642 | 44.6% | 21897 | 61.2% | 21284 | 56.7% |
| 25 | 15291 | 21906 | 43.3% | 24902 | 62.9% | 24699 | 61.5% |
| 50 | 16558 | 23582 | 42.4% | 27236 | 64.5% | 27253 | 64.6% |
| 100 | 17815 | 25354 | 42.3% | 29469 | 65.4% | 29827 | 67.4% |
| 200 | 19068 | 27089 | 42.1% | 31935 | 67.5% | 32466 | 70.3% |
| 500 | 20721 | 29358 | 41.7% | 34866 | 68.3% | 35931 | 73.4% |
| 1000 | 21971 | 31009 | 41.1% | 37152 | 69.1% | 39153 | 78.2% |

## 4.6. Kurram River Basin

100. The flood frequency analysis for the Kurram River Basin indicates notable variations in flood estimates between the historical period (1981–2010) and the projected future periods under two different scenarios—SSP 245 and SSP 585. Both SSP 245 and SSP 585 show an increase in future floods. The SSP 585 scenario shows more intense and frequent floods compared to SSP 245 scenario.

101. Overall, the magnitude of the 100-year flood in the Kurram River basin is projected to increase in the future compared to the historical period under both the SSP 245 and SSP 585 scenarios. The percentage increase ranges from approximately 11.8 % to 14.6% for SSP 245 scenario while for SSP 585 scenario the percentage increase ranges from approximately 9.9 % to 33.7% indicating a significant potential increase in flood severity.

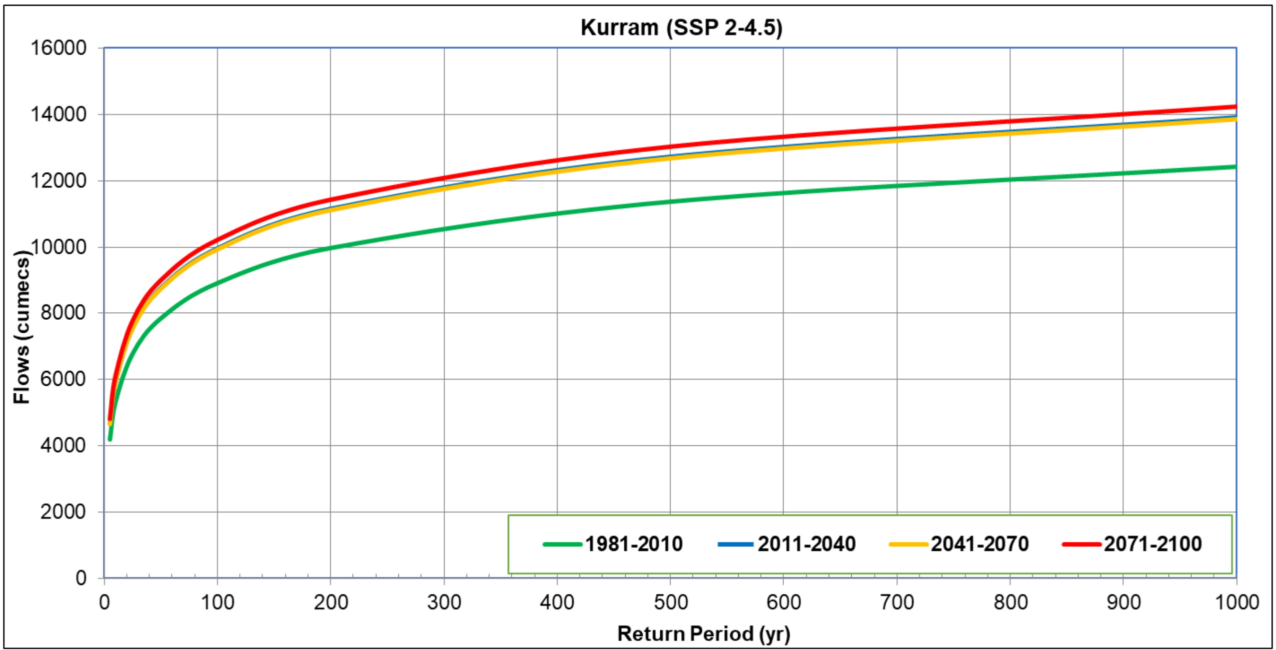


Figure 31.Flood frequency plots for Kurram River Basin under SSP 2-4.5 scenario

Table 33.Various return period flood for Kurram River under SSP 2-4.5 scenario

| Return Period | Historical Period | Kurram SSP 245 | | | | | |
|---|---|---|---|---|---|---|---|
| | 1981-2010 | 2011-2040 | | 2041-2070 | | 2071-2100 | |
| Years | $m^3/s$ | $m^3/s$ | % | $m^3/s$ | % | $m^3/s$ | % |
| 5 | 4197 | 4664 | 11.1% | 4656 | 10.9% | 4807 | 14.5% |
| 10 | 5339 | 5949 | 11.4% | 5934 | 11.1% | 6116 | 14.5% |
| 25 | 6783 | 7572 | 11.6% | 7549 | 11.3% | 7771 | 14.6% |
| 50 | 7853 | 8776 | 11.8% | 8747 | 11.4% | 8998 | 14.6% |
| 100 | 8916 | 9971 | 11.8% | 9937 | 11.4% | 10217 | 14.6% |
| 200 | 9975 | 11162 | 11.9% | 11121 | 11.5% | 11430 | 14.6% |
| 500 | 11372 | 12733 | 12.0% | 12685 | 11.5% | 13032 | 14.6% |
| 1000 | 12427 | 13921 | 12.0% | 13866 | 11.6% | 14242 | 14.6% |

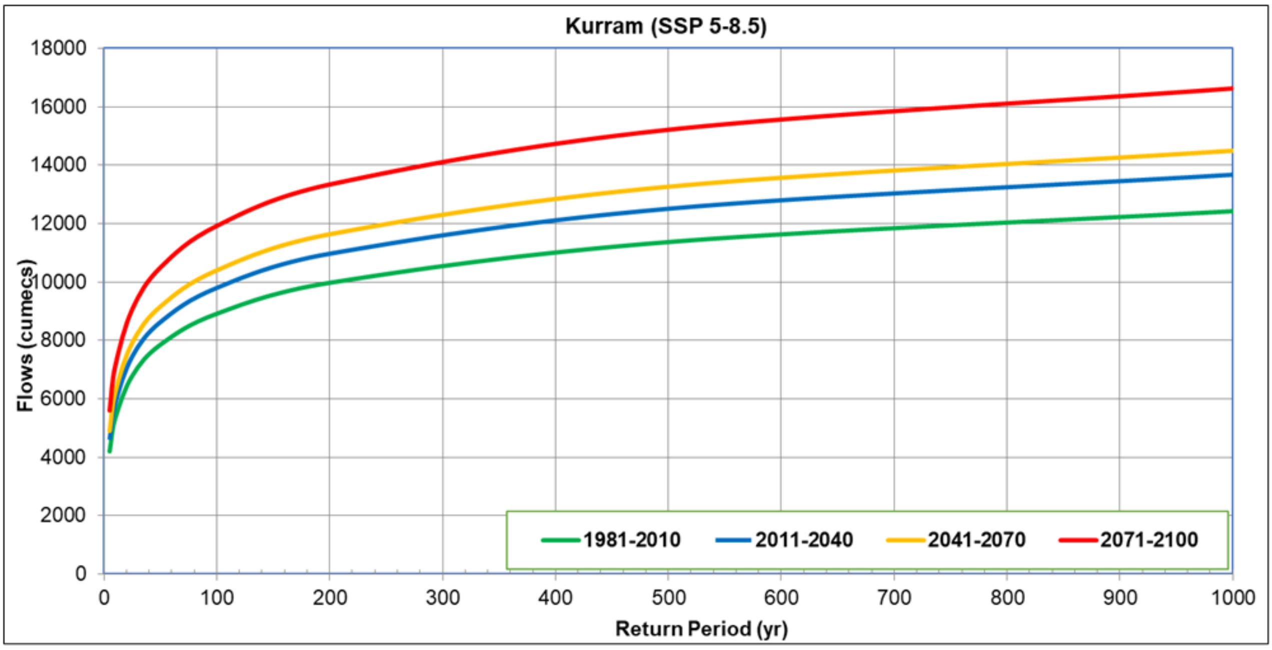


Figure 32.Flood frequency plots for Kurram River Basin under SSP 5-8.5 scenario

Table 34.Various return period flood for Kurram River under SSP 5-8.5 scenario

| Return Period | Historical Period | Kurram SSP 585 | | | | | |
|---|---|---|---|---|---|---|---|
| | 1981-2010 | 2011-2040 | | 2041-2070 | | 2071-2100 | |
| Years | $m^3/s$ | $m^3/s$ | % | $m^3/s$ | % | $m^3/s$ | % |
| 5 | 4197 | 4597 | 9.5% | 4916 | 17.1% | 5607 | 33.6% |
| 10 | 5339 | 5856 | 9.7% | 6247 | 17.0% | 7136 | 33.7% |
| 25 | 6783 | 7446 | 9.8% | 7929 | 16.9% | 9068 | 33.7% |
| 50 | 7853 | 8625 | 9.8% | 9177 | 16.9% | 10502 | 33.7% |
| 100 | 8916 | 9796 | 9.9% | 10415 | 16.8% | 11924 | 33.7% |
| 200 | 9975 | 10963 | 9.9% | 11649 | 16.8% | 13342 | 33.8% |
| 500 | 11372 | 12502 | 9.9% | 13277 | 16.8% | 15212 | 33.8% |
| 1000 | 12427 | 13666 | 10.0% | 14507 | 16.7% | 16625 | 33.8% |

## 4.7. Tank Zam River Basin

102. The flood frequency analysis results for the Tank Zam River Basin are provided under two different scenarios—SSP 245 and SSP 585. Comparing the historical period (1981–2010) to the future scenarios, both SSP 245 and SSP 585 show an increase in flood estimates during future periods, for various return. This suggests a higher risk of more frequent and severe flooding events

in the coming years. Under both scenarios, the flood estimates rise from near to far future However, when comparing SSP 245 and SSP 585, the flood estimates tend to be higher under SSP 585 in far future indicating a potentially greater impact of climate change in terms of flood risk.

103. The results shown in Figures 31 and 32 and provided in Tables 35 and 36 show that a 100-year return period flood in the Tank Zam River basin corresponds to a magnitude of 2,294 cumecs based on the base period estimate. Considering the SSP 245 scenario, the projected 100-year flood magnitudes for future periods vary between 2,923 cumecs and 2,711 cumecs. For SSP 585 scenario, the 100-year return period flood ranges between 2,656 cumecs and 3,012 cumecs.

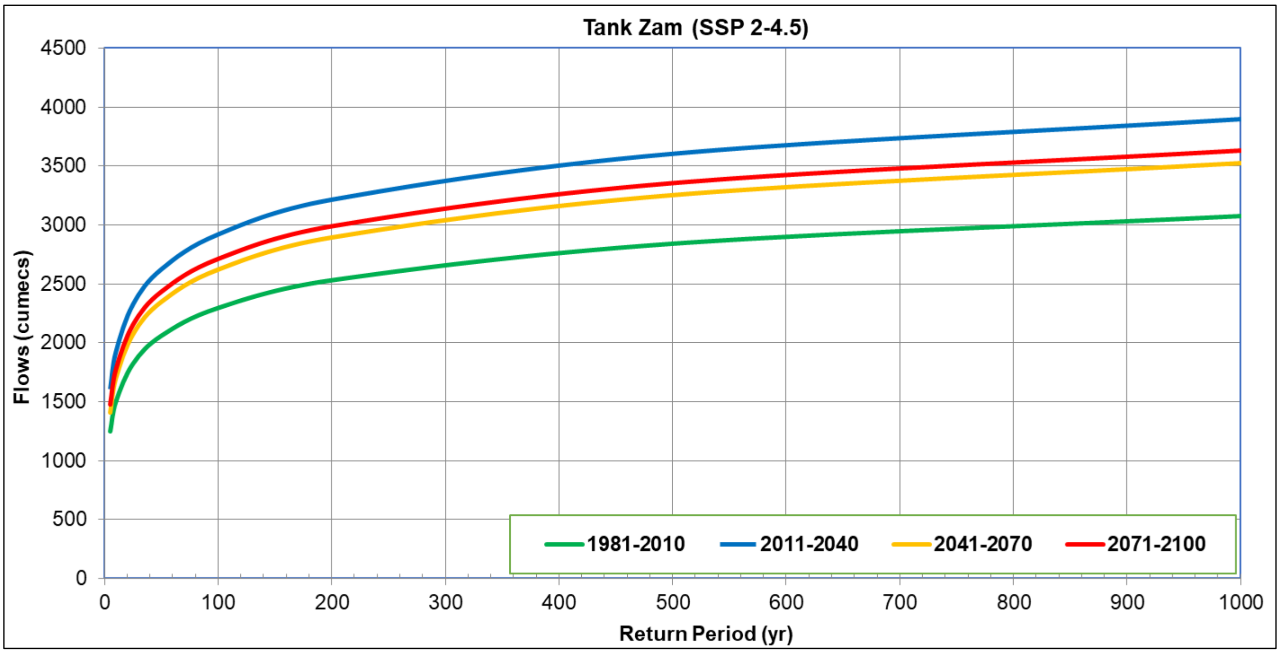


Figure 33.Flood frequency plots for Tank Zam River Basin under SSP 2-4.5 scenario

Table 35.Various return period flood for Tank Zam River under SSP 2-4.5 scenario

| Return Period | Historical Period | Tank Zam SSP 245 | | | | | |
|---|---|---|---|---|---|---|---|
| | 1981-2010 | 2011-2040 | | 2041-2070 | | 2071-2100 | |
| Years | m³/s | m³/s | % | m³/s | % | m³/s | % |
| 5 | 1245 | 1609 | 29.2% | 1410 | 13.2% | 1478 | 18.7% |
| 10 | 1499 | 1927 | 28.6% | 1703 | 13.6% | 1776 | 18.5% |
| 25 | 1820 | 2329 | 28.0% | 2074 | 14.0% | 2153 | 18.3% |
| 50 | 2058 | 2627 | 27.7% | 2349 | 14.2% | 2433 | 18.2% |
| 100 | 2294 | 2923 | 27.4% | 2623 | 14.3% | 2711 | 18.2% |
| 200 | 2530 | 3218 | 27.2% | 2895 | 14.4% | 2987 | 18.1% |
| 500 | 2840 | 3606 | 27.0% | 3254 | 14.6% | 3352 | 18.0% |
| 1000 | 3075 | 3900 | 26.8% | 3525 | 14.6% | 3628 | 18.0% |

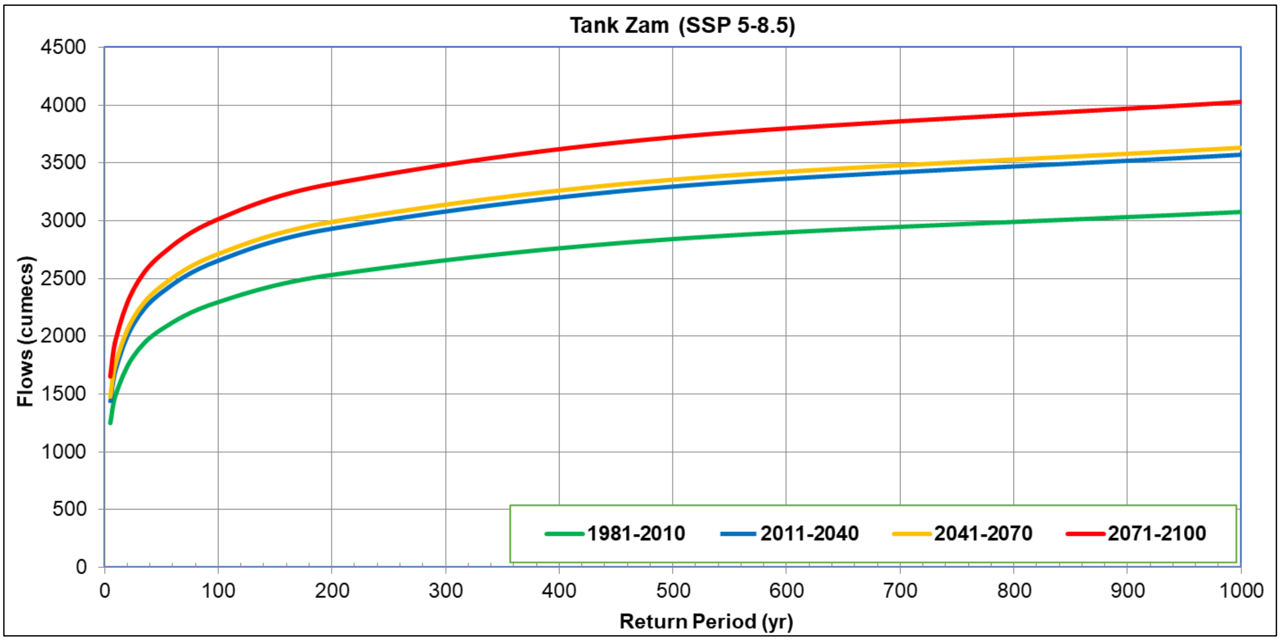


**Figure 34.Flood frequency plots for Tank Zam River Basin under SSP 5-8.5 scenario**

**Table 36.Various return period flood for Tank Zam River under SSP 5-8.5 scenario**

| Return Period | Historical Period | Tank Zam SSP 585 | | | | | |
|---|---|---|---|---|---|---|---|
| | 1981-2010 | 2011-2040 | | 2041-2070 | | 2071-2100 | |
| Years | $m^3/s$ | $m^3/s$ | % | $m^3/s$ | % | $m^3/s$ | % |
| 5 | 1245 | 1424 | 14.4% | 1477 | 18.6% | 1651 | 32.6% |
| 10 | 1499 | 1722 | 14.9% | 1776 | 18.5% | 1981 | 32.1% |
| 25 | 1820 | 2099 | 15.3% | 2153 | 18.3% | 2397 | 31.7% |
| 50 | 2058 | 2378 | 15.6% | 2433 | 18.2% | 2706 | 31.5% |
| 100 | 2294 | 2656 | 15.8% | 2711 | 18.2% | 3012 | 31.3% |
| 200 | 2530 | 2932 | 15.9% | 2988 | 18.1% | 3318 | 31.2% |
| 500 | 2840 | 3297 | 16.1% | 3354 | 18.1% | 3721 | 31.0% |
| 1000 | 3075 | 3572 | 16.2% | 3630 | 18.0% | 4026 | 30.9% |

## 4.8. GOMAL RIVER BASIN

104. The flood frequency analysis for the Gomal River Basin indicates notable variations in flood estimates between the historical period (1981–2010) and the projected future periods under two different scenarios—SSP 245 and SSP 585. Both SSP 245 and SSP 585 show an increase in future floods. The SSP 585 scenario shows more intense and frequent floods compared to SSP 245 scenario.

105. Overall, the magnitude of the 100-year flood in the Gomal River basin is projected to increase in the future compared to the historical period under both the SSP 245 and SSP 585 scenarios. The percentage increase ranges from approximately 98.6 % (near future) to 72.9% (far future) for SSP 245 scenario while for SSP 585 scenario the percentage increase ranges from approximately 109.1% (near future) to 76.4% (far future) indicating a significant potential increase in flood severity.

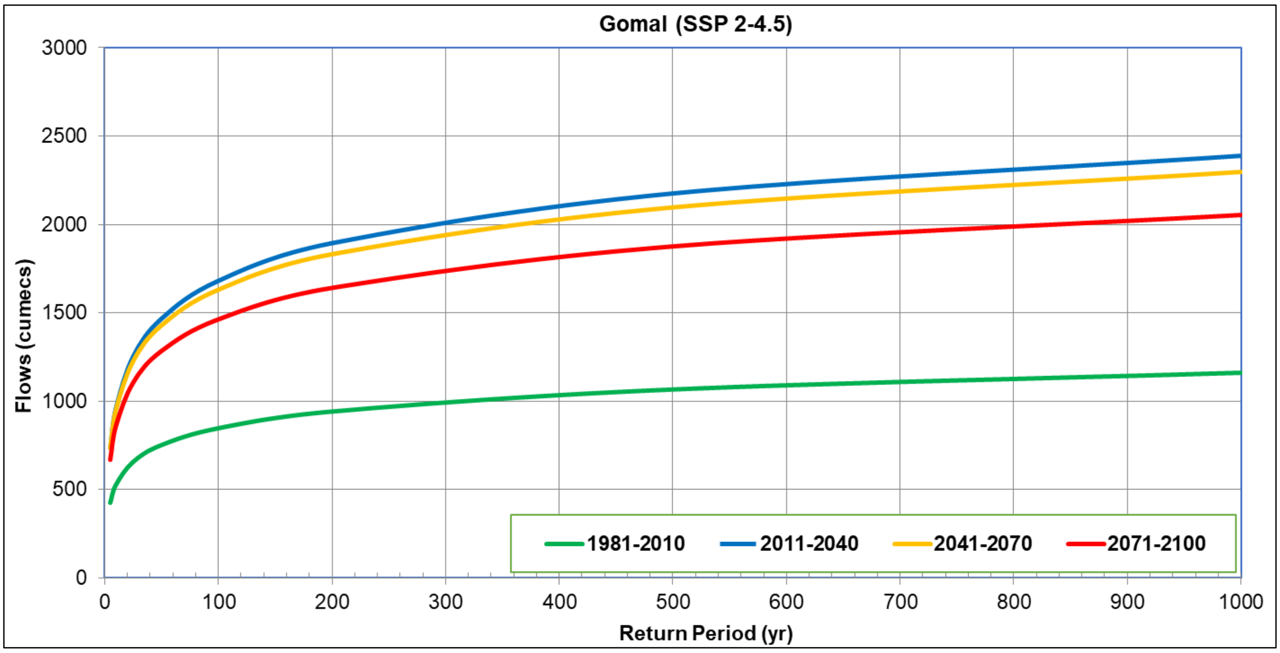


Figure 35.Flood frequency plots for Gomal River Basin under SSP 2-4.5 scenario

Table 37.Various return period flood for Gomal River under SSP 2-4.5 scenario

| Return Period | Historical Period | Gomal SSP 245 | | | | | |
|---|---|---|---|---|---|---|---|
| | 1981-2010 | 2011-2040 | | 2041-2070 | | 2071-2100 | |
| Years | m³/s | m³/s | % | m³/s | % | m³/s | % |
| 5 | 422 | 728 | 72.6% | 734 | 74.0% | 667 | 58.1% |
| 10 | 524 | 958 | 82.7% | 951 | 81.3% | 859 | 63.9% |
| 25 | 654 | 1249 | 91.0% | 1225 | 87.3% | 1102 | 68.6% |
| 50 | 750 | 1465 | 95.3% | 1428 | 90.5% | 1283 | 71.1% |
| 100 | 845 | 1679 | 98.6% | 1630 | 92.9% | 1462 | 72.9% |
| 200 | 940 | 1892 | 101.3% | 1831 | 94.8% | 1640 | 74.4% |
| 500 | 1065 | 2174 | 104.0% | 2096 | 96.7% | 1875 | 76.0% |
| 1000 | 1160 | 2386 | 105.7% | 2297 | 98.0% | 2053 | 77.0% |

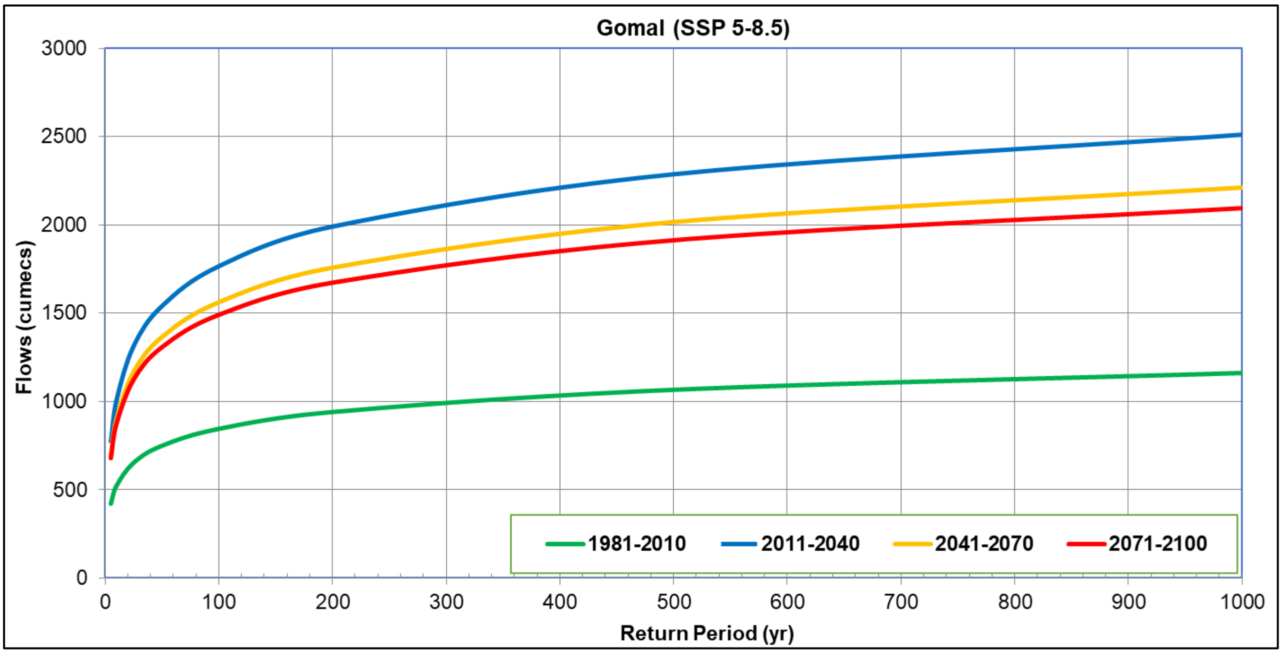


Figure 36.Flood frequency plots for Gomal River Basin under SSP 5-8.5 scenario

**Table 38.Various return period flood for Gomal River under SSP 5-8.5 scenario**

| Return Period | Historical Period | Gomal SSP 585 | | | | | |
|---|---|---|---|---|---|---|---|
| | 1981-2010 | 2011-2040 | | 2041-2070 | | 2071-2100 | |
| Years | $m^3/s$ | $m^3/s$ | % | $m^3/s$ | % | $m^3/s$ | % |
| 5 | 422 | 766 | 81.6% | 688 | 63.2% | 678 | 60.8% |
| 10 | 524 | 1009 | 92.3% | 900 | 71.7% | 875 | 66.9% |
| 25 | 654 | 1315 | 101.1% | 1168 | 78.6% | 1124 | 71.9% |
| 50 | 750 | 1542 | 105.6% | 1366 | 82.2% | 1308 | 74.4% |
| 100 | 845 | 1767 | 109.1% | 1563 | 84.9% | 1491 | 76.4% |
| 200 | 940 | 1992 | 111.8% | 1759 | 87.1% | 1674 | 78.0% |
| 500 | 1065 | 2288 | 114.7% | 2018 | 89.4% | 1914 | 79.7% |
| 1000 | 1160 | 2512 | 116.5% | 2214 | 90.8% | 2096 | 80.7% |

# A-5. CONCLUSIONS AND RECOMMENDATIONS

106. The “Report on Climate Change Projections” (January 2024) project wetter and hotter near to far future. The climate change inclusive flood modelling results show an increase in various return period floods. The projected flood intensities vary among the basins as well as for various return periods.

107. The Gomal River Basin shows the highest increase across the study area. The increase in 100-year return flood is 98.6%, 92.9%, and 72.9% for 2011-2040, 2041-2070, and 2071-2100 under SSP 2-4.5 scenario. The rise in 100-year flood under SSP 5-8.5 is projected to be 109.1%, 84.9%, and 76.4% for 2011-2040, 2041-2070, and 2071-2100.

108. Similarly, the Upper Indus Basin, shows the second highest increase across the study area. The increase in 100-year return flood is 36.8%, 59.1%, and 57.9% for 2011-2040, 2041-2070, and 2071-2100 under SSP 2-4.5 scenario. The rise in 100-year flood under SSP 5-8.5 is projected to be 42.3%, 65.4%, and 67.4% for 2011-2040, 2041-2070, and 2071-2100.

109. In addition, the Swat, Chitral, Kabul, Kurram, Tank, and Kunhar river basins also show an increase in 100-year floods. The increase in 100-year flood ranges between 10% to 40% in various time periods under both scenarios. The maximum increase in various return period may occur in different future time periods.

110. Furthermore, the potential increase in various return period floods is likely to increase significant sediment, boulders and debris flows in the Gomal, UIB, Kunhar, Swat, Chitral and Kabul River basins. The deposition of these sediments, boulders and debris may block water ways, reduce river carrying capacities (such as witnessed in Swat River during flood 2022) together with reduction in reservoir capacities (such as witnessed in the Tarbela Dam and Chashma Barrage). The future hotter and wetter climate will also increase risk of increase in Glacier Lake Outburst Flood (GLOF) events, which may also bring large quantity of boulders and debris (particularly in the UIB, Chitral and Swat River Basin). Reduction in water carrying capacities and potential increase in floods may rise risks of inundation and damages in near to far future.

111. Therefore, the basin-level future flood projections suggest to carry-out sub-basin level climate change inclusive flood modelling together with sub-basin-level integrated flood management dynamic adaptation pathways planning for the near, mid and long-term basis. It is also recommended that the climate inclusive Climate Risk Vulnerability Risk Assessment (CRVA) should be carried out at the basin and sub-basin levels. Adequate policy measures are also mandatory for better climate change inclusive flood adaptation and mitigation measures in the near to far future.